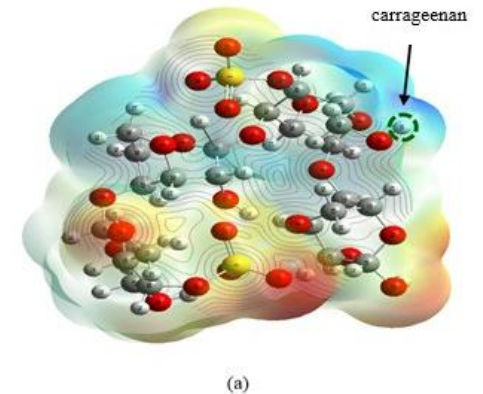
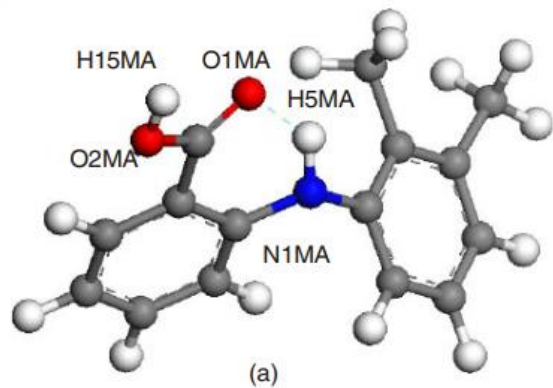


Molecular Modelling & Simulation

Application For Sustainable Engineering

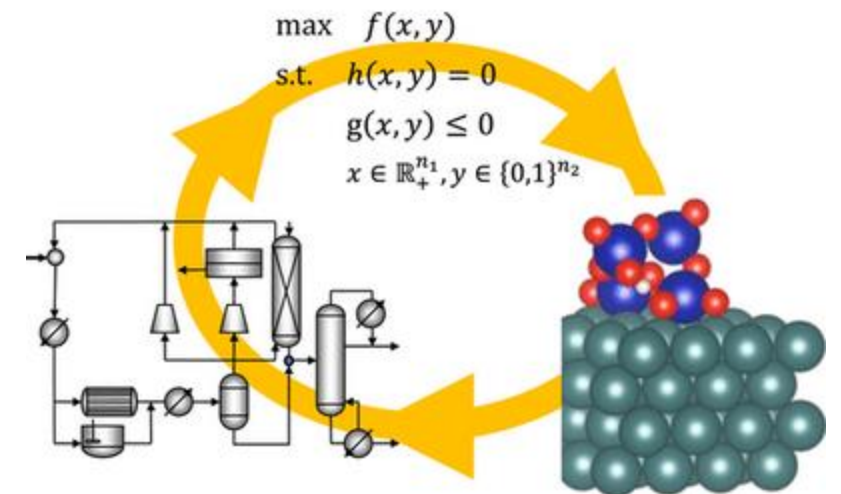
Process Design : Microscopic linking to Macroscopic Property



Associate Professor Dr Fatmawati binti Adam
Faculty of Chemical & Process Engineering Technology

Why Molecular Modelling?

- MD can provide atomistic picture of how a polymorph is selected by crystallisation.
- Model to understand the molecular level interactions of solvent-solute systems for which experimental work is limited.
- Potentially alternative tool to predict and screen the polymorphism in the development phase, i.e. solvent screening.
- Modelling and simulation helps to understand and control materials structure, properties and processes.
- Sustainable method in interplay between process design and the design of molecules and materials



Macroscopic vs Microscopic

The **key difference** is:

macroscopic properties are the properties of matter in bulk

microscopic properties are properties of the constituents of matter in bulk.

*Properties of matter in bulk are macroscopic properties. Examples are **density, volume, viscosity of a liquid, surface tension of a liquid, resistance of a conductor** and many more properties like these.*

*Microscopic properties are properties of constituents of the bulk matter, i.e. **properties of atoms and molecules constituting the bulk matter.***

These properties of individual atoms or molecules are called microscopic properties.

Dynamics Simulation

- The Newton equation of motion produced the deterministic trajectory in phase space (three positions, three momenta per particle) $F = ma$.

- Total Energy= Kinetic E + Potential E

- Potential energy:

$$E = E_{bond} + E_{angles} + E_{torsions} + E_{non-bonded}$$

- (Leach, 2001)

- Diffusion coefficient, D using Einstein equation :

- Mean Square Displacement = $6Dt + C$

- (Rahman, 1964), (Charati and Stern, 1998), (Hofman, 2000)

- D = self-diff coefficient

- C = finite displacement constant

- Radial distribution function is calculated as:

$$g_{xy}(r) = \frac{\langle N_y(r, r + dr) \rangle}{\rho_y 4\pi r^2 dr}$$

(Jorgensen and Ibrahim, 1980)

N_y = number of atom of type y at distances fr r to r+dr from reference atoms

ρ_y = Number density of atom of type y

Dreiding FF parameters

$$E_{pot} = E_{bond} + E_{angle} + E_{dihed} + E_{coul} + E_{vdw}$$

Valence terms:

$$E_{bond} = \frac{1}{2} k_e (r - r_e)^2$$

$$E_{angle} =$$

$$E_{dihed} = \frac{1}{2} V [1 - \cos(n_{jk} (\varphi - \varphi^\theta))]$$

$$E_{coul} = 322 \left(\frac{q_i q_j}{\epsilon r_{ij}} \right)$$

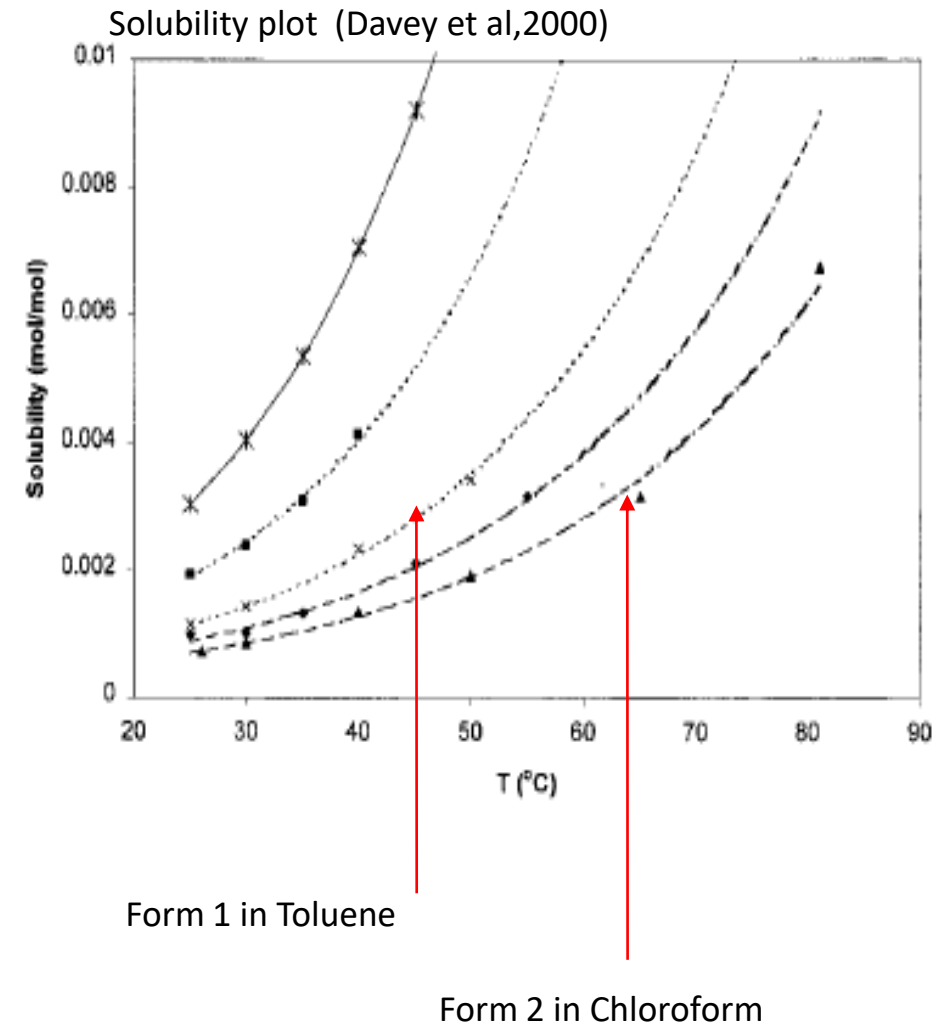
$$E_{vdw} = 4\epsilon \left[\left(\frac{\sigma}{r_{ij}} \right)^{12} - \left(\frac{\sigma}{r_{ij}} \right)^6 \right]$$

Solvent box creation

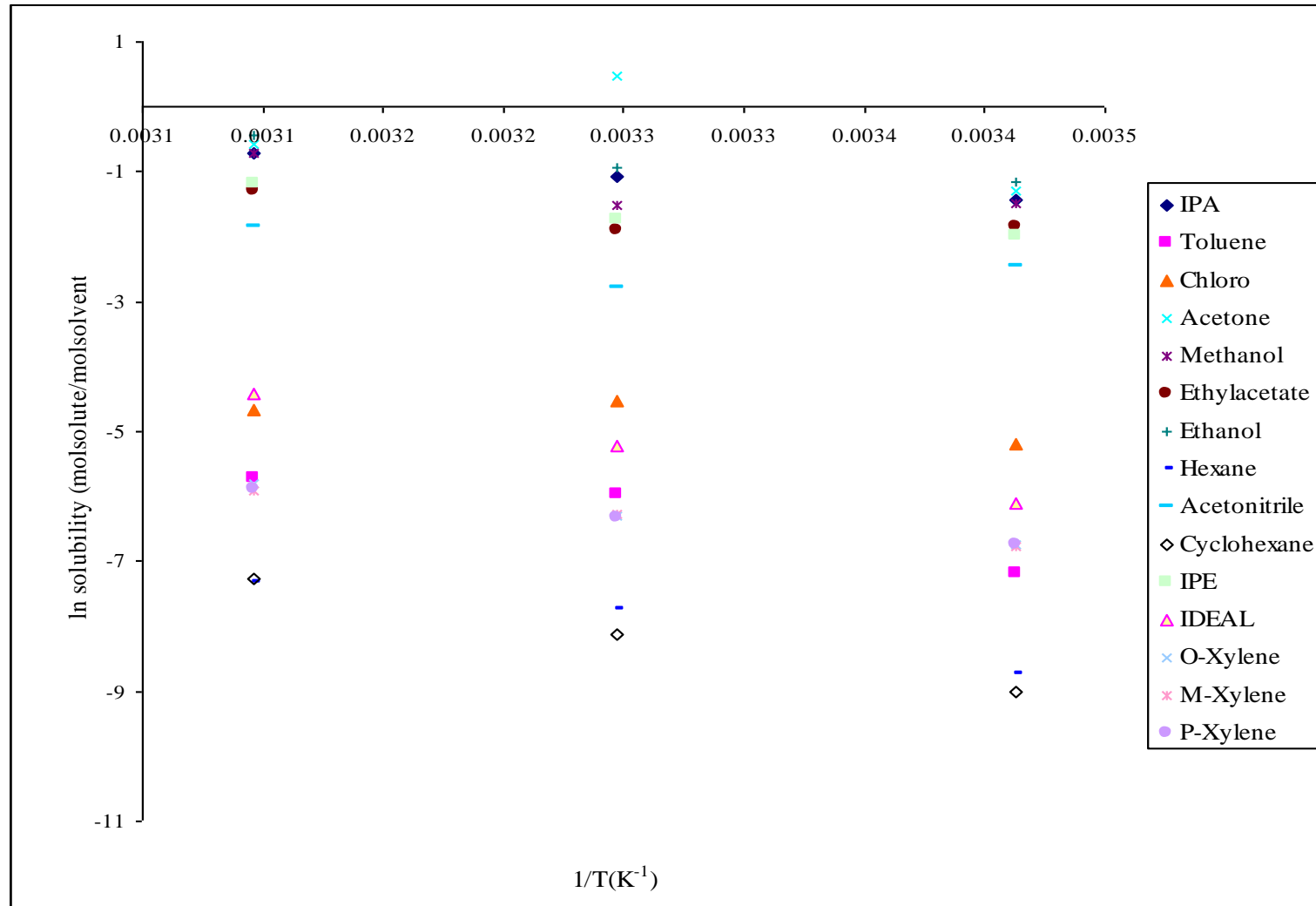
- -based on solubility data-
- mol solute/mol solvent

$$\rho_{mix} = \frac{Mass_{solute} + Mass_{solvent}}{V_{total} x N_{avogadro}}$$

- -Using Amorphous cell module i||
- Materials Studio

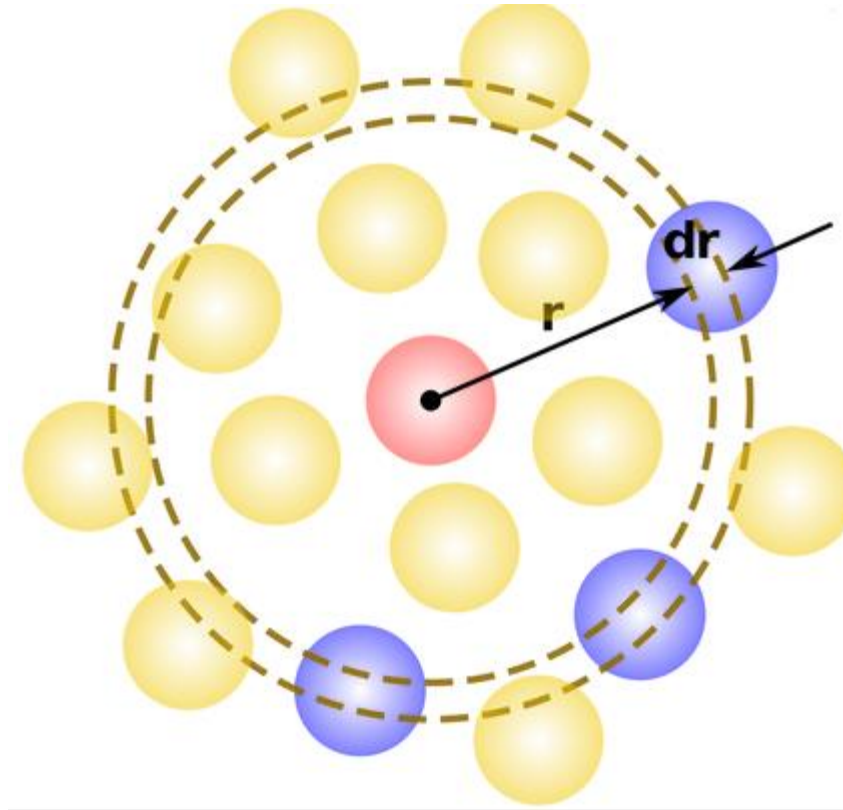


Ideal Solubility and Solubility

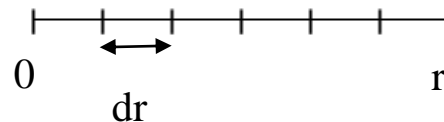


Van Hoff Plot
describes
Solute-solvent
Solvent-solvent
Solute-solute
INTERACTION

Radial Distribution Function



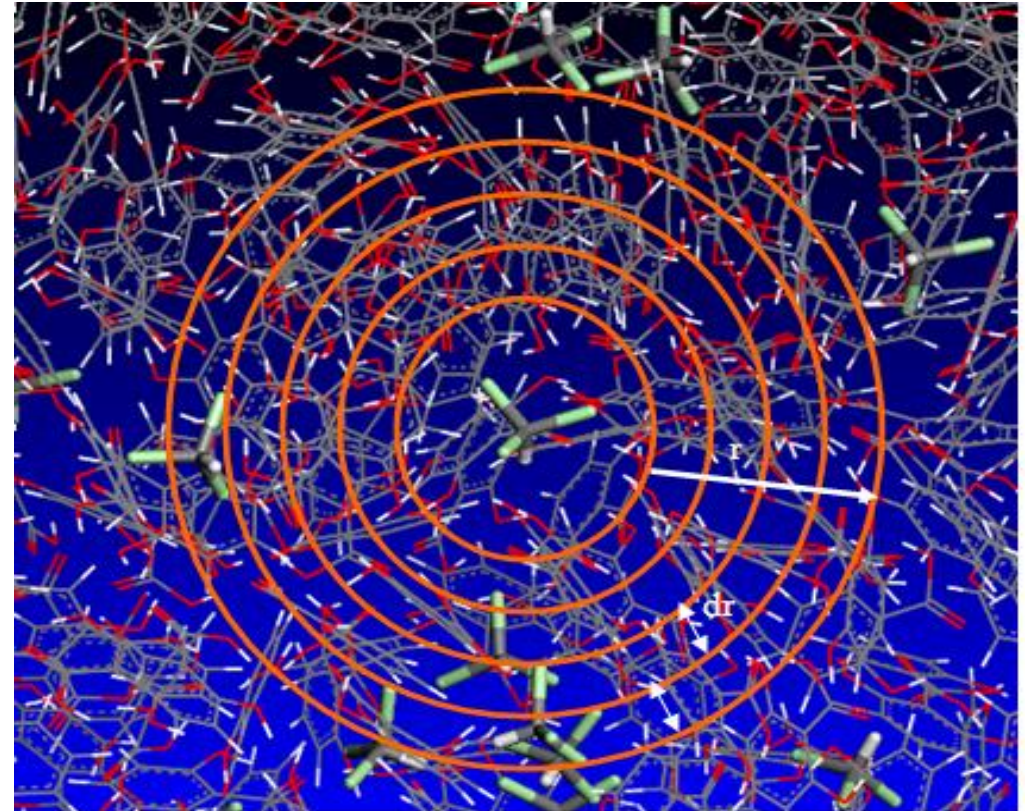
Probability of how frequently of nearest neighbour atoms moves along the spherical radius, r .



Reference atom
is surrounded
by the nearest
neighbour
atoms (1st, 2nd, ...)

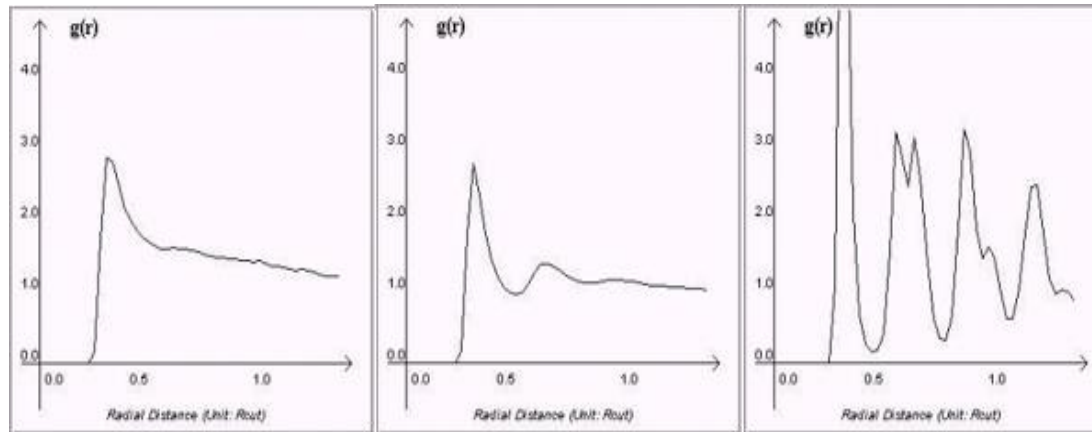
$$g_{xy}(r) = \frac{\langle N_y(r, r + dr) \rangle}{\rho_y 4\pi r^2 dr}$$

Radial Distribution Function



Radial Distribution Function

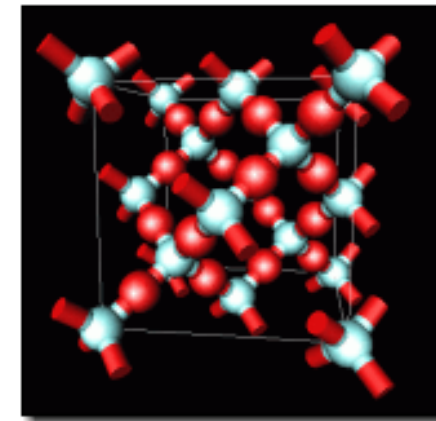
- describes how, on average, the atoms in a system are packed around each other.
- effective way of describing the average structure of disordered molecular systems such as liquids



a) Gas

b) Liquid

c) Solid



SiO solid

Source:

<http://www.cse.scitech.ac.uk/ccg/software/Democritus/Theory/rdf.html>

CASE STUDY 1

*An Examination into The Influence
and Change of Solution Structure on
The polymorphic Behaviour of 2,6-
Dihydroxybenzoic Acid*

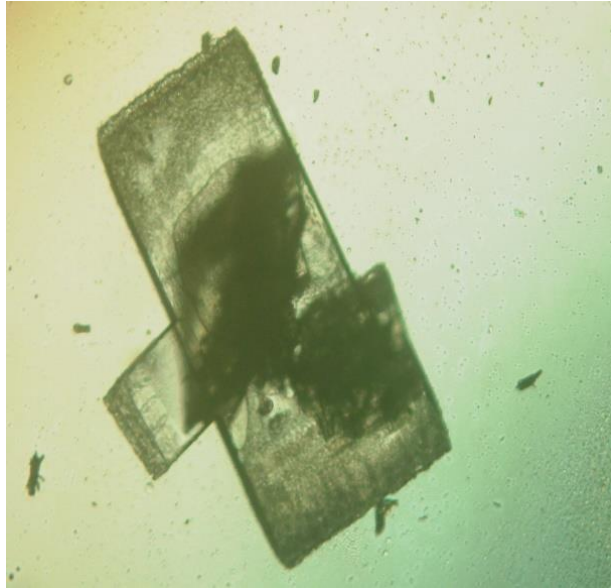
Introduction

- Polymorphism- key issue for pharmaceutical crystallisation processes & product storage.
- Compounds exist in two or more solid forms with different crystal structures exhibit differences in physical properties, i.e. density, solubility, particle shape, dissolution rates & stability.
- Ritonavir® (AIDS drug) transformed from anhydrous to hydrous (Bauer et al, 2001) form after launched to market changed bioavailability -recall for reformulation

Benzoic acid Application

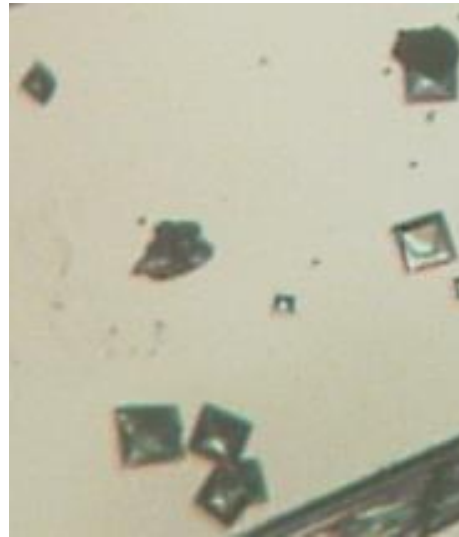
- **Antimicrobial** preservative in **beverages** ie carbonated beverage
- Antimicrobial preservative in **food** in the form of sodium salt ie sodium benzoate
- **Antifungal**
- Tablet and capsule **lubricant**
- Nitrogen binding Agent ie ammonium ion binding activity
- Syrups, fruit salads, icings, jellies

2,6-Dihydroxybenzoic Acid

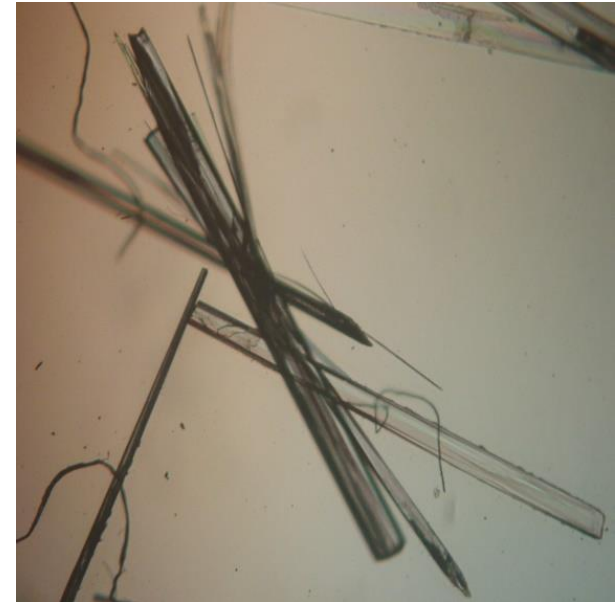


Form I growth from
Toluene

Unstable



Monohydrate from traces of H₂O in
Wet Ethylacetate



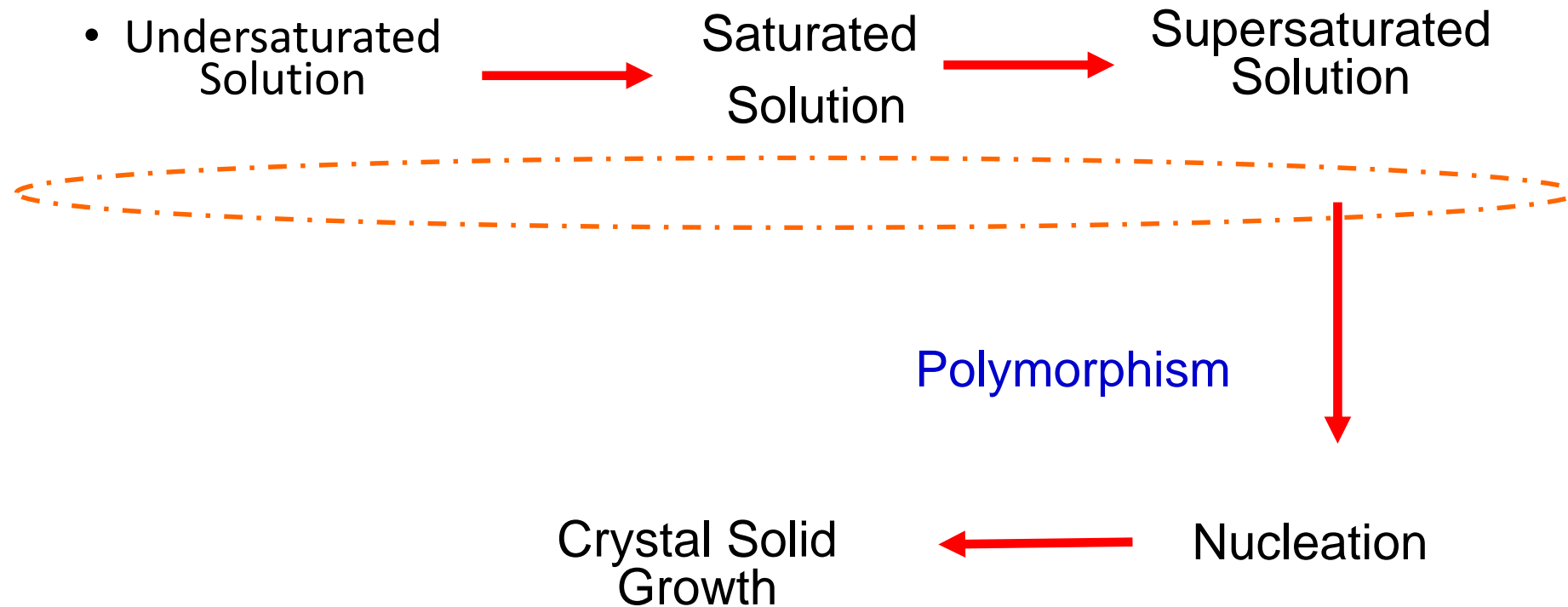
Form II growth from
Chloroform

Stable

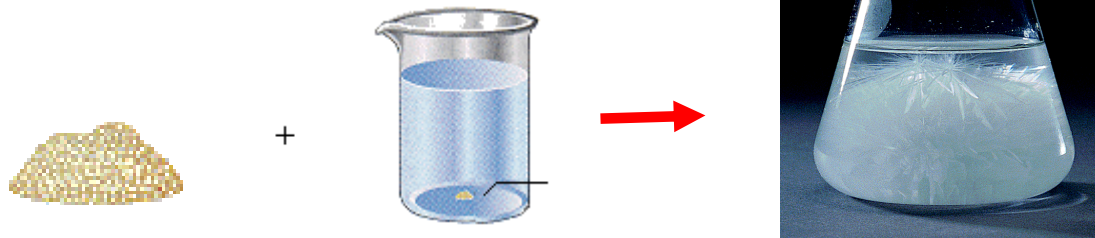
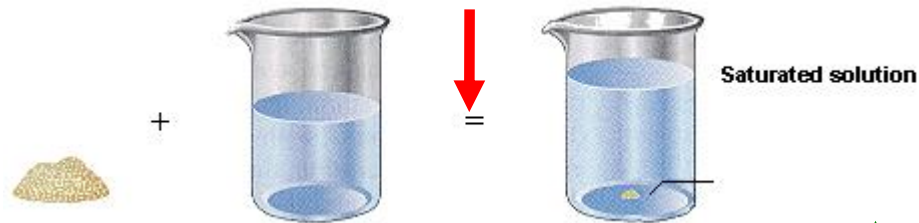
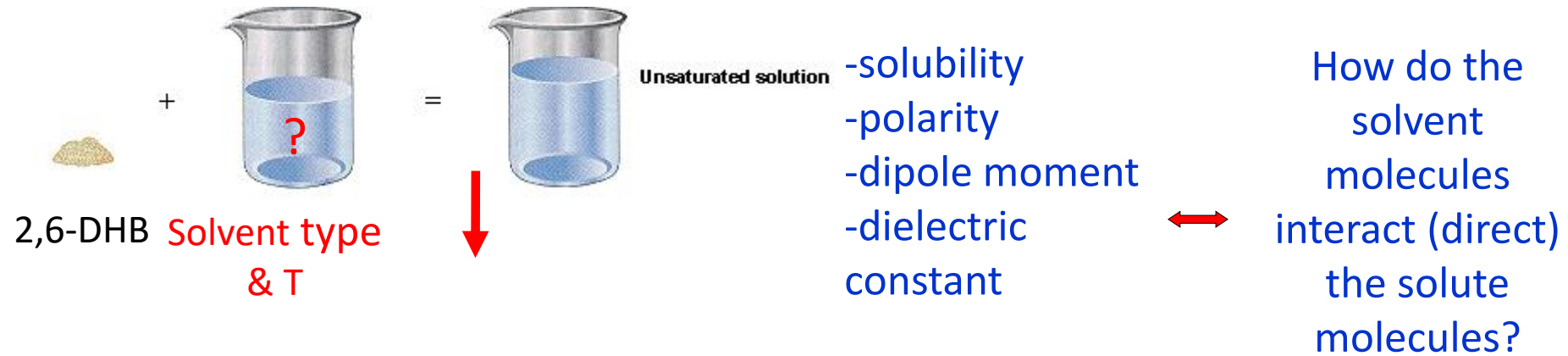
Crystallisation

a process whereby **solid crystals**
are formed from another phase,
typically **a liquid solution or melt**

Crystallisation Process Step



Problem Statement

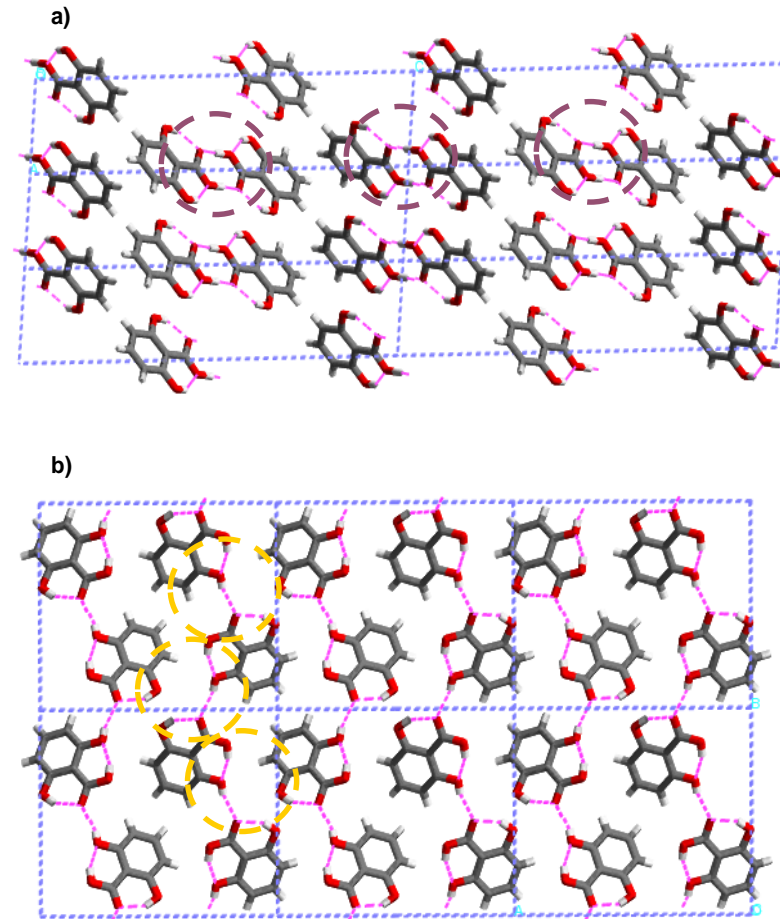


WHICH CRYSTAL POLYMORPH?

- Polymorphism- key issue for pharmaceutical crystallisation processes & product storage - 2/3 of API exhibits polymorphism (Rohani, 2009).
- There is less effort and work being done to model polymorphism in crystallisation of organic compound using the MD simulation to understand the process at molecular level.
- The subtle change in rdfs, diffusion –give insight to understand polymorphism as a function of solvent type, T and concentration. Agreed by many scientists (Maeda et al, 2005; Davey 2008) in crystallisation matter – to recognize how the solute molecule cluster in the solution, how the cluster and nuclei present in the solution

- Investigate the correlation of solubility and which polymorph will crystallise under given process conditions particularly as a function of solvent choice and temperature - solution chemistry & thermodynamics. MSZW compares the kinetics of FI and FII – different solution chemistry properties
- Assessing correlations in the inter-atomic distances between specified atoms on solute molecules by examining
 - i) time-averaged rdf calculated from MD simulations. probability of forming specific solute-solute versus specific solute-solvent intermolecular interactions
 - ii) check the degree of H-bond exist in crystal & solution in relation to the diffusion trend

- 2,6-Dihydroxybenzoic acid is observed experimentally to exhibit different polymorphs depending on the choice of crystallisation solvent.
- **Form I** (a) crystallises from **toluene** whereas **Form II** (b) crystallises from **chloroform**.
- Form I manifests acid **hydrogen-bonded dimers** centro-symmetric, carboxylic whereas Form II manifests **‘infinite’ chains of hydrogen bonded** molecules.



Summary of 2,6-DHB Polymorph Solvent Screening

Crystal Form	T _{melt} °C	Solvent Role	Solvents	Morphology
FI	165	Neither H-bond donor nor acceptor	Toluene, ortho, para, meta-xylene	Plate-Like
FII	165, 170	H-bond donor or acceptor	Chloroform, methanol, ethanol, IPA, IPE, acetone, acetonitrile, ethyl acetate, tert-butyl-methyl ether, diethyl ether, n-hexane, cyclohexane, EA, Methanol, Acetonitrile, IPA	Needle-like Rectangular prism
Monohydrate	- 172	H-bond donor and acceptor	Water/ methanol Water	Prismatic Needle-like

methanol > ethanol > IPA > EA > acetonitrile > acetone > IPE > diethylether > tert-butyl methyl ether >
IDEAL > chloroform > toluene > o-xylene > m-xylene > p-xylene > hexane > cyclohexane

ΔH_{diss} lower, ΔG_{diss} lower, Activity coefficient higher

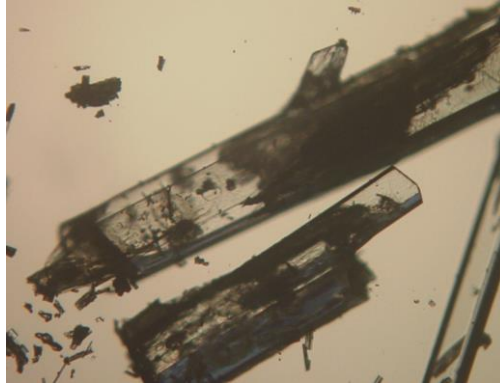
> **IDEAL** > Activity coefficient lower, ΔG_{diss} higher, ΔH_{diss} higher

Solvent-solute interaction stronger > **IDEAL** > Solvent-solute interaction weaker

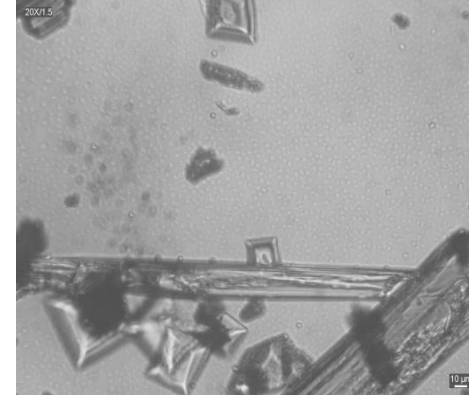
2,6-Dihydroxybenzoic Acid Morphology and MSZW Study



Form I growth from m-xylene

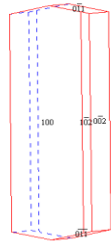


Form II growth from Chloroform

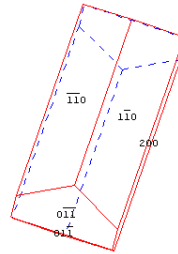


Monohydrate growth from anhydrous solvent
(H₂O sensitive) !!!

Morphology Prediction



FI



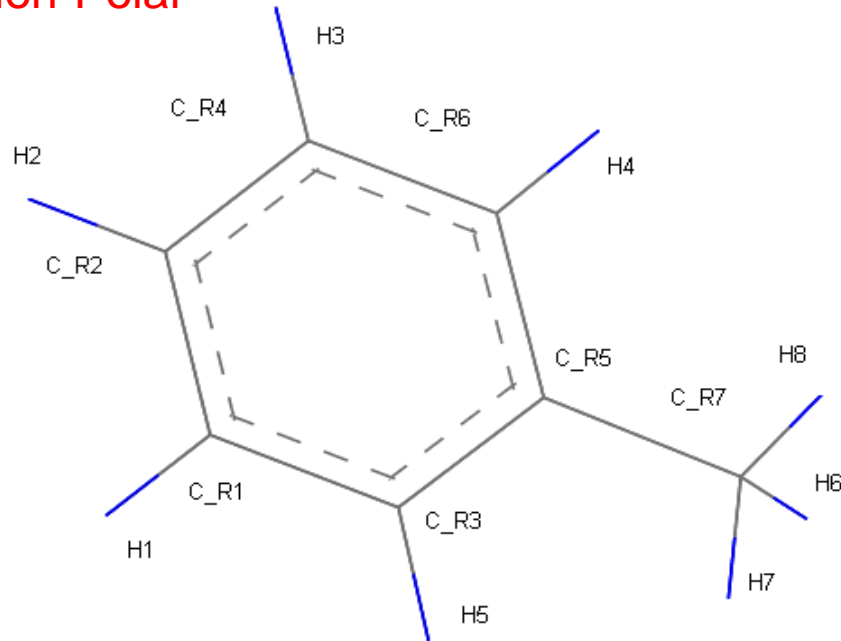
FII

Needle like and plate like shape -
agreement to experimental morphology

Different chemical nature with polar acetonitrile and nonpolar ortho-xylene compounds gave different supersaturation and nucleation of FII and FI polymorph respectively. The nucleation order is lower and narrow MSZW in acetonitrile compared to ortho-xylene which might increase probability of contact between solute molecules for self assembly and nucleation to occur.

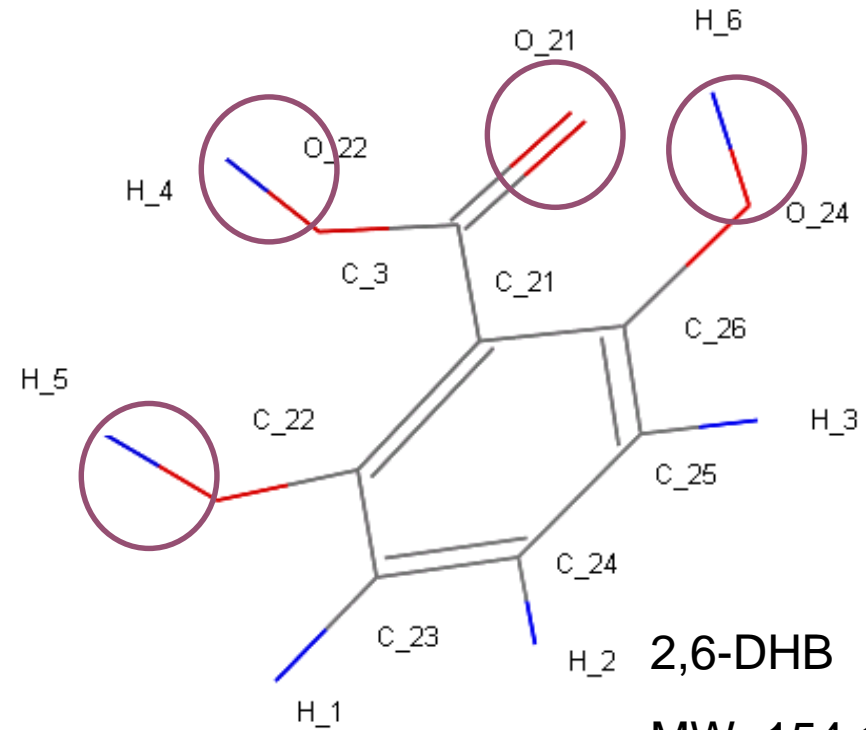
Molecular Diagrams On Atomistic Approach

Non-Polar



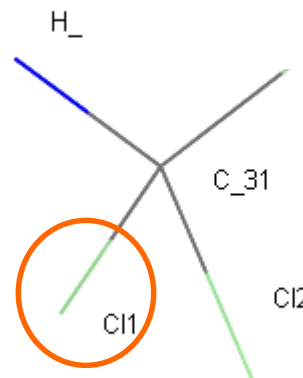
Toluene

MW=92.14



2,6-DHB

MW=154.12



Chloroform

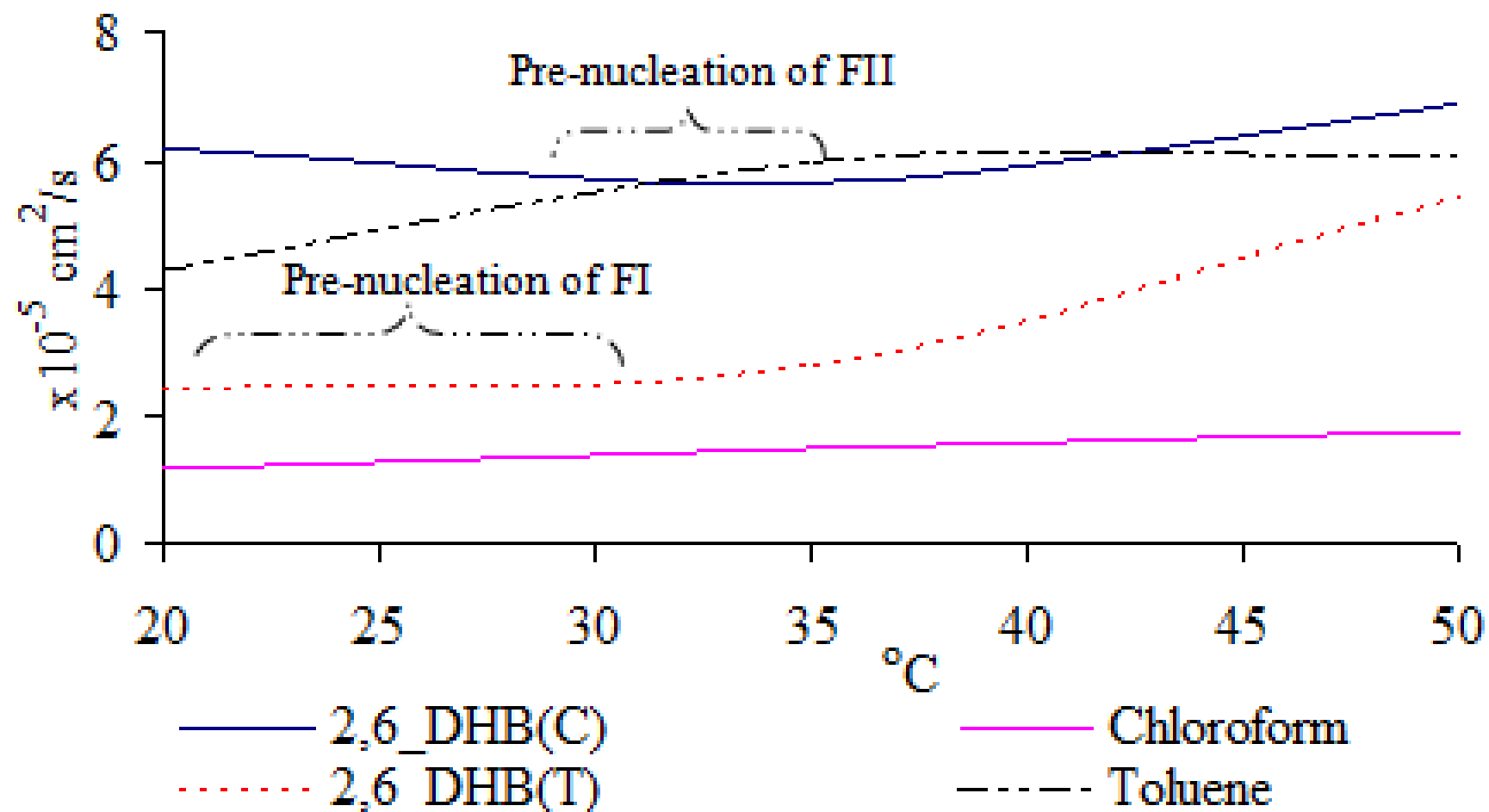
MW=119.38

Polar

Overview of MD Simulation Findings

- MD simulation able to give the insight into the polymorphism of 2,6-DHB as the experimental work is limited
- Dreiding and OPLSAA work excellently to model the pure solvent to reproduce properties in agreement to the experimental & theoretical value.
- Binary system
- Diffusion
- In general, 2,6-DHB acid solute diffuses faster in chloroform compared in toluene solution at highly supersaturated solution- more degree of H-bond forms amongst the solute molecule to drive the self aggregation/self assembly. The diffusion of toluene & chloroform diffuses slower compared to the 2,6-DHB solute due to the repulsion forces and high MW respectively in the solution mixture.

Overview of MD Simulation Findings



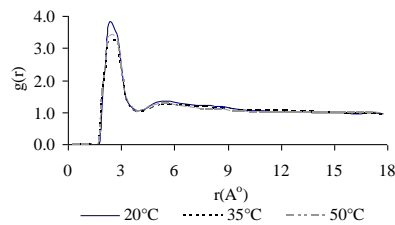
Overview of MD Simulation Findings

The crystal polymorph in 2,6-DHB is due to the particular H-bond of

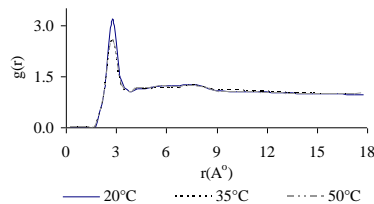
- FI - O₂₁---H₄, O₂₁---H₅, O₂₄---H₆

FI – O₂₁---H₄

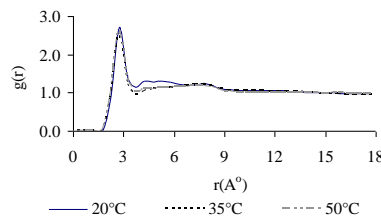
Chloroform Solution



O₂₁---H₄



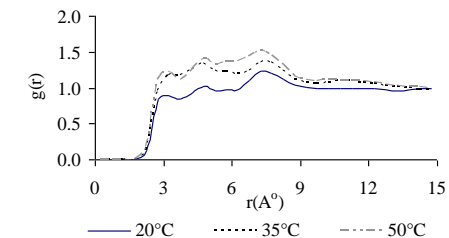
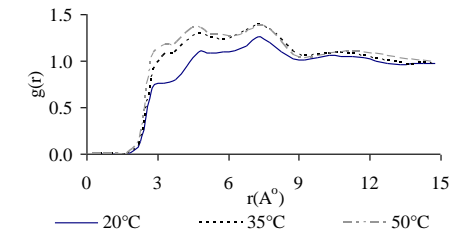
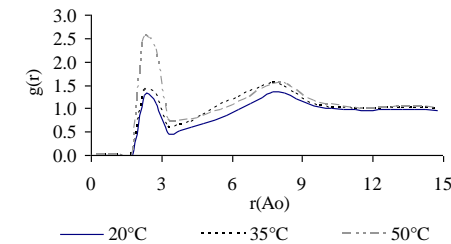
O₂₁---H₅



O₂₄---H₆

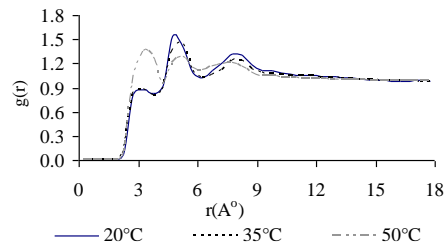
Strong H-bond interaction for O₂₁---H₄, O₂₁---H₅ & O₂₁---H₆ & more probable upon cooling

Toluene Solution

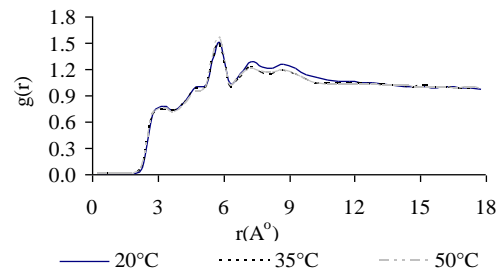


Contrary, strong H-bonds for O₂₁---H₄ but a weak H-bond interaction for O₂₁---H₅ & O₂₁---H₆ but become less probable upon cooling.

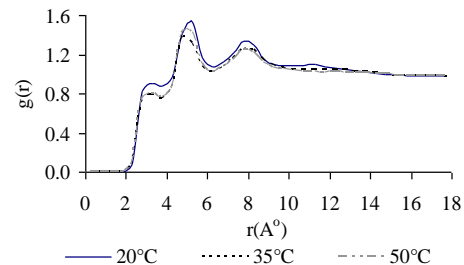
Overview of MD Simulation Findings



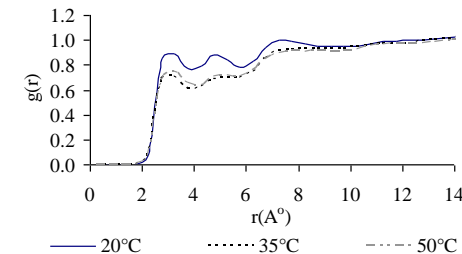
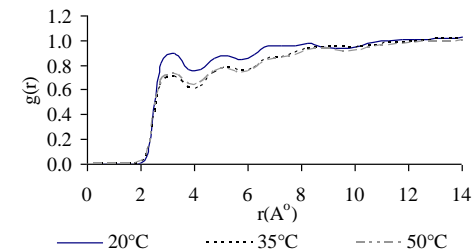
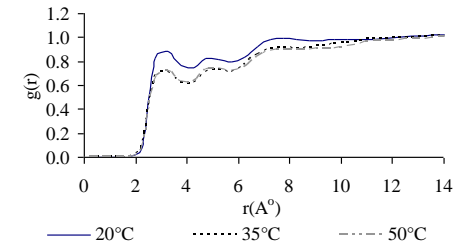
$\text{O}_{21}\cdots\text{H}_1$



$\text{O}_{21}\cdots\text{H}_2$



$\text{O}_{21}\cdots\text{H}_3$



Weak interaction is found for $\text{O}_{21}\cdots\text{H}_1$, $\text{O}_{21}\cdots\text{H}_2$, & $\text{O}_{21}\cdots\text{H}_3$ which reflects to the preserve of infinite H-bond chains

$\text{O}_{21}\cdots\text{H}_1$, $\text{O}_{21}\cdots\text{H}_2$ & $\text{O}_{21}\cdots\text{H}_3$ intermolecular interaction has stronger interaction but less probable when the temperature decreases

Importance of the selection of Solvent in Chemical Processes

CASE STUDY 2

Molecular Recognition of Wax Inhibitor Through
Pour Point Depressant Type Inhibitor Solvent

Crude Oil Waxes

The major constituents of solid deposit in waxy crude oil are known as paraffin waxes

Mixture of long chain hydrocarbon C₁₈-C₆₅

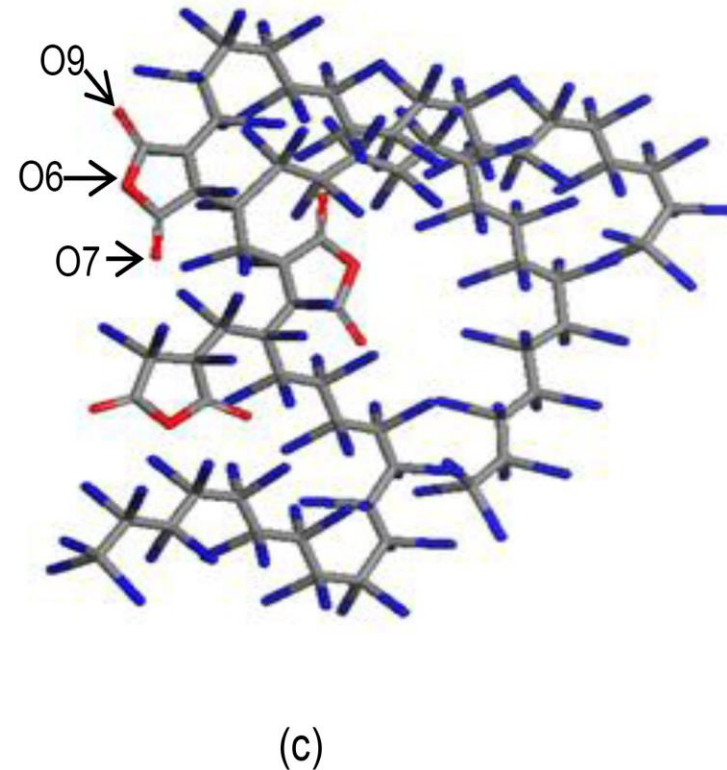
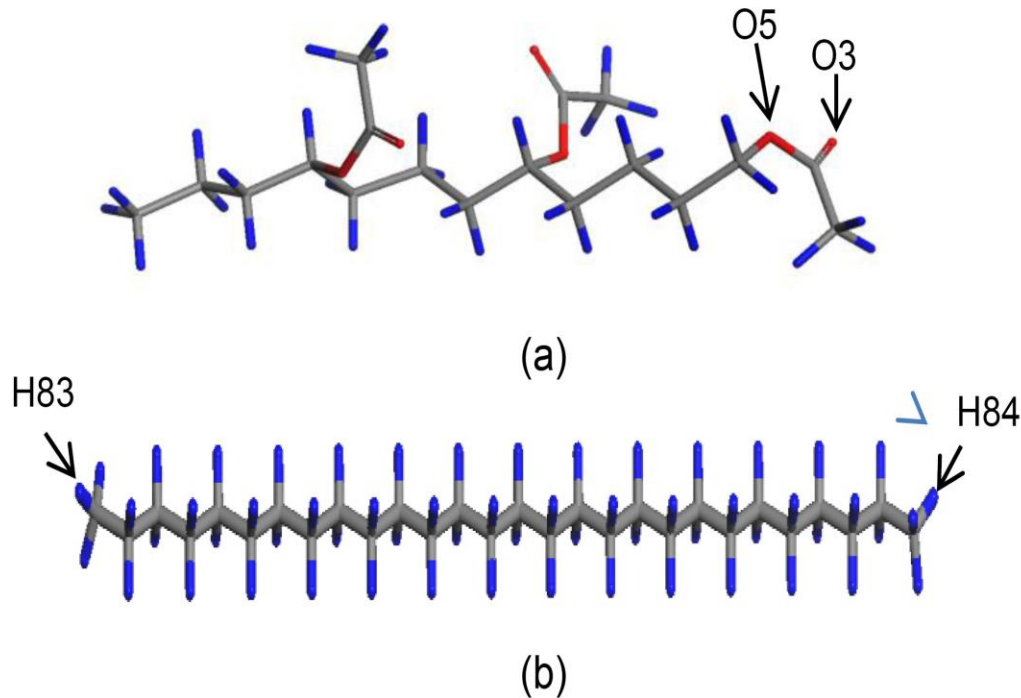
Crystal formation and solid deposition from waxy mixture in the pipeline

Chemical inhibitor is one of the methods to prevent and control the wax crystal formation

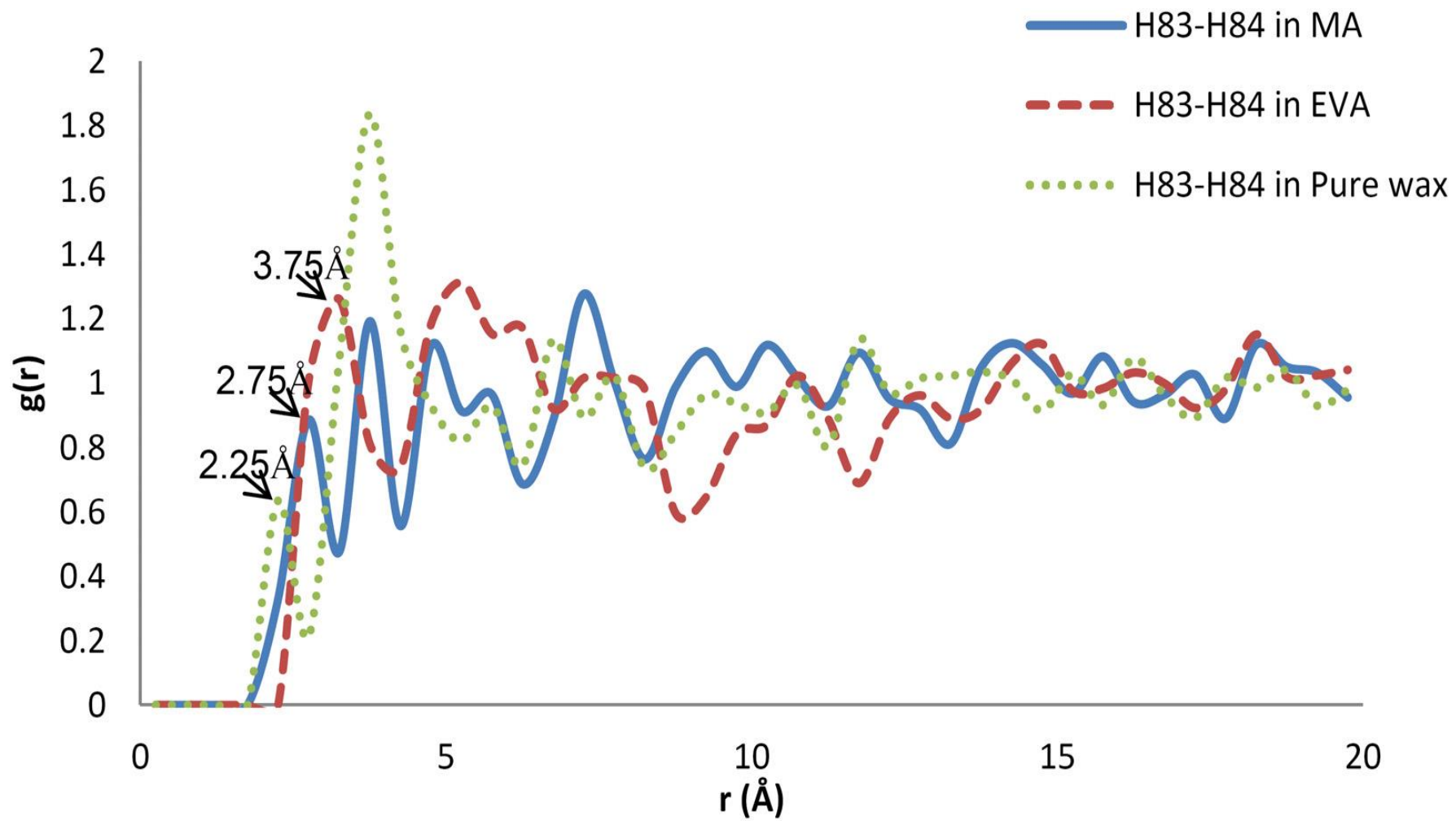


Crude Oil Wax

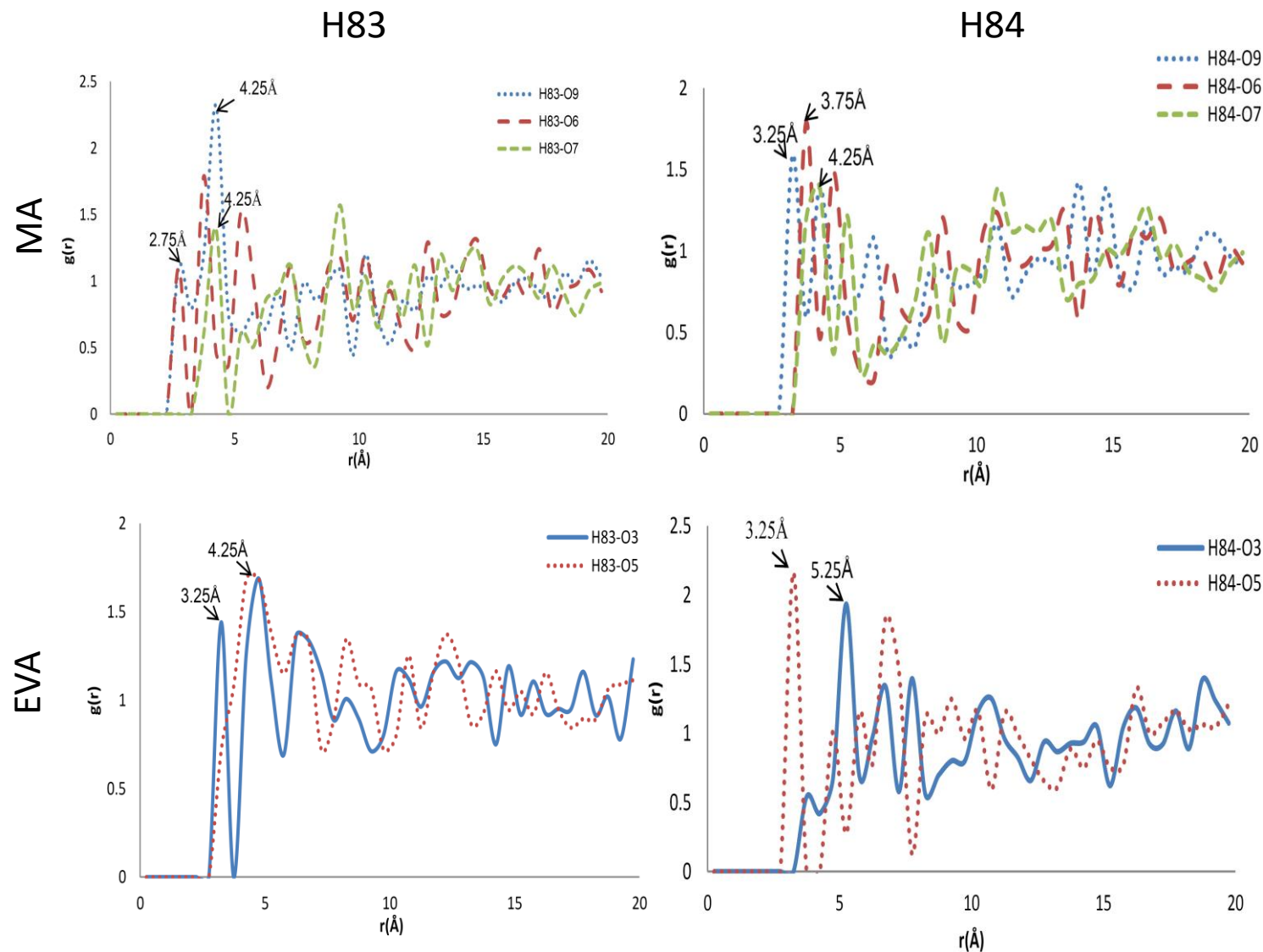
Objective: To investigate poly(ethylene-co-vinyl acetate(EVA)) and Poly(maleic anhydride-*alt*-1-octadecene)(MA) polymer inhibitors on the van der Waals intermolecular interaction between the major wax component molecule n-octacosane C₂₈H₅₈, via molecular dynamics simulation (MD).



The structure properties defining the active atom of (a)poly(ethylene-co-vinyl acetate(EVA)) (b)n-Octacosane (c) Poly(maleicanhydride-alt-1-octadecene)(MA)



Rdf pattern H83-H84 of n-octacosane in MA and EVA inhibitors



Chemical inhibitor	Weight of wax deposited from crude (g)	Paraffin Inhibitor Efficiency (PIE) (wt. %)
Blank	1.3	-
Poly(maleic anhydride- <i>α</i> /t-1-octadecene) (MA)	1.2	7.5
Poly (ethylene vinyl acetate) (EVA)	1.0	23.1

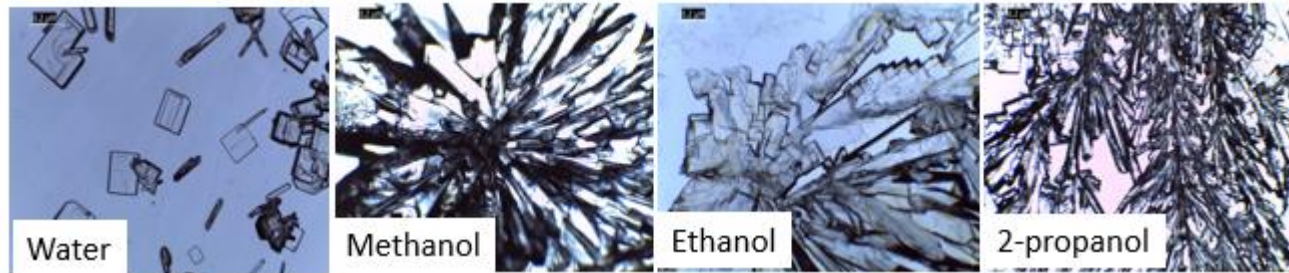
Experimental result for wax deposition study

Study Findings

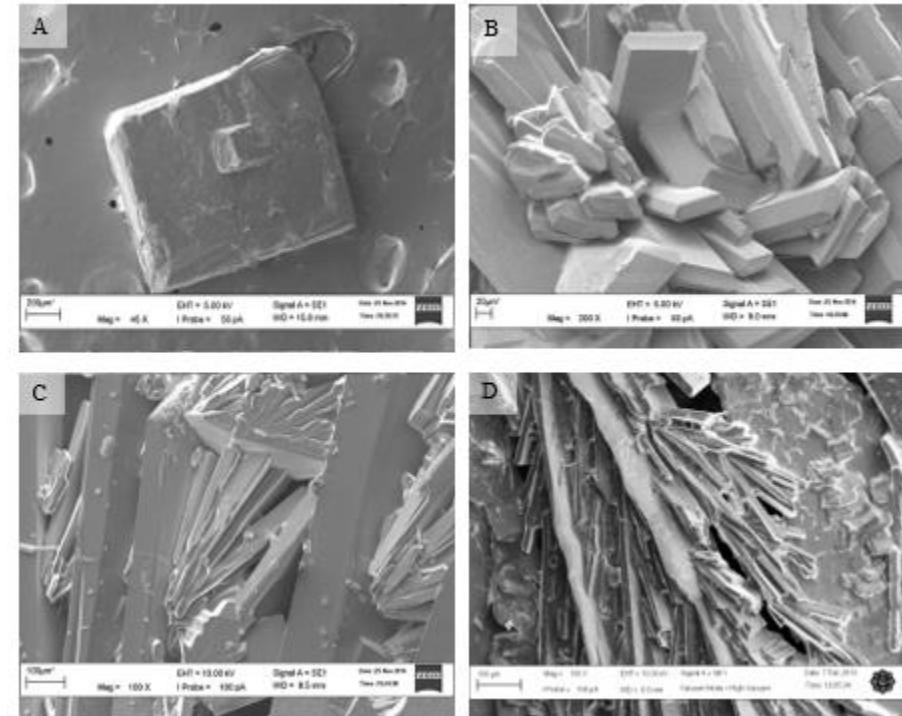
The present of **carbonyl oxygen in EVA** play a significant role to **inhibit the wax formation** through the van der Waals interaction between active hydrogen atoms in **n-Octacosane** molecule. Therefore the chances of wax inhibition in octacosane is less by introduce EVA as inhibitor compare to MA.

Importance of the selection of Solvent in Crystallisation Process of Ascorbic Acid (Vit C)

Crystal Characterization Morphology



- Reduce in **polarity**, reduce in **size**
- Shape from **cubic/prism** become more **elongated like needle shape**

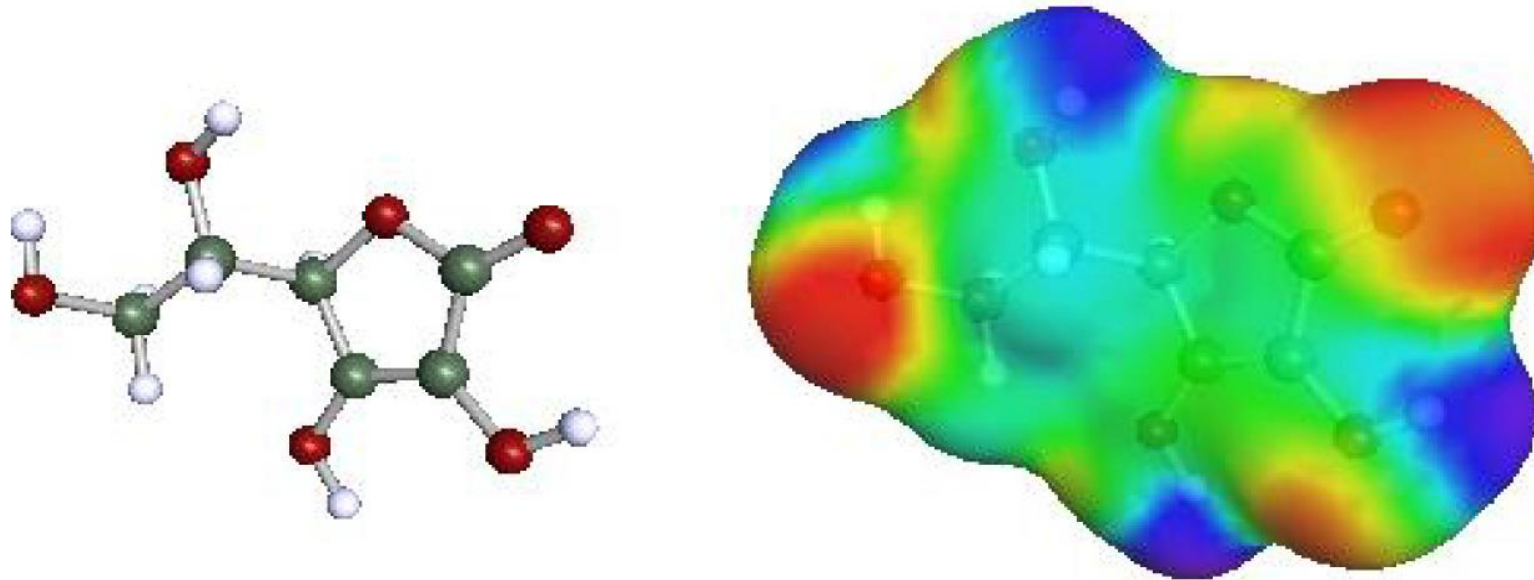


Evaluation of solvents' effect on solubility, intermolecular interaction energies and habit of ascorbic acid crystals

S. Hassan, F. Adam, M.R. Abu Bakar, S.K. Abdul Mudalip, Journal of Saudi Chemical Society, 2019

Objective: To evaluation solvents' effect on solubility, intermolecular interaction energies and habit of ascorbic acid crystals

Method: COSMO RS and experimental.



L-ascorbic acid molecular structure; and COSMO sigma profile image

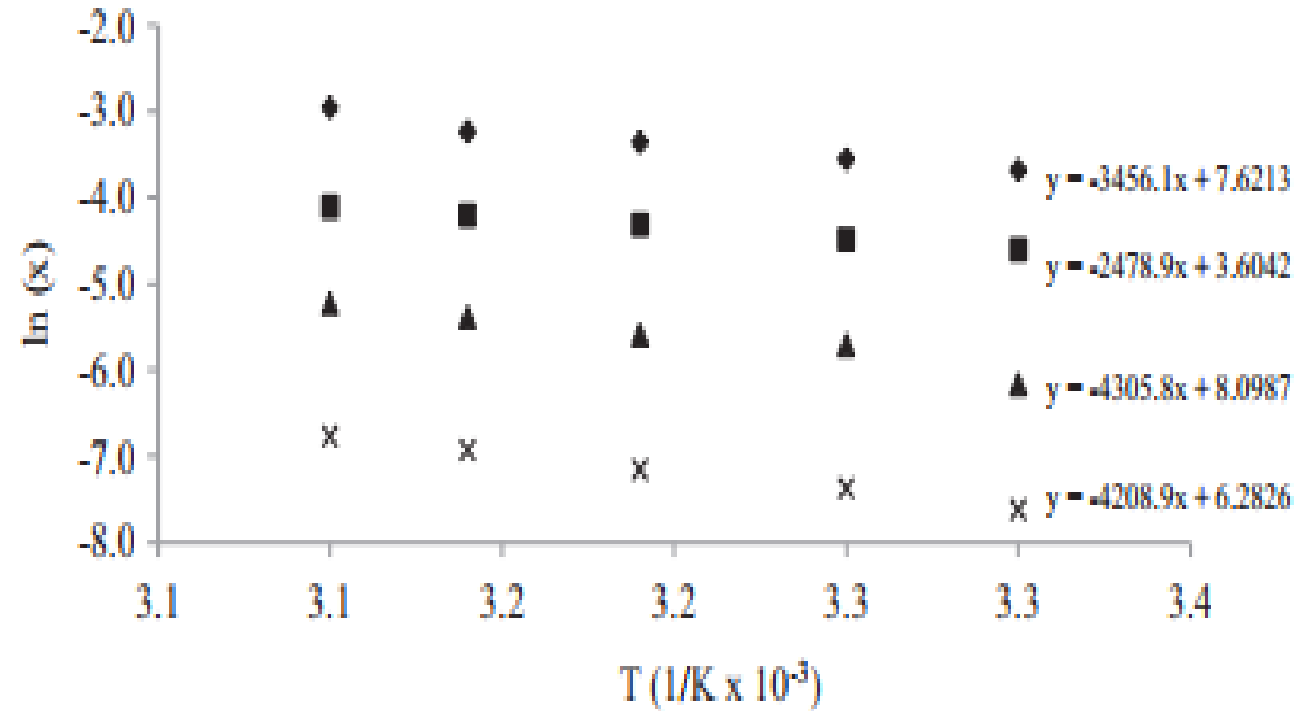
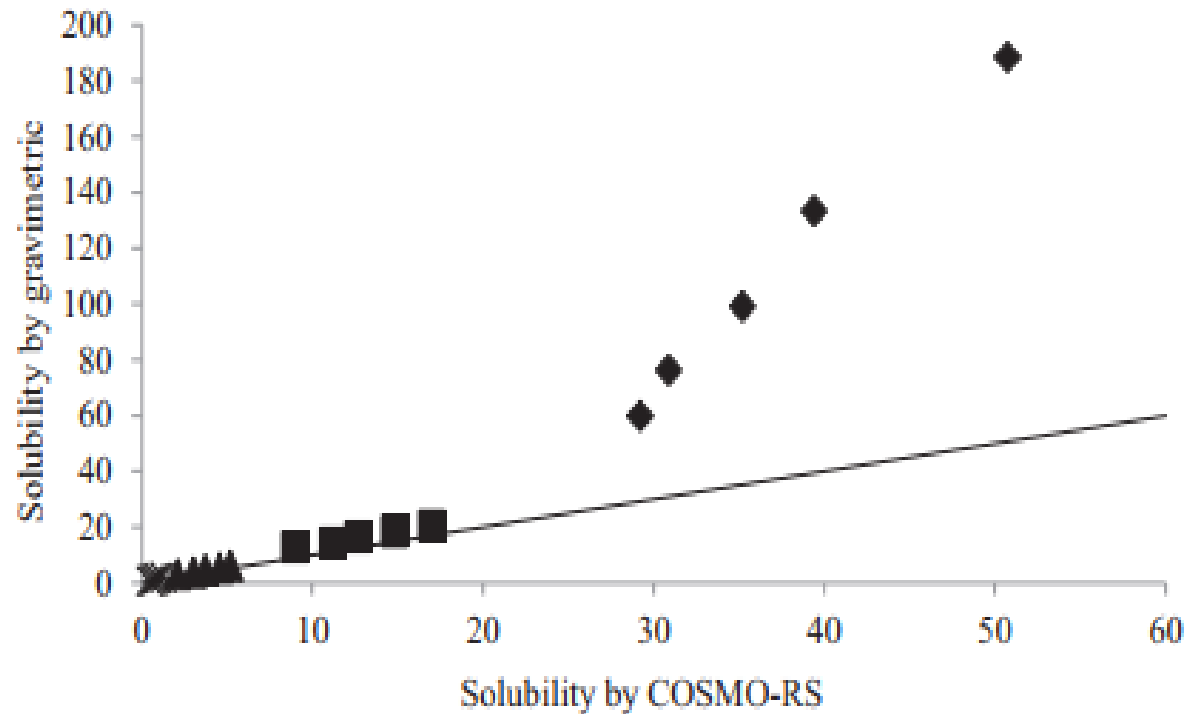
Evaluation of solvents' effect on solubility, intermolecular interaction energies and habit of ascorbic acid crystals

Solvent	T (K)	$10^3 x_{\text{exp}}$	$10^3 x_{\text{COSMO}}$	Standard deviation for x_{exp}
Water	303	25.20	59.90	0.02
	308	28.70	76.40	0.03
	313	35.00	99.10	0.03
	318	39.40	133.50	0.03
	323	52.10	188.50	0.04
Methanol	303	10.10	13.00	0.04
	308	11.30	14.30	0.02
	313	13.50	16.50	0.05
	318	14.90	18.50	0.05
	323	16.50	20.40	0.07
Ethanol	303	2.10	3.20	0.04
	308	3.30	3.90	0.05
	313	3.70	4.70	0.04
	318	4.60	5.50	0.07
	323	5.40	6.10	0.06
2-Propanol	303	0.50	0.80	0.08
	308	0.60	1.00	0.07
	313	0.80	1.20	0.08
	318	1.00	1.70	0.10
	323	1.20	2.10	0.09

Saturated mole fraction solubility x of ascorbic acid in different organic solvents at experimental pressure (0.1 MPa) and temperatures T from (303 to 323) K

Evaluation of solvents' effect on solubility, intermolecular interaction energies and habit of ascorbic acid crystals

S. Hassan, F. Adam, M.R. Abu Bakar, S.K. Abdul Mudalip, Journal of Saudi Chemical Society, 2019



van't Hoff plot of ascorbic acid in water (◆), methanol (■), ethanol (▲) and 2-propanol (×).

Material Studio

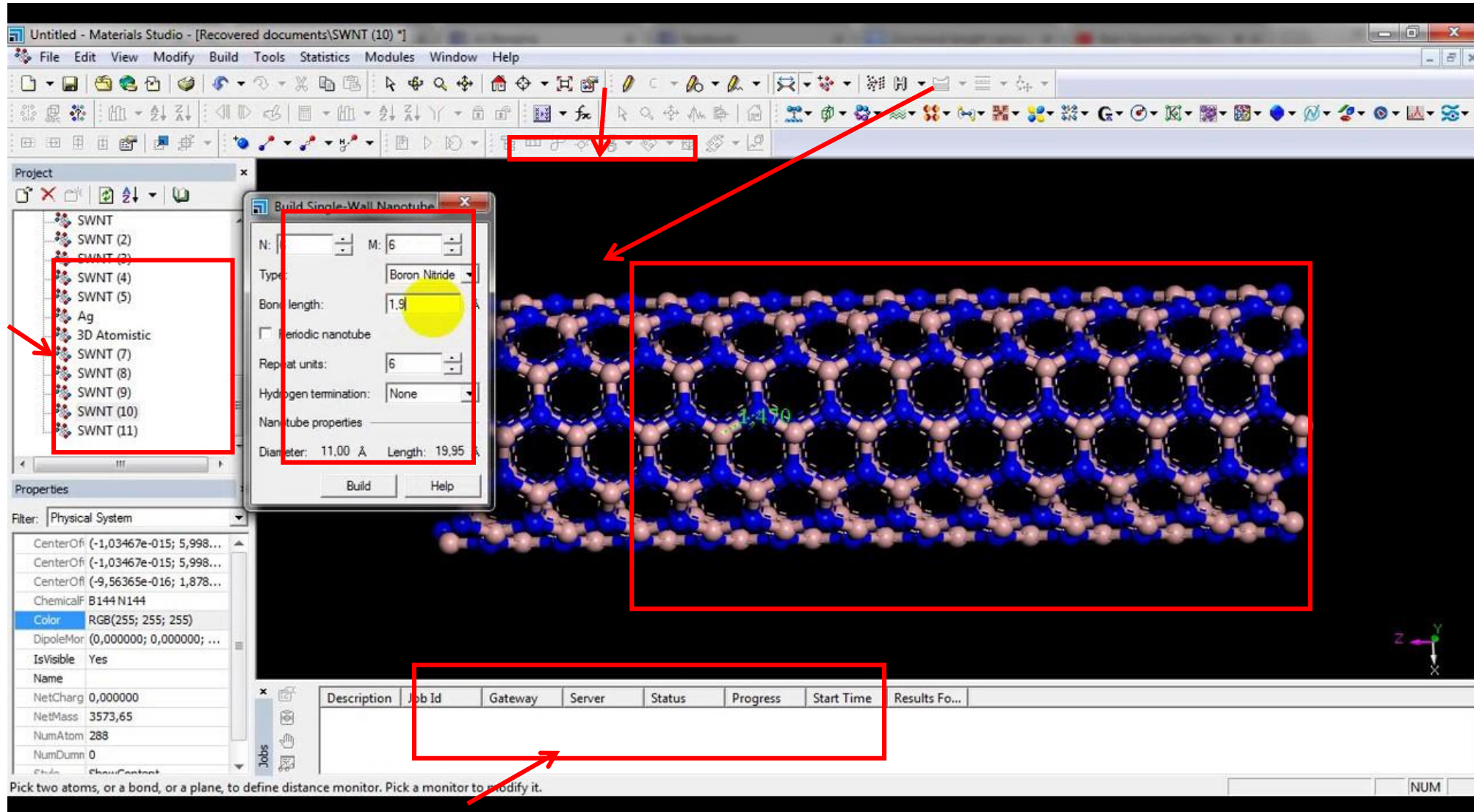
Material Studio User Interface

Simulation Work & Setting
Dialog Box

Cursor control

Simulation
Library

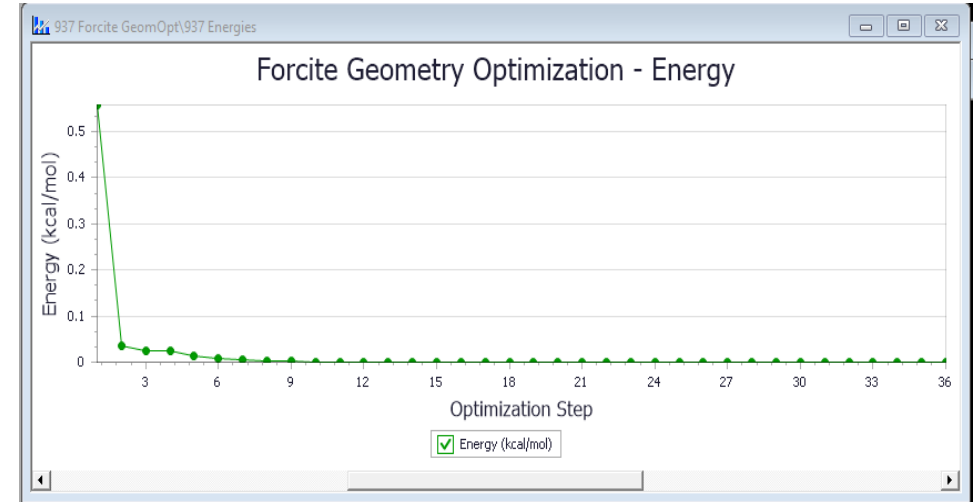
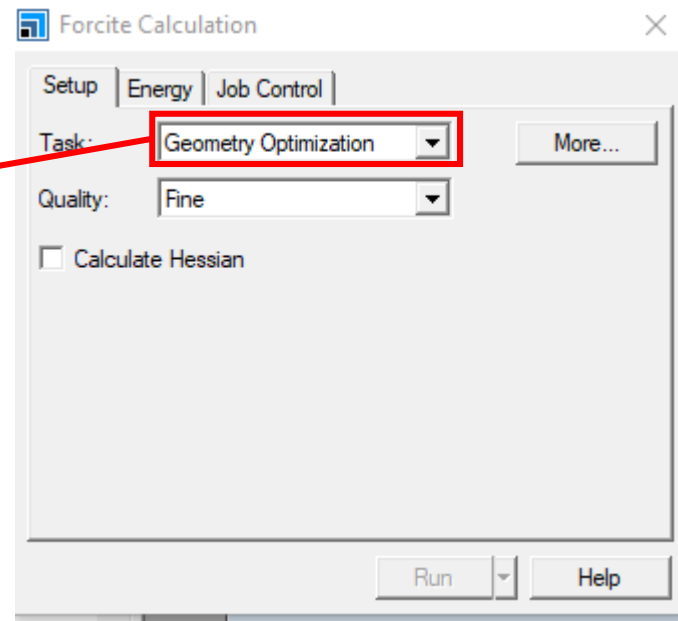
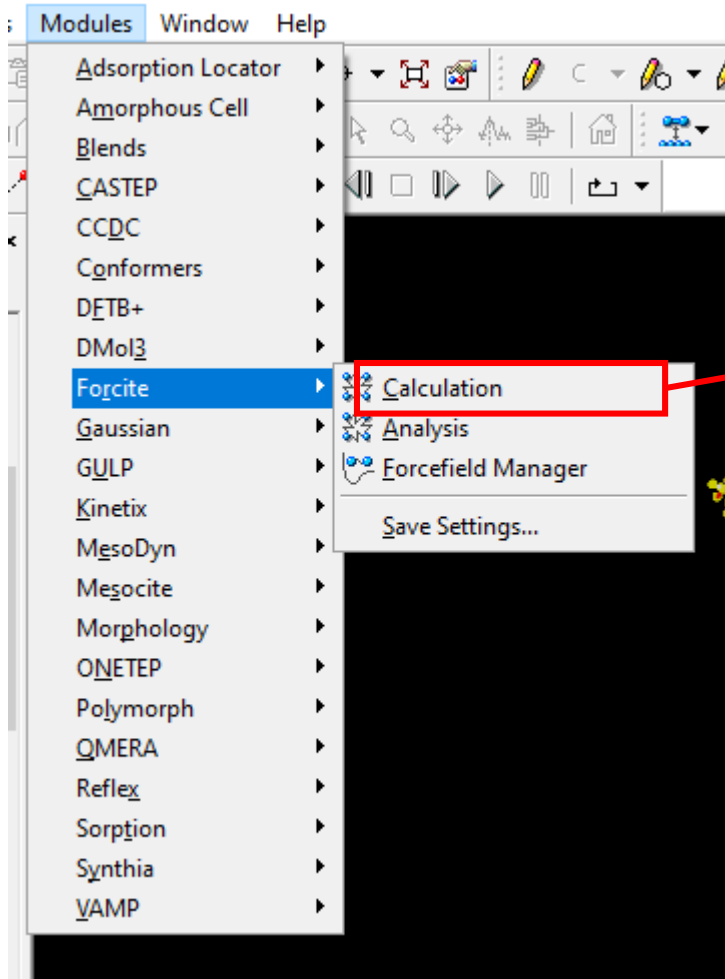
Simulation
Display



Job Description and Status

Geometry Optimization

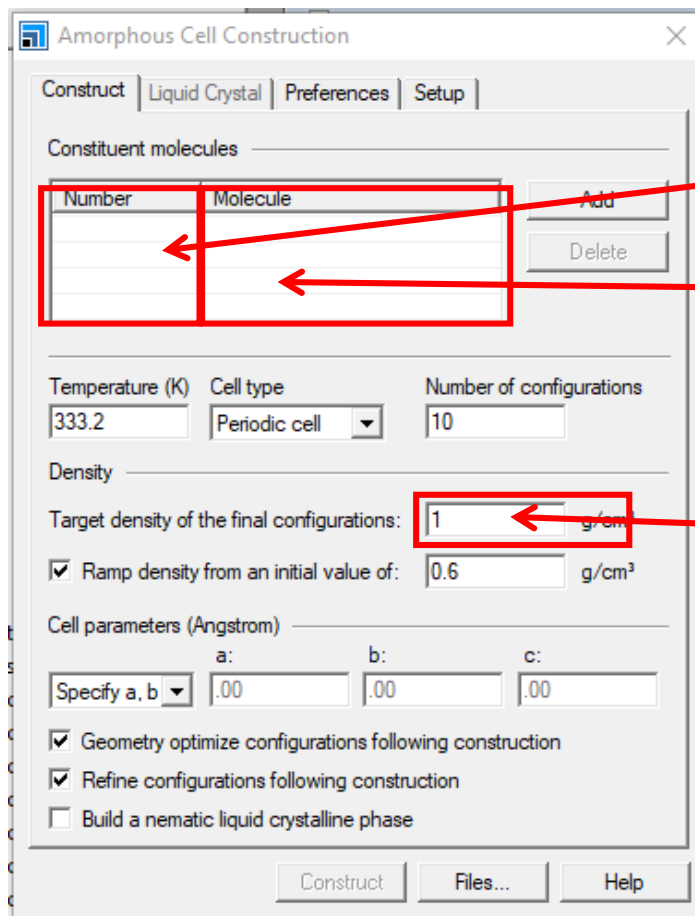
To optimised the energy of the molecular structure



Energy optimisation graph

Amorphous Cell Construction (Simulation Box)

Module > Amorphous Cell > Construction



The screenshot shows the 'Amorphous Cell Construction' dialog box with the 'Construct' tab selected. It features a table for 'Constituent molecules' with columns for 'Number' and 'Molecule'. Below the table are fields for 'Temperature (K)' (333.2), 'Cell type' (Periodic cell), and 'Number of configurations' (10). The 'Density' section includes a 'Target density of the final configurations' field (1 g/cm³) and a checkbox for 'Ramp density from an initial value of: 0.6 g/cm³'. The 'Cell parameters (Angstrom)' section has a dropdown for 'Specify a, b' and input fields for 'a:', 'b:', and 'c:' (all .00). At the bottom are checkboxes for 'Geometry optimize configurations following construction', 'Refine configurations following construction', and 'Build a nematic liquid crystalline phase'. Buttons for 'Construct', 'Files...', and 'Help' are at the bottom.

Number	Molecule

Temperature (K): 333.2 Cell type: Periodic cell Number of configurations: 10

Density: Target density of the final configurations: 1 g/cm³

☒ Ramp density from an initial value of: 0.6 g/cm³

Cell parameters (Angstrom): Specify a, b: a: .00 b: .00 c: .00

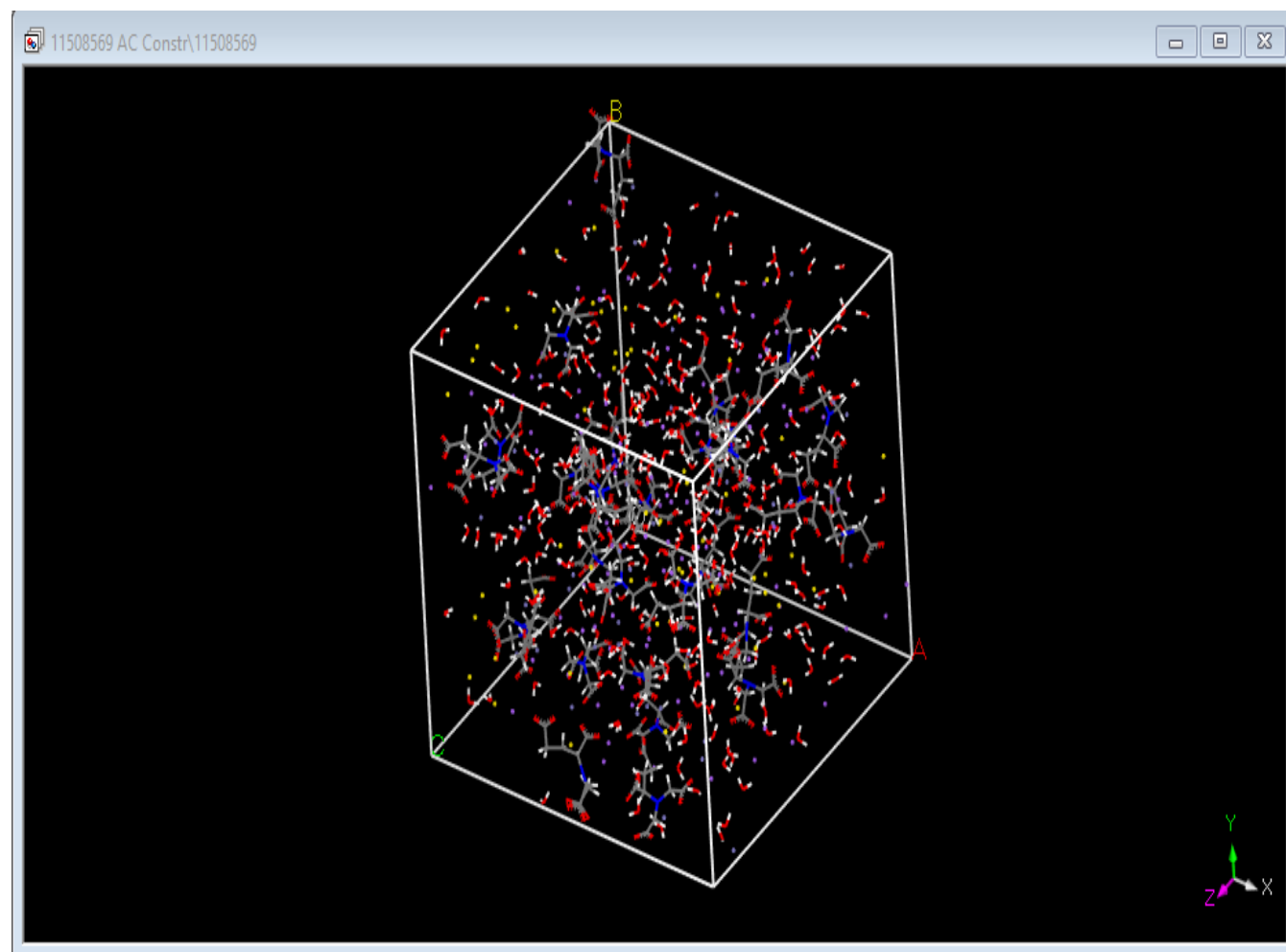
☒ Geometry optimize configurations following construction
☒ Refine configurations following construction
☐ Build a nematic liquid crystalline phase

Construct Files... Help

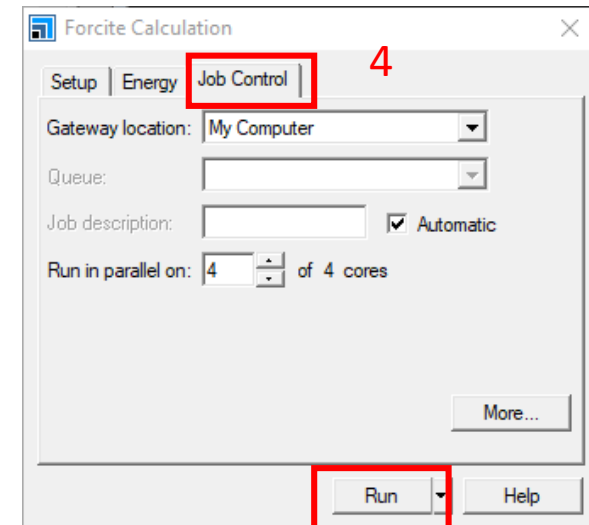
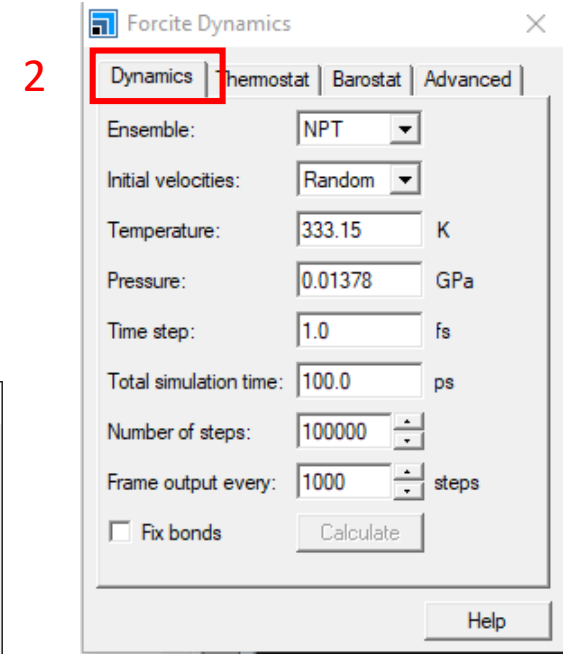
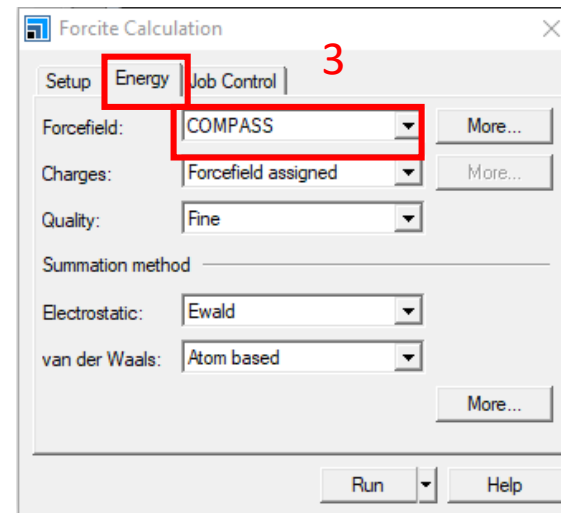
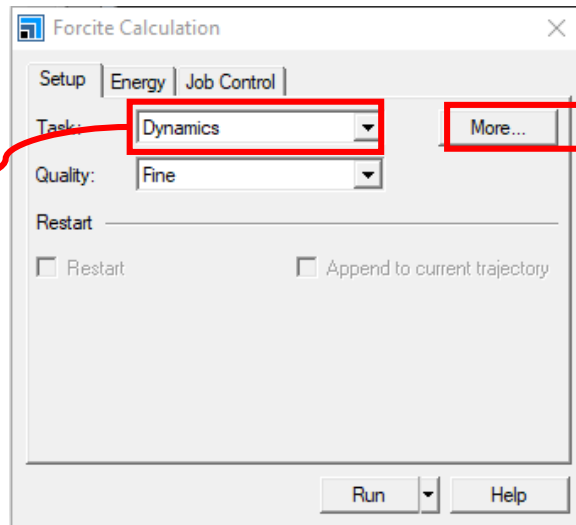
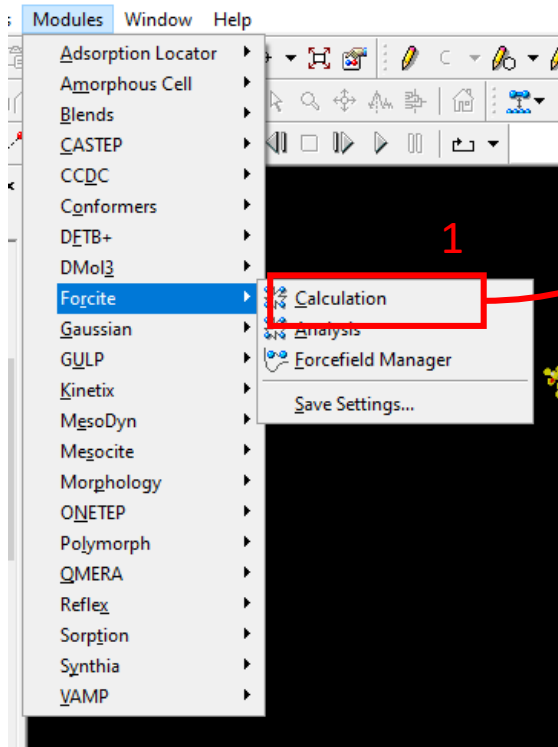
Number of
molecules

Name
(code) of
molecules

Density



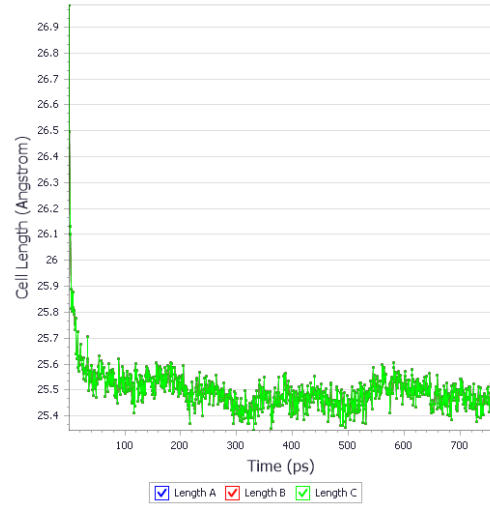
COMPASS Forcefield Calculation



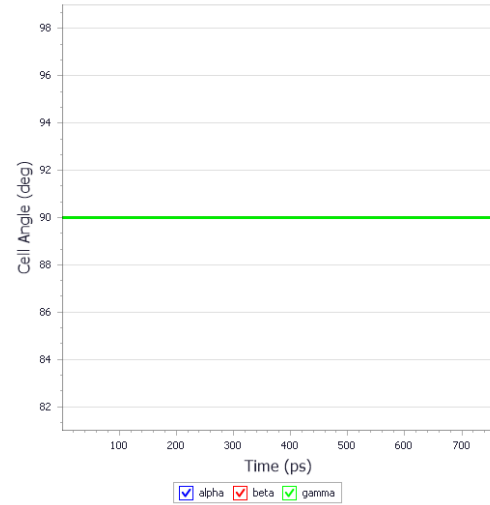
- 1) Modules > Forcite > Calculation > Dynamic (Quality Fine)
- 2) In Dynamics, Click more > Dynamics :Set NPT, NVE, and other setting.
- 3) Select Energy in Forcite Calculation, Select COMPASS, Forcefield Assigned, Fine quality
- 4) Select Job Control, Set Gateway to My Computer, and parallel run for CPU core and click run.

Graph and Data generated during simulation

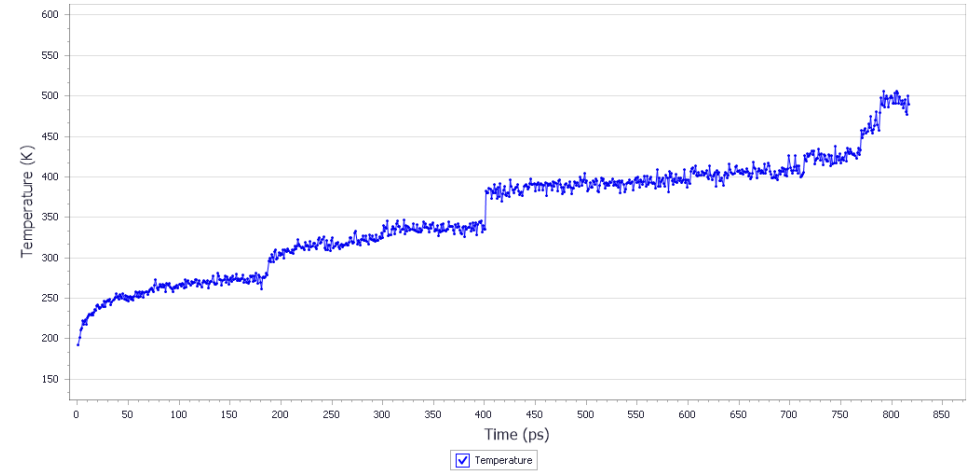
Forcite Dynamics Cell Lengths



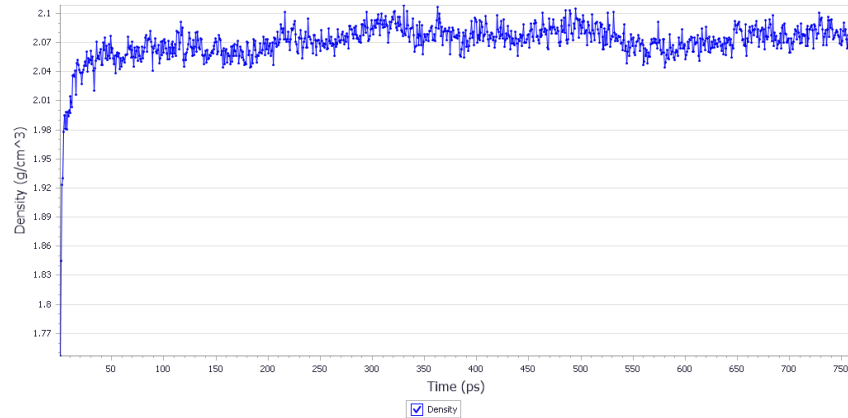
Forcite Dynamics - Cell Angles



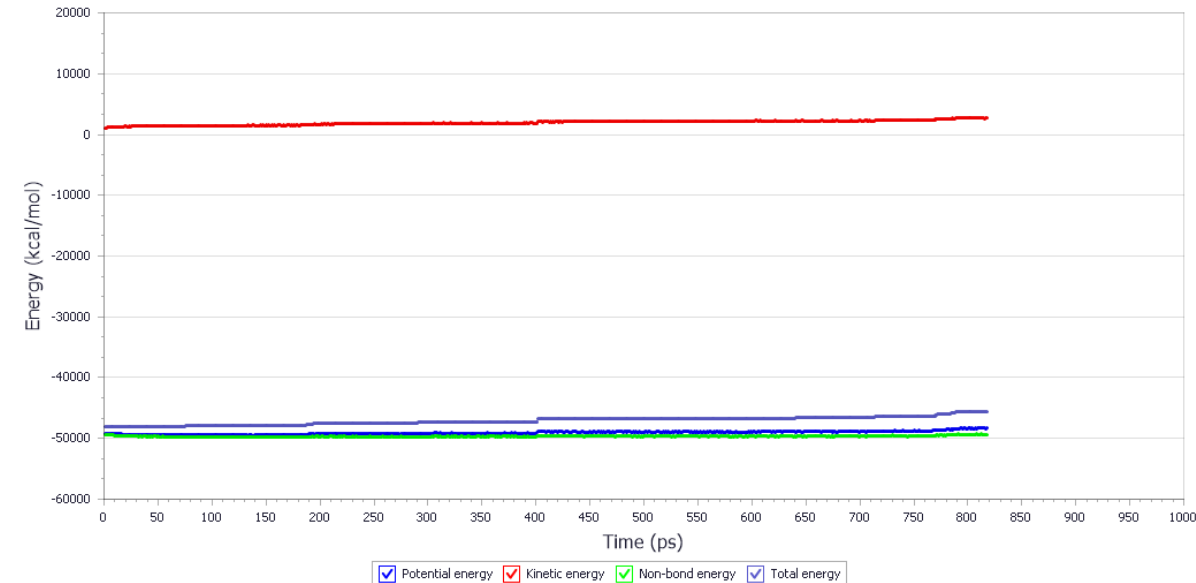
Forcite Dynamics - Temperature



Forcite Dynamics Density

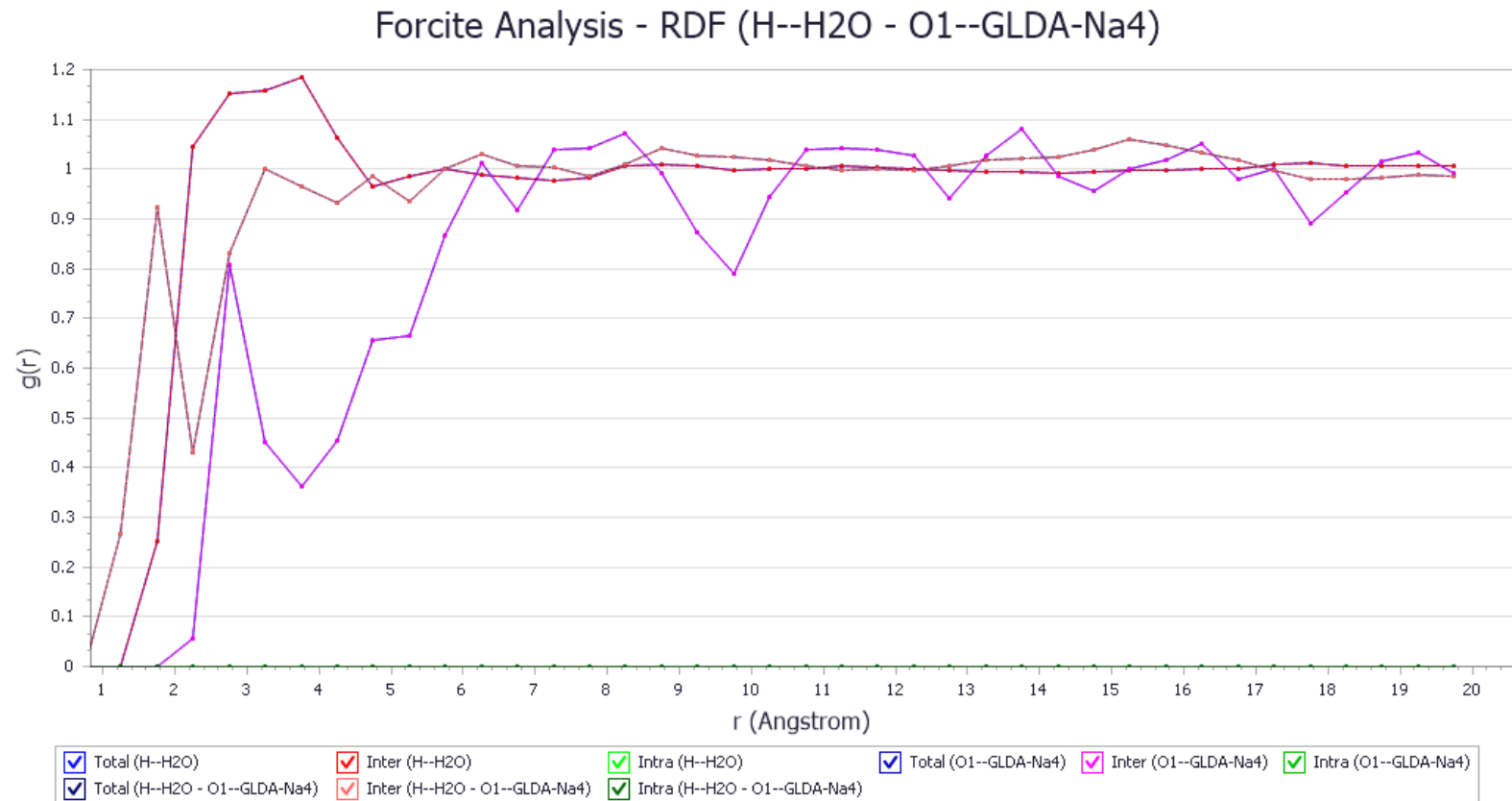
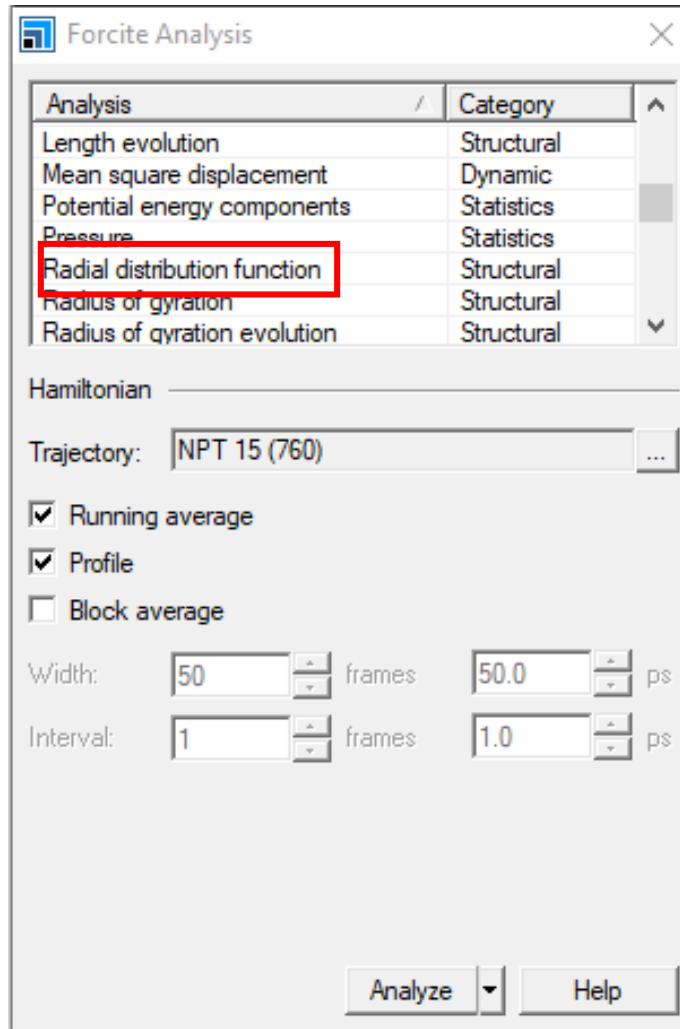



Forcite Dynamics - Energies



RDF Analysis

Modules > Forcite > Analysis



A rustic, handcrafted 'Thank you!' tag made of brown cardboard is the central focus. It features a small, irregular hole on the left side, through which a dark, thin string or twine is threaded. The tag is placed on a light-colored, textured wooden surface. Three white daisies with bright yellow centers are scattered around the tag: one is in the foreground to the right, and two are in the background, slightly out of focus. The overall aesthetic is warm, natural, and handmade.

Thank
you!

Molecular Dynamic Simulation of the Patchouli Oil Extraction Process : Chemical Solvents Interaction Role



اونيورسيتي ملايسيا قهغ
UNIVERSITI MALAYSIA PAHANG



Associate Professor Dr Fatmawati binti Adam
Faculty of Chemical & Process Engineering Technology

Patchouli

- Patchouli or Pogostemon cablin
- The name 'patchouli' also originated in India
- had been used for many centuries in Asian countries such as Indonesia, Malaysia
- The extracted essential oil is used for fragrance application. characteristic woody scent and is used commercially as an ingredient in fragrance and cosmetic products.
- The active chemical compound in the essential oil is patchoulol alcohol ($C_{15}H_{26}O$)

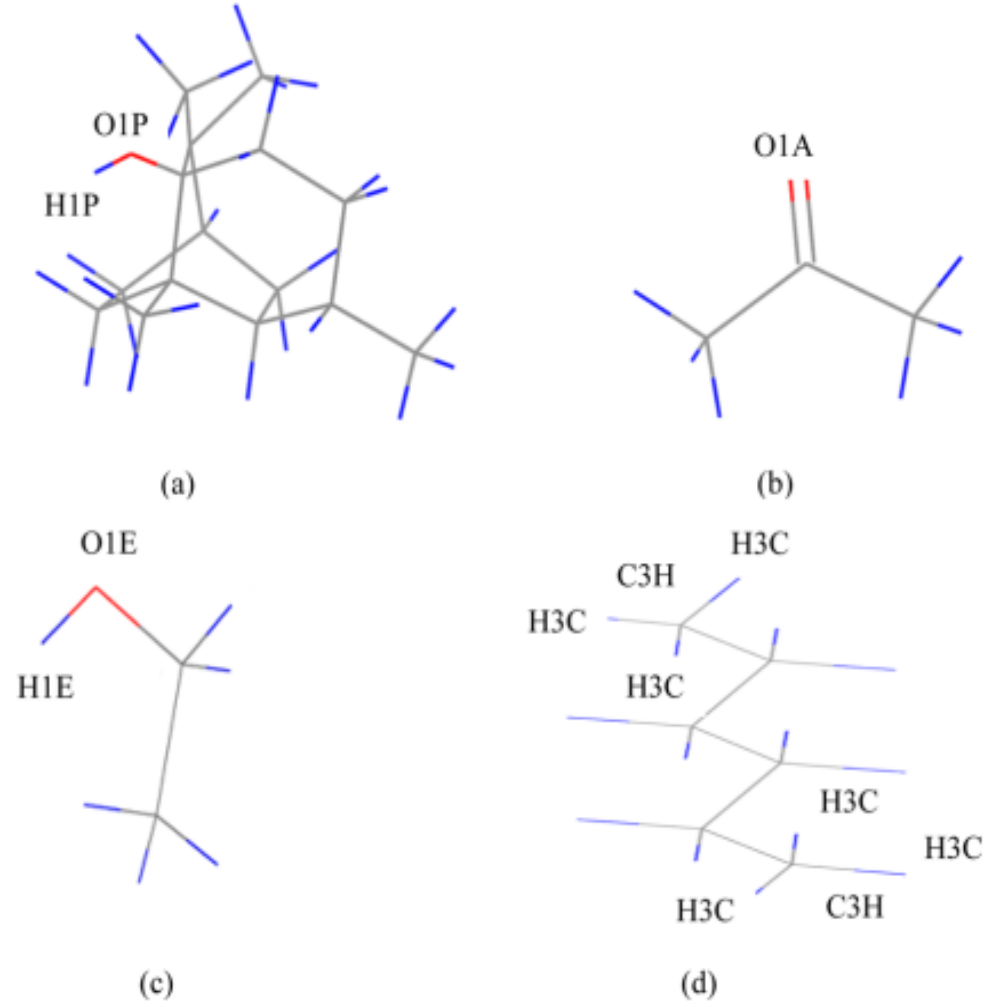


Molecular Dynamic Simulation of the Patchouli Oil Extraction Process

Method: Material Studio, COMPASS Forcefield.

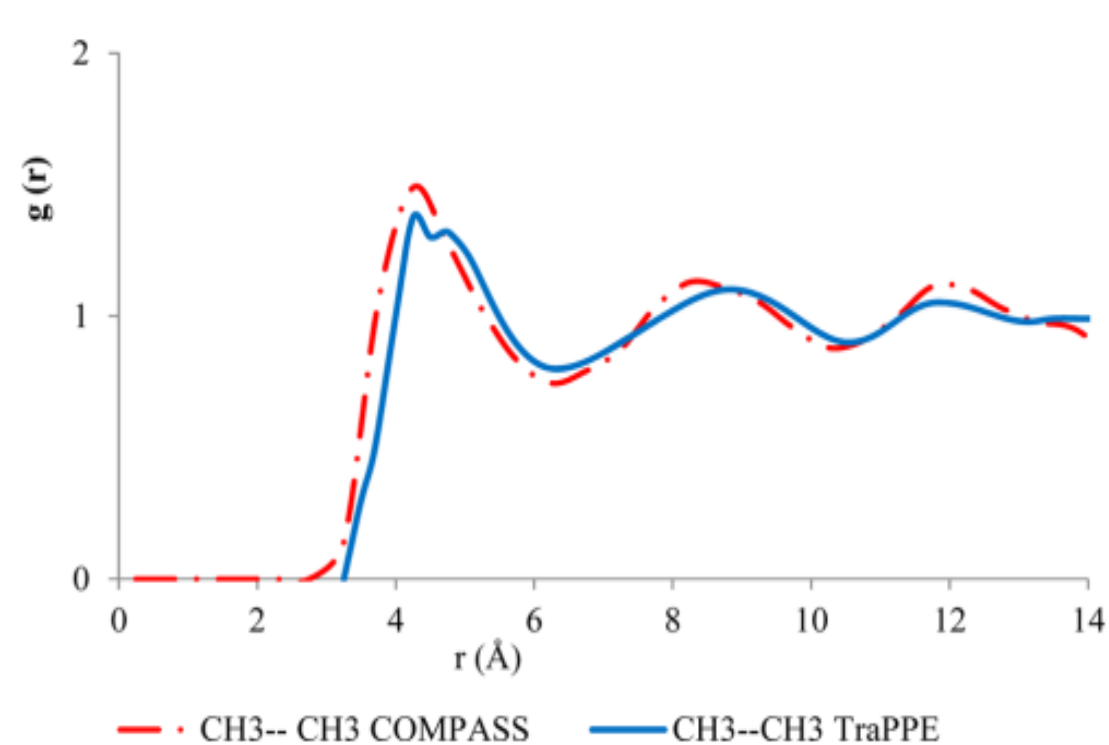
Objective:

To simulate the patchouli oil extraction process using patchoulol as a modeled molecule in different solvents, namely acetone, ethanol, and hexane.

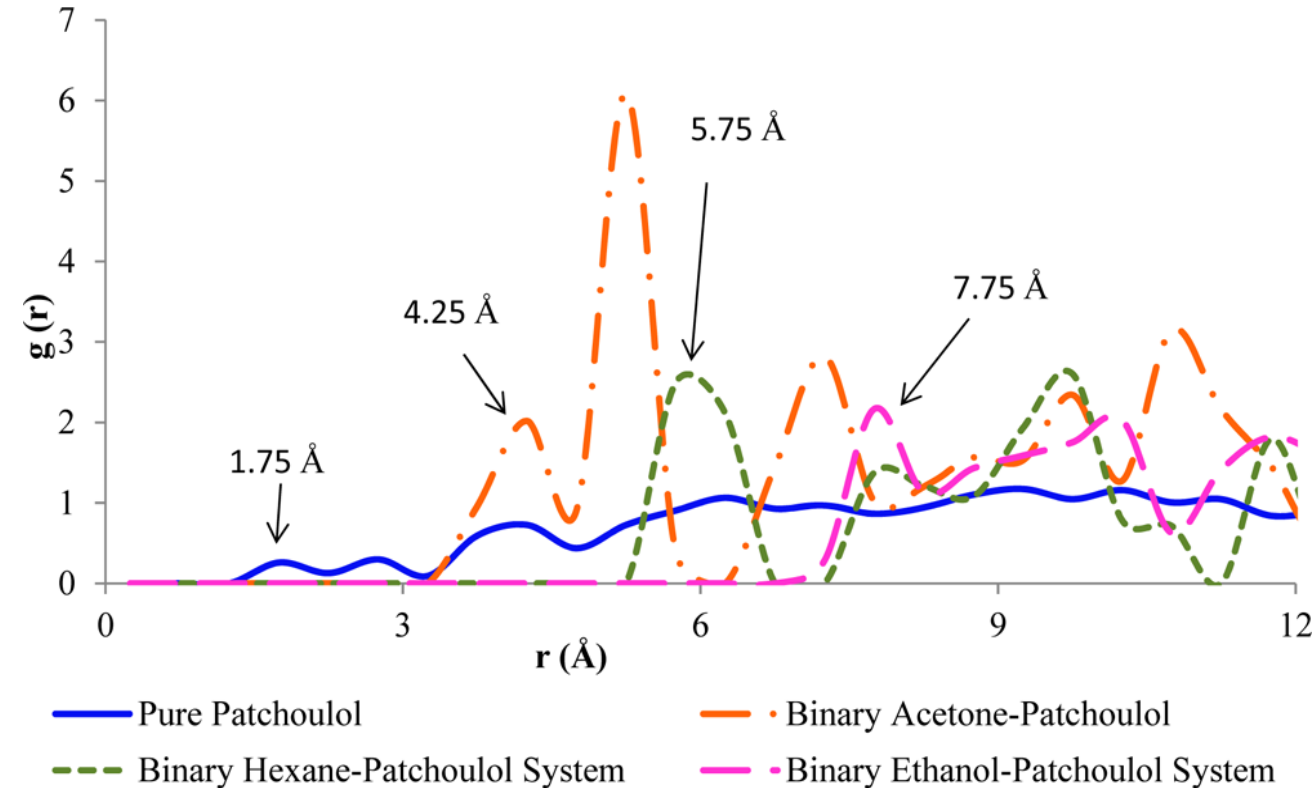


Schematic labeling of **patchoulol (a)**, **acetone (b)**, **ethanol (c)**, and **hexane (d)** molecular structure.

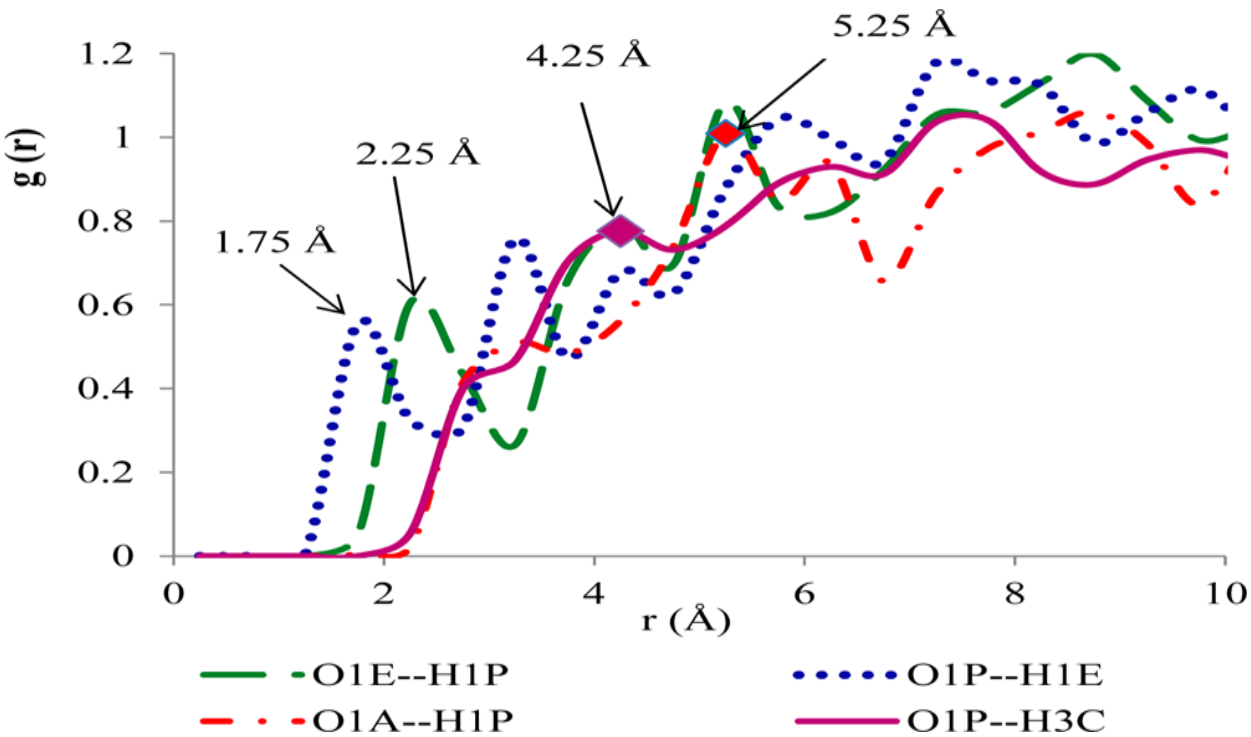
Molecular Dynamic Simulation of the Patchouli Oil Extraction Process



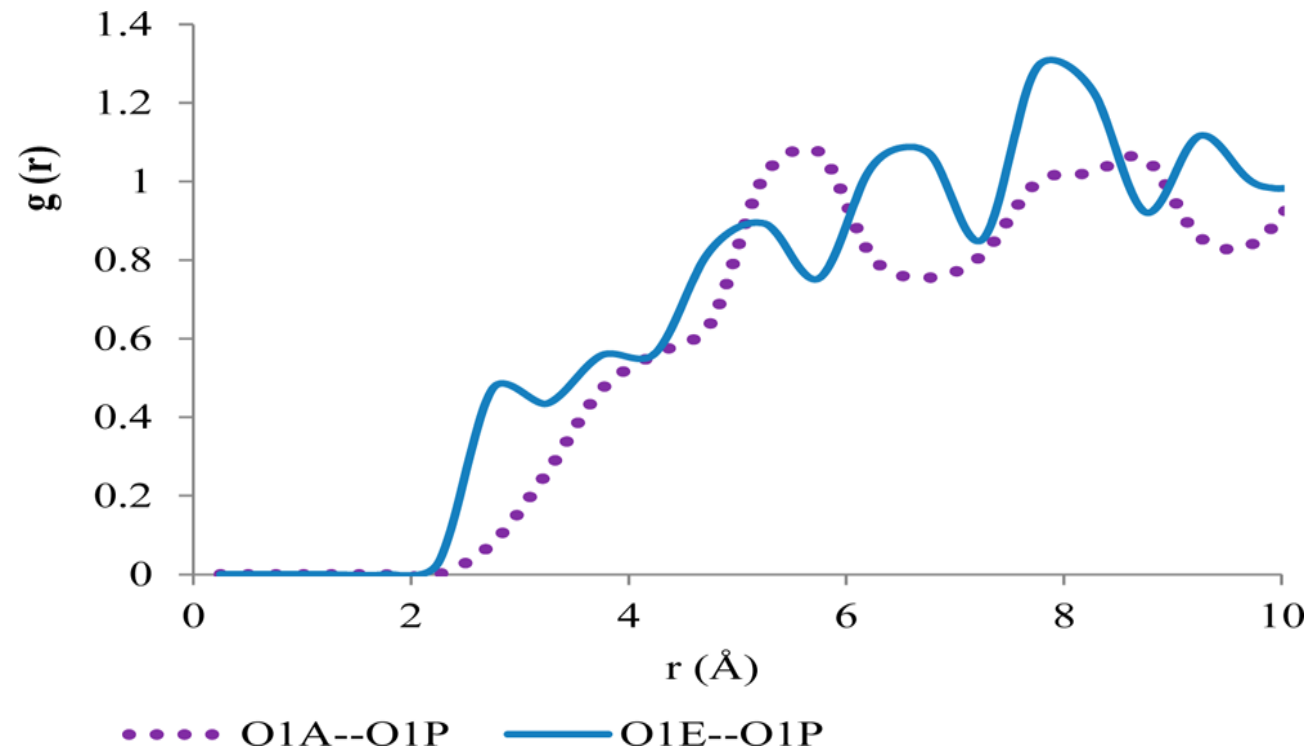
Comparison COMPASS/TraPPE
for CH3...CH3 interaction in pure
hexane liquid system



Solute-solute interaction in the
pure patchoulol system and
binary systems



The solvent-solute intermolecular interaction in a binary acetone-patchoulol, ethanol-patchoulol, and hexane-patchoulol system



The repulsion phenomena in a binary acetone-patchoulol system and ethanol-patchoulol system.

The Extraction Experiment Yield for Patchouli Oil Extracted Using the Solvent Extraction Method

solvent	average patchouli oil yield	average patchoulol identified by GC– MS
	wt/wt %	% area
acetone	8.34	58.04
ethanol	30.99	66.17
hexane	13.15	64.55

The pattern observed in the simulations is **in agreement with extraction yield results** obtained from the extraction experiment.

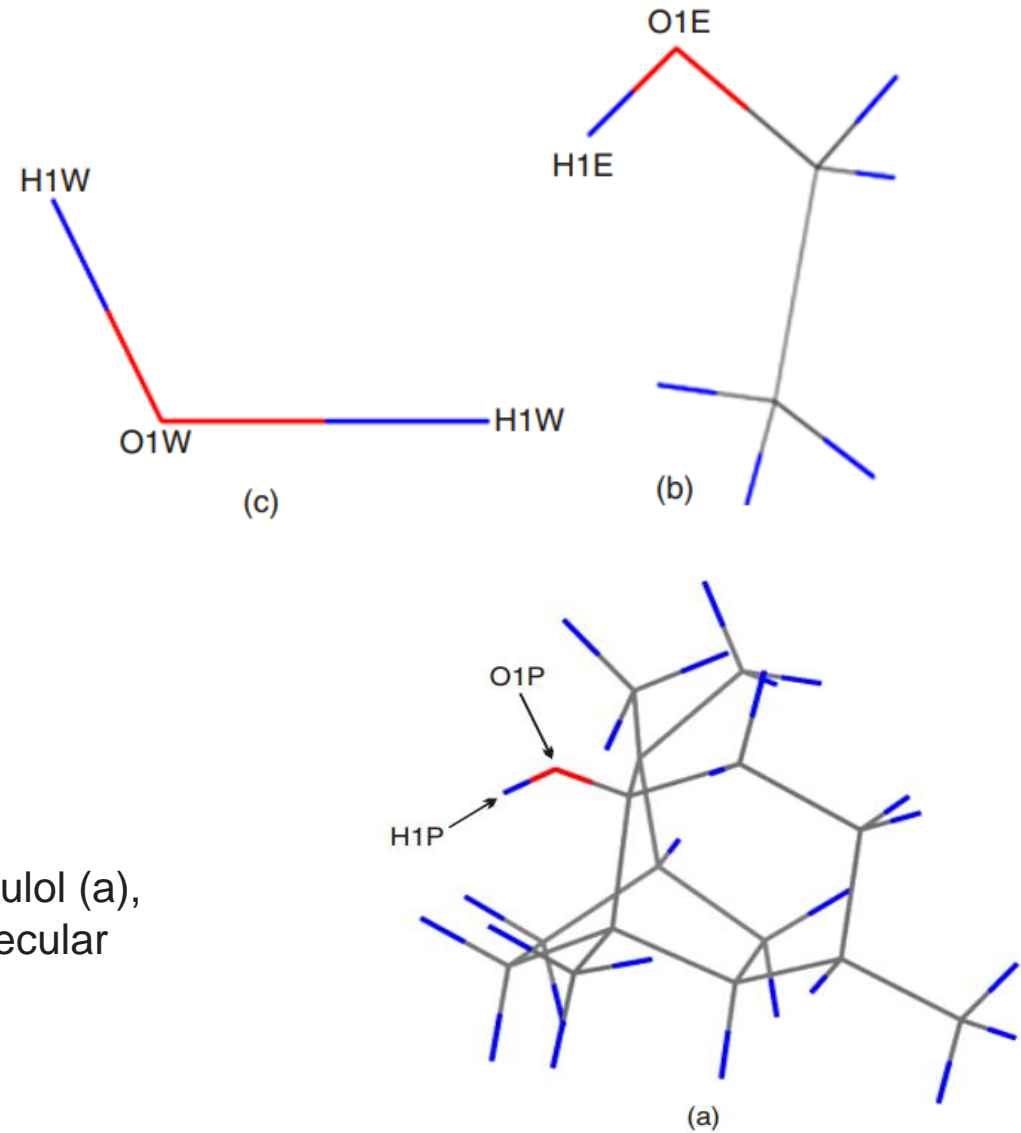
Study Summary

- The rdf trend found that the interaction between patchoulol solutes is through the oxygen atom (O1P) and hydrogen (H1P) atom from the hydroxyl functional group of the patchoulol molecule.
- In the acetone–patchoulol and hexane–patchoulol systems, the patchoulol solutes tend to self-agglomerate indicated by first neighboring molecules in the range of 4.25 Å and 5.75 Å, respectively
- The first neighboring molecules of patchoulol solutes in the binary ethanol–patchoulol system is located at 7.75 Å. This might suggest that the patchoulol is much more soluble in ethanol than in acetone and hexane.

Solvent Role in Molecular Recognition of Patchouli Extraction Process

Objective: **To simulate the patchouli oil extraction process using patchoulol as a modeled molecule in ethanol and water**

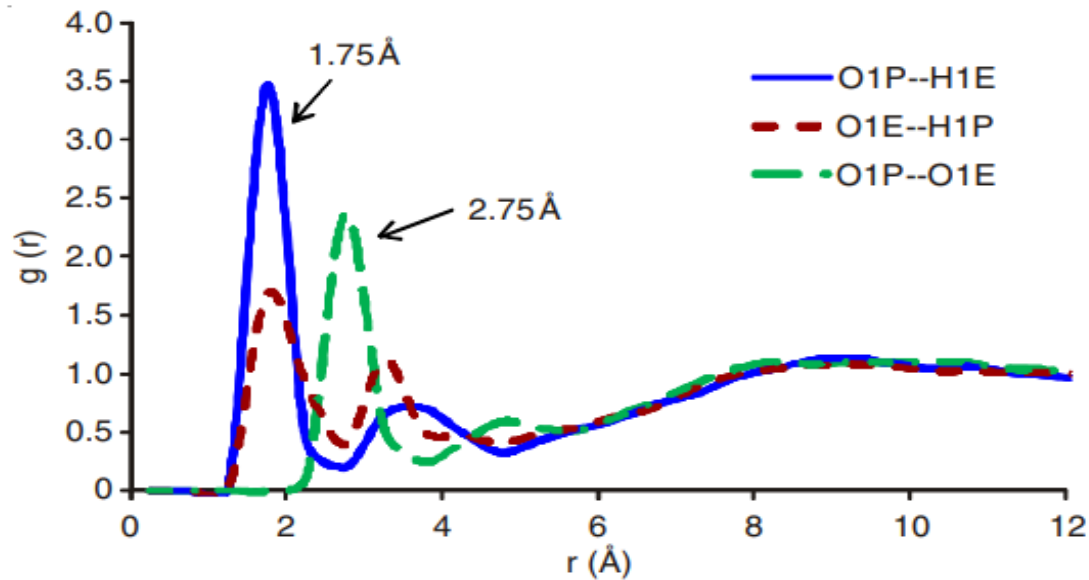
Schematic labelling of patchoulol (a), ethanol (b) and (c) water molecular structures



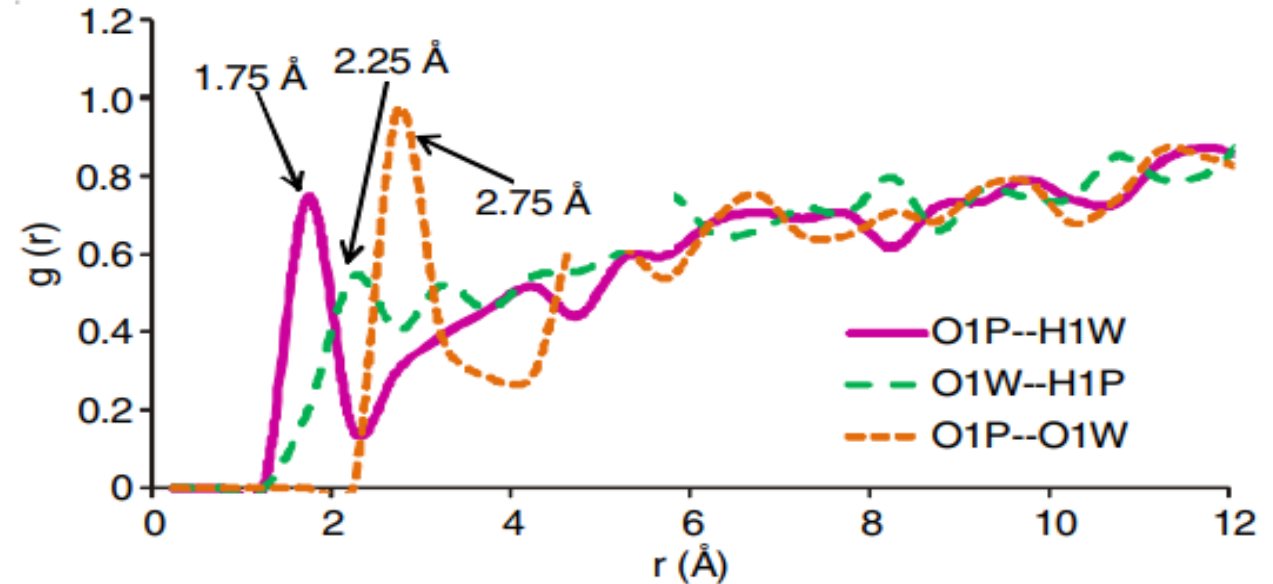
Methods

TABLE-1 LIST OF SIMULATED SYSTEMS APPLYING EWALD SUMMATION METHOD [Ref. 9]		
Systems	Number of molecules	Density (g/cm ³)
Pure system at 298 K		
Ethanol	1000	0.780
Water	1000	1.000
Patchoulol	50	1.001
Binary system at 298 K		
Ethanol:Patchoulol	1000:20	0.795
Water:Patchoulol	1000:20	1.000

Solvent Role in Molecular Recognition of Patchouli Extraction Process

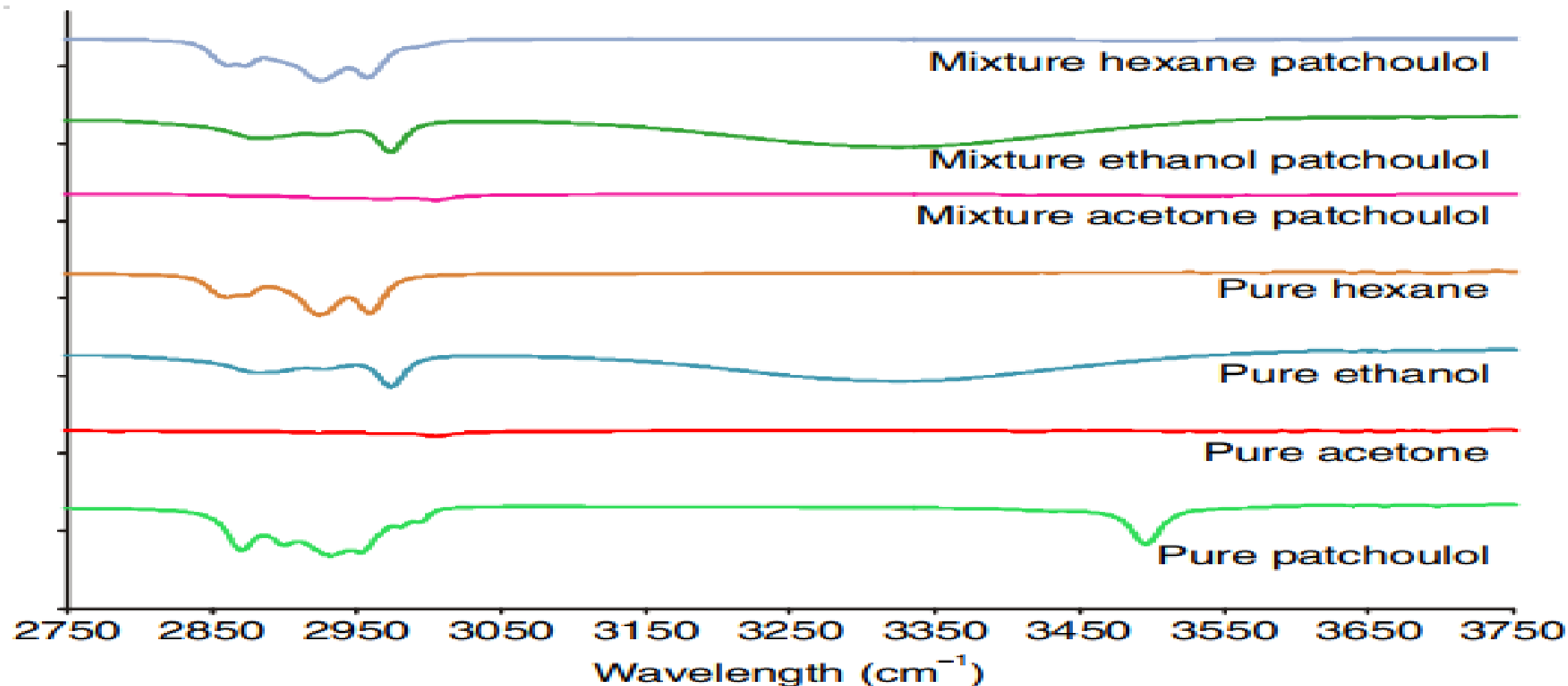


Solute-solvent interaction (binary ethanol patchoulol system) with oxygen and hydrogen atoms as reference atoms



Solute-solvent interaction in water (binary water-patchoulol system) with O and H atoms as reference atoms

Solvent Role in Molecular Recognition of Patchouli Extraction Process



Infrared spectroscopy of pure patchoulol, pure solvent and mixture of solvent and patchoulol with acetone, ethanol and hexane as the solvent

Solvent Role in Molecular Recognition of Patchouli Extraction Process

TABLE-2
CHEMICAL CONSTITUENTS OF PATCHOULI ESSENTIAL OIL EXTRACTED
USING ACETONE, ETHANOL AND HEXANE SOLVENTS

No.	Chemical compound	Area (%)			CAS number	Hydrogen bond donor/acceptor
		Acetone	Ethanol	Hexane		
1	β -Patchoulene	4.93	5.69	0.67	331-09-0	None
2	α -Patchoulene	2.80	3.21	3.71	560-32-7	None
3	Caryophyllene oxide	1.51	1.53	1.75	1139-30-6	Acceptor
4	Longifolenaldehyde	–	1.48	1.45	19890-847	Acceptor
5	Ledol	–	1.87	1.76	577-27-5	Acceptor/Donor
6	Patchouli alcohol	58.04	66.17	63.71	5986-55-0	Acceptor/Donor
7	Aristolone	1.64	1.68	1.74	6831-17-0	Acceptor
8	<i>n</i> -Hexadecanoic acid	1.76	2.09	1.17	57-10-3	Acceptor/Donor

Constituents are listed in the order of their relative content 1.0 %; MS by comparison of the MS with those of the NIST98 library (80 % matching from the library).

Study Summary

- The rdf trend demonstrated a stronger hydrogen bonding networking formed in ethanol solution in comparison to water.
- This suggests that a higher patchoulol composition extracted in ethanol.
- In polar solvent such as ethanol and acetone and nonpolar hexane, H-bond only can be detected in ethanol from infra red trend.
- H-bond can control the solubility of solute in solvent during extraction process

Agarwood Essential Oil Extraction Process



- Agarwood or oud or Gaharu (Malay term), khasnya *Aquilaria malaccensis*, is categorised in genus *Aquilaria* (Thymelaeaceae)
- **Black resinous** produced from the agarwood or oud or agarwood tree.



Agarwood Commercial Grade



A is Premium grade



B is medium grade

Black Resin chemical component



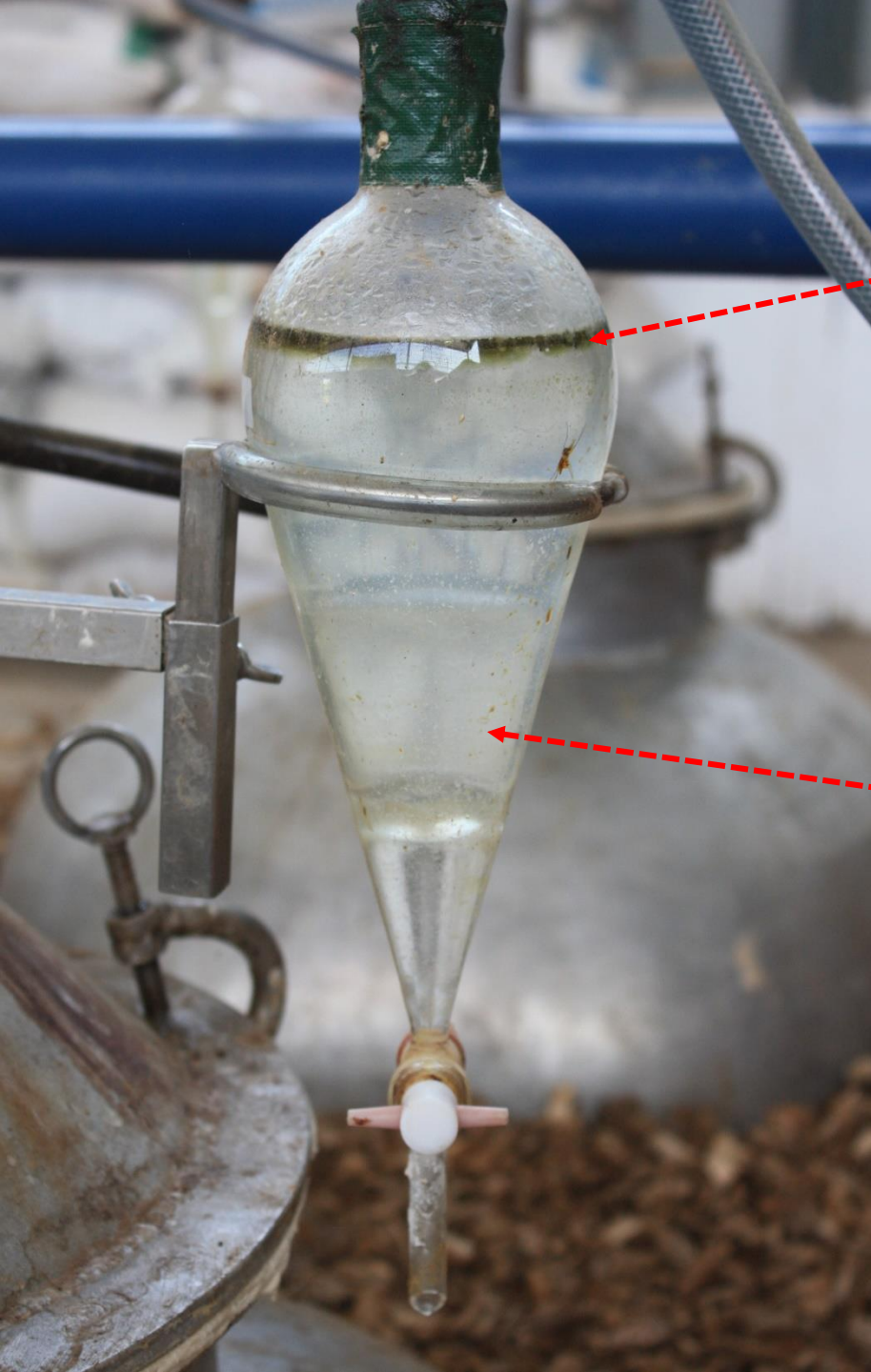
- Chemical composition profile is **complex and varies** of hydrocarbon and sesquiterpene oxide
- Chemical Marker compounds are **agarospirol**, **jinkohol-eremol**, **jinkohol** and **kusenol** in the extracted essential oil of agarwood
- The marker was identified using GCMC based on the MW and retention time.

Extraction of Agarwood



C or D grade will be extracted for agarwood essential oil. The essential oil is used for perfume and fragrance industry





Essential oil

Hydrosol

Low yield of extraction, also some of marker compound loss in the water solvent during extraction process.

Need a novel and new solution to recover the chemical marker compound.

Agarwood sesquiterpene

Table-1. Properties of agarwood sesquiterpenoids.

Compound & Formula	Structure	Functional groups	MW (Da)
Agarospinol $C_{15}H_{26}O$		Aromatic Hydroxyl Alkene Alkane	222.36
Jinkohol $C_{15}H_{26}O$		Aromatic Hydroxyl Alkene Alkane	222.36

Jinkohol $C_{15}H_{26}O$		Aromatic Hydroxyl Alkene Alkane	222.36
Kusenol $C_{15}H_{26}O$		Aromatic Hydroxyl Alkene Alkane	222.36

Retrace Code
01082471

SCHOTT
DURAN
150 ml



Essential Oil Chemical component

Chemical Component	Percentage composition(%)	
	Brownish Colour	Greenish Colour
4-phenyl-2-butanone	3.92	4.52
α -guaiene	0.17	0.13
β -agarfuran	0.24	0.39
β -bulnesene	2.29	-
α -muuralene	-	2.94
nor-ketoagarofuran	1.69	2.43
elemol	1.50	1.43
agarospirol	15.4	7.01
kusunol	-	7.61
selina-3,11-dien-9-ol	4.95	0.66
selina-3,11-dien-9-one	-	6.14
selina-4,11-dien-14-oic acid	2.96	-
selina-3,11-dien-14-al	2.71	2.91
selina-3,11-dien-14-ol	0.84	3.61

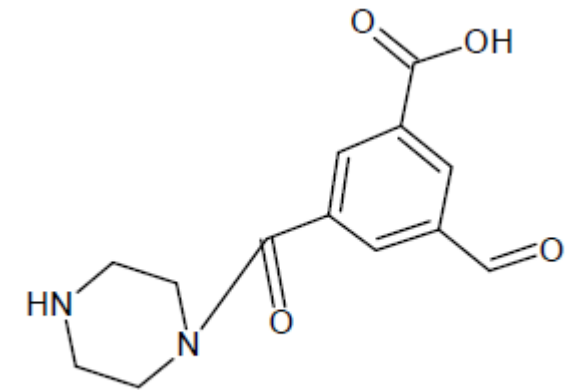
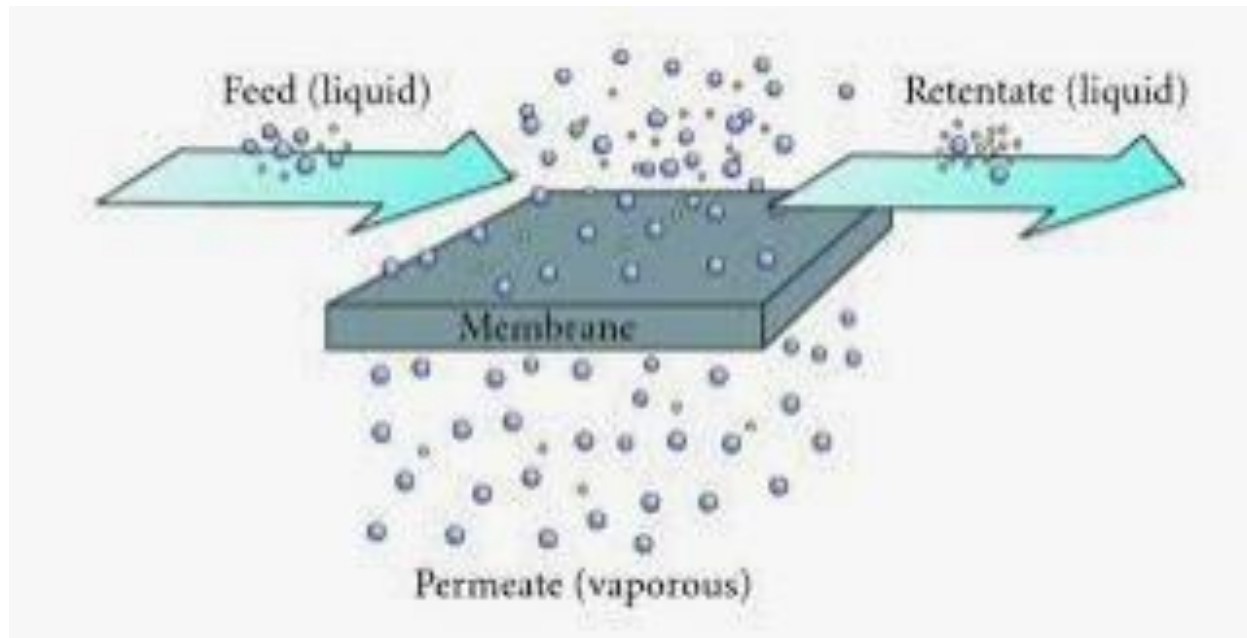
Membrane Separation for Agarwood Marker Compound Recovery

Water soluble marker compounds affect the quality of agarwood essential oil



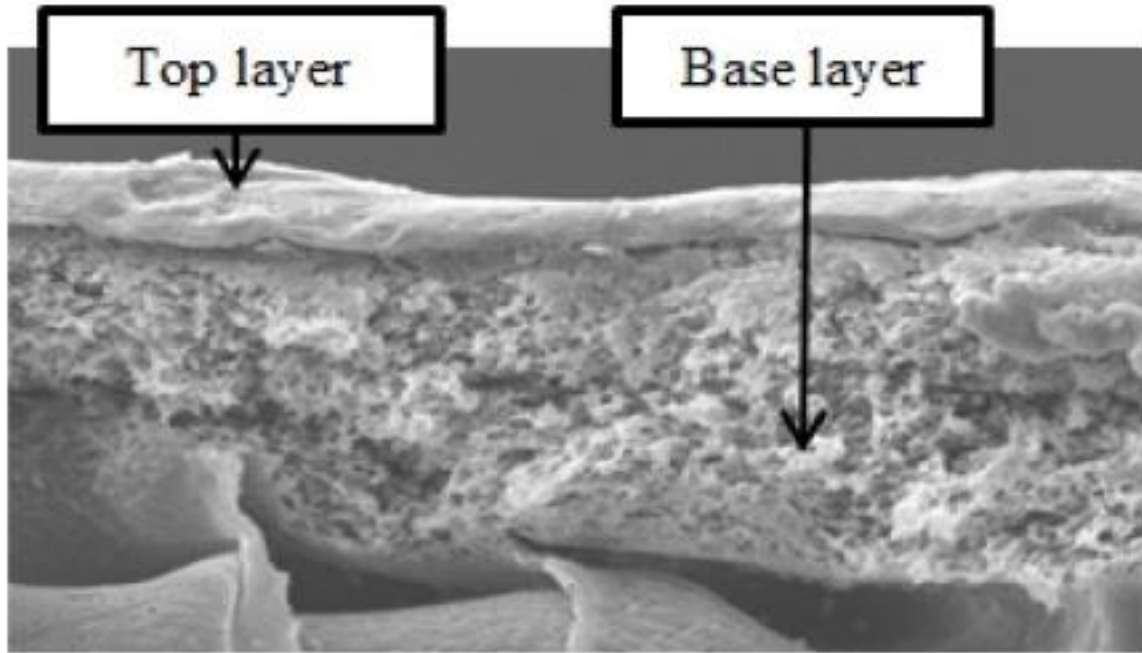
Technique to separate the soluble marker compound from water solvent

Polypiperazine Nanofiltration membrane

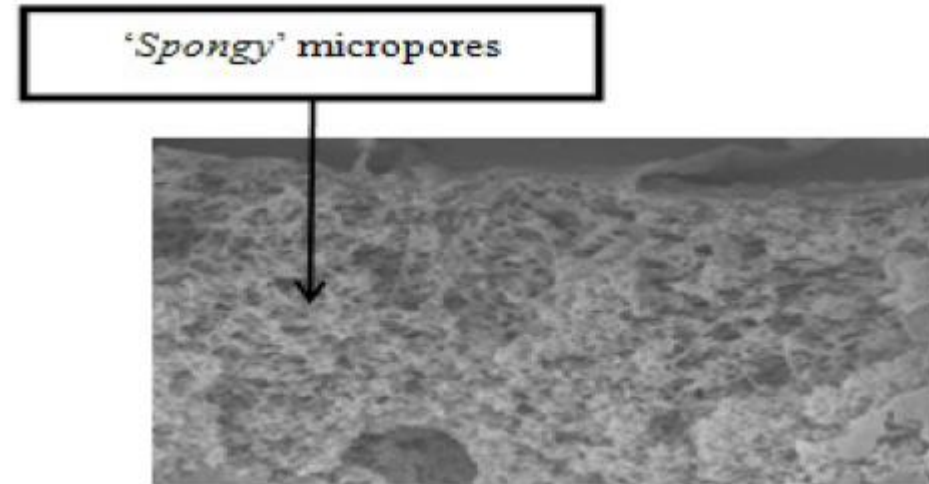


Chemical structure of poly(piperazine) (PPA).

PPA membrane for Agarwood Hydrosol Recovery



(a)



(b)

Essential Oil Chemical component

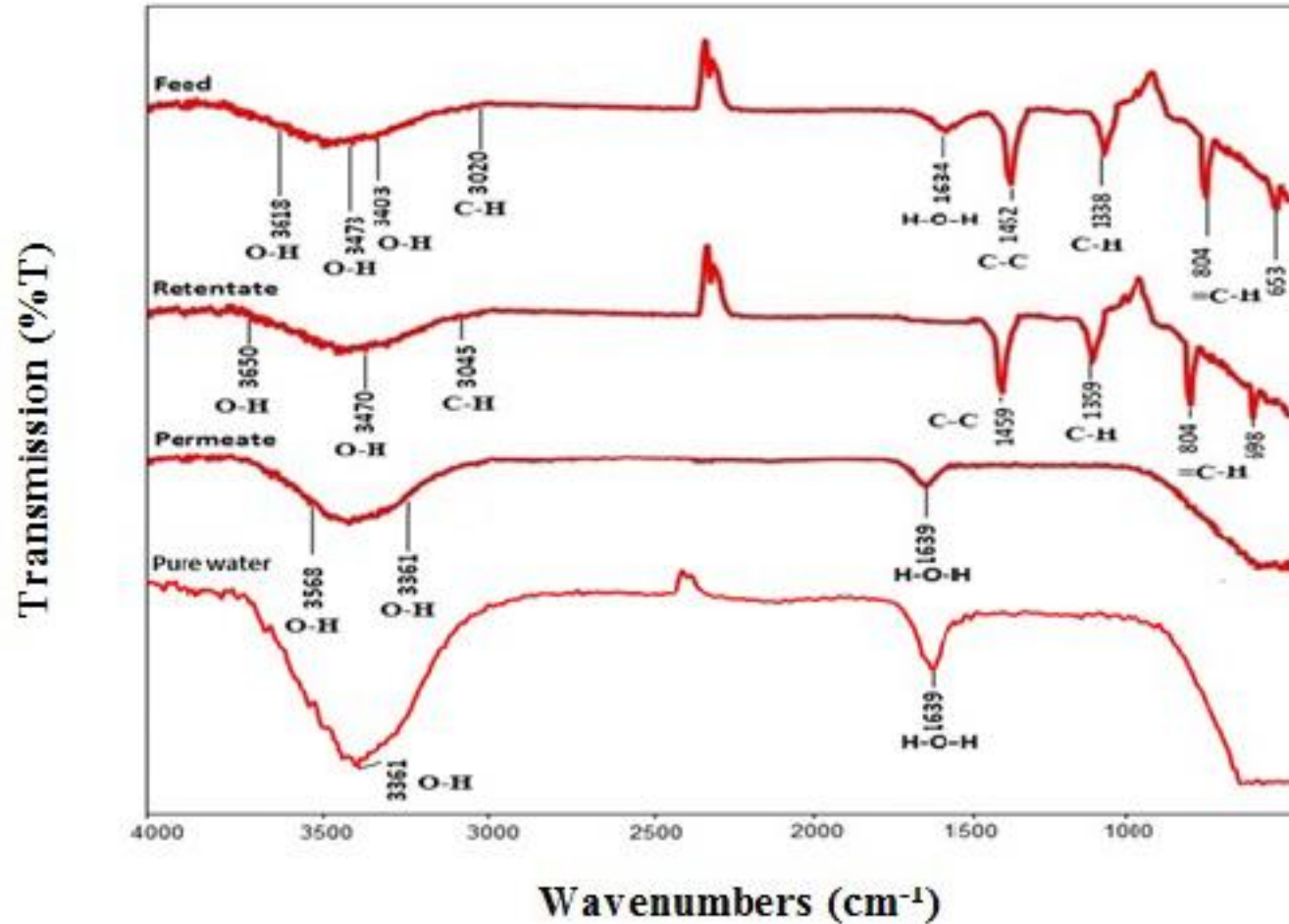
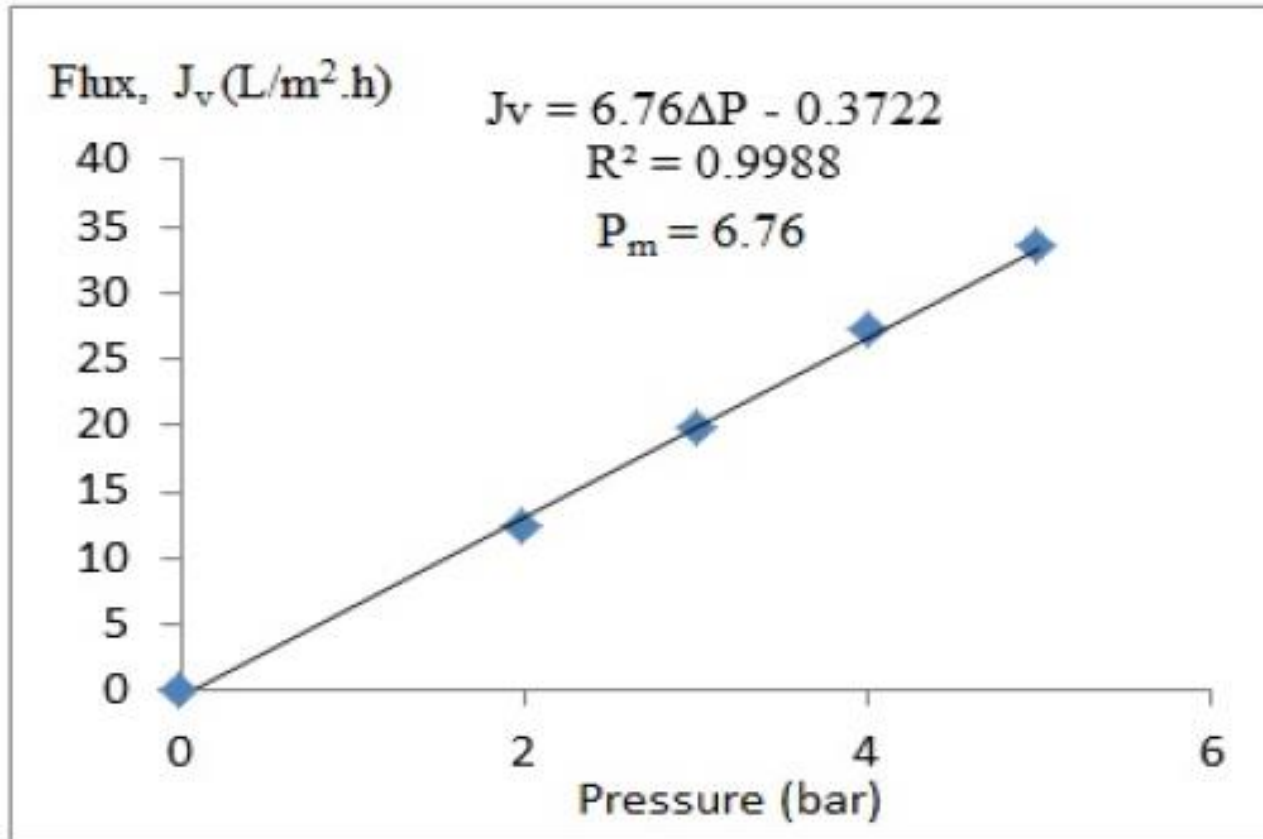


Table-2. Vibrational bands assignments of feed, retentate, permeate and pure water [(Schulz *et al.* 2005), (Fang *et al.* 2011), (Li *et al.* 2013), (Santosa *et al.* 2013)].

Wavenumbers (cm ⁻¹)	Band assignment
3400- 3600	O-H (alcohol)
3000-3100	C-H (aromatic alkane)
1400- 1500	In ring C-C stretches (aromatic alkane)
1330-1370	C-H (alkane)
650-800	=C-H bending (alkene)
3300-3400	O-H (water)
1630-1640	H-O-H (water)

Study Findings



Flux of PPA membrane at different operating pressure.

Permeability Coefficients
 P_M is 6.76 L/m².hr.bar

Average mass transfer Flux
is 23.20 L/m².hr

Study Summary

- Positive separation outcome from PPA nanofiltration membrane
- Hydroxyl bearing component (sesquiterpenoid) has been extracted into permeate
- Working flux is still low and need a new formulation of thin film composite (TFC) NF membraneto achieve optimum flux for industrial application

Crystallisation of Active Pharmaceutical Ingredient: Chemical Solvents Interaction Role

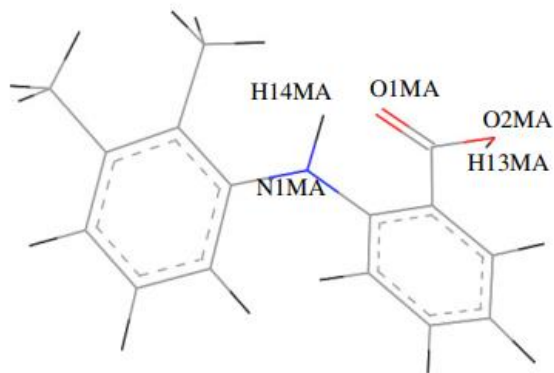
Structures and Hydrogen Bonding Recognition of Mefenamic Acid Form I Crystals in Mefenamic Acid/Ethanol Solution

Author: Siti Kholijah Abdul Mudalip, Mohd Rushdi Abu Bakar, Fatmawati Adam and Parveen Jamal

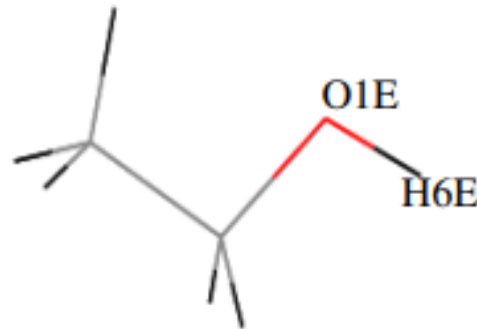
International Journal of Chemical Engineering and Applications, 2013.

Method: Material Studio, COMPASS Forcefield, FTIR

Objective: To verify the effect of hydrogen bonding is considered as the on the polymorphism of mefenamic acid in ethanol.

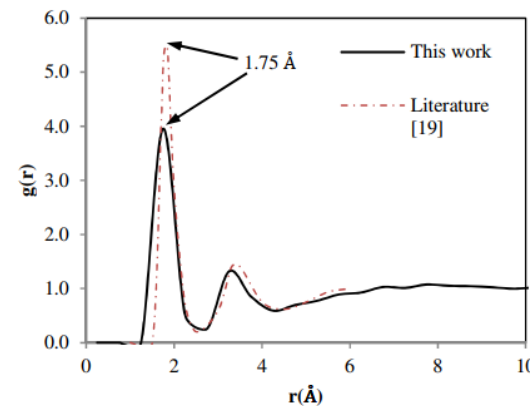


Mefenamic Acid

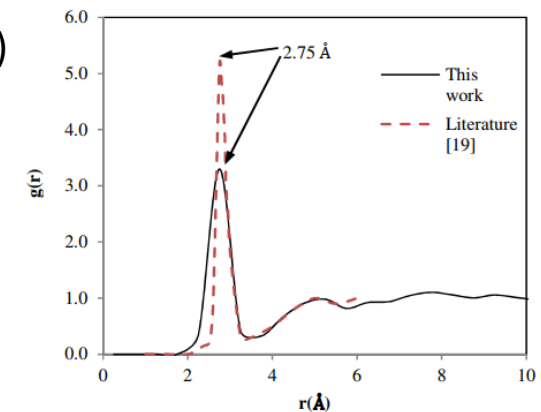


Ethanol

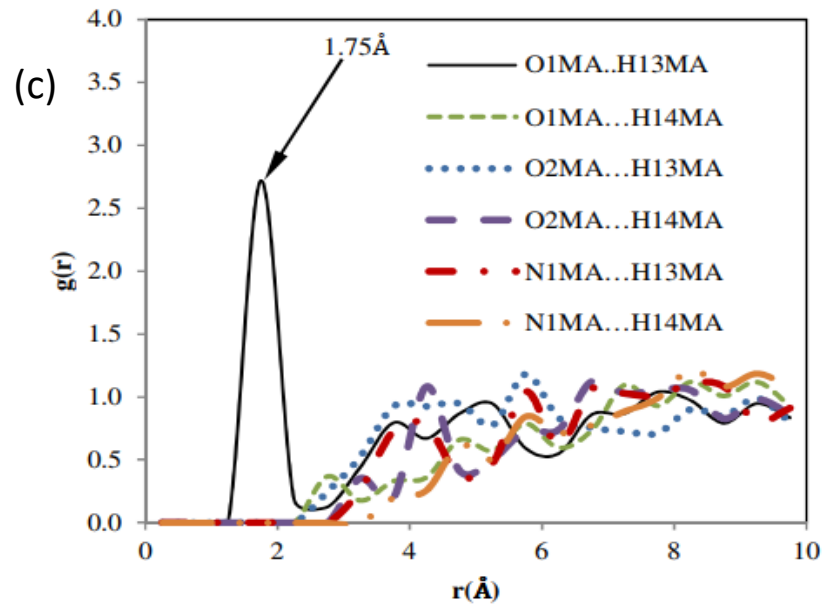
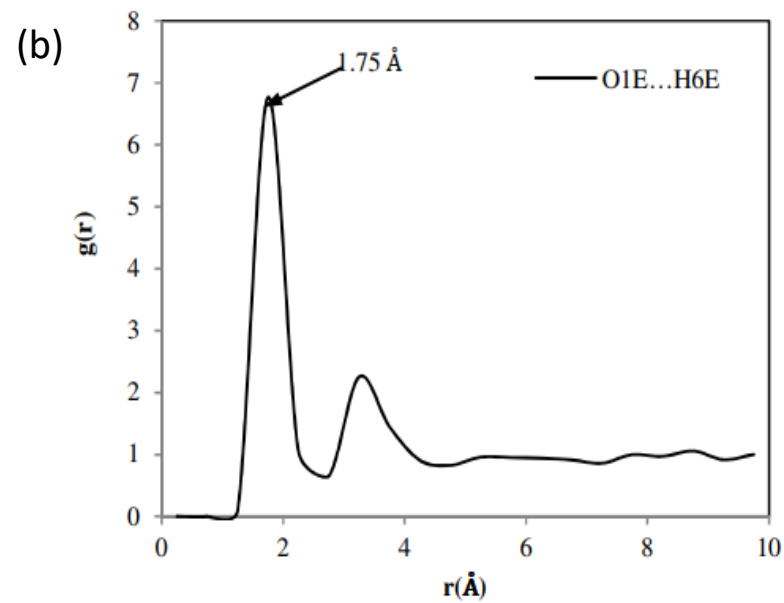
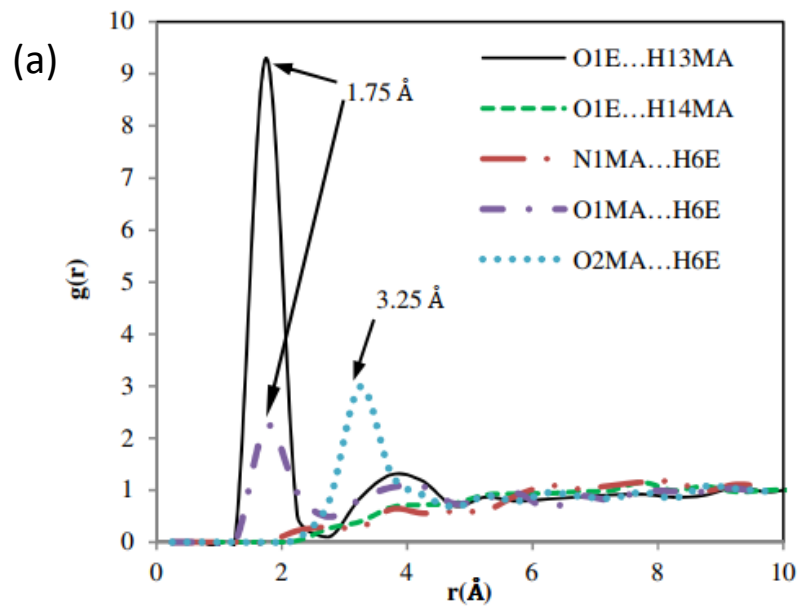
(a)



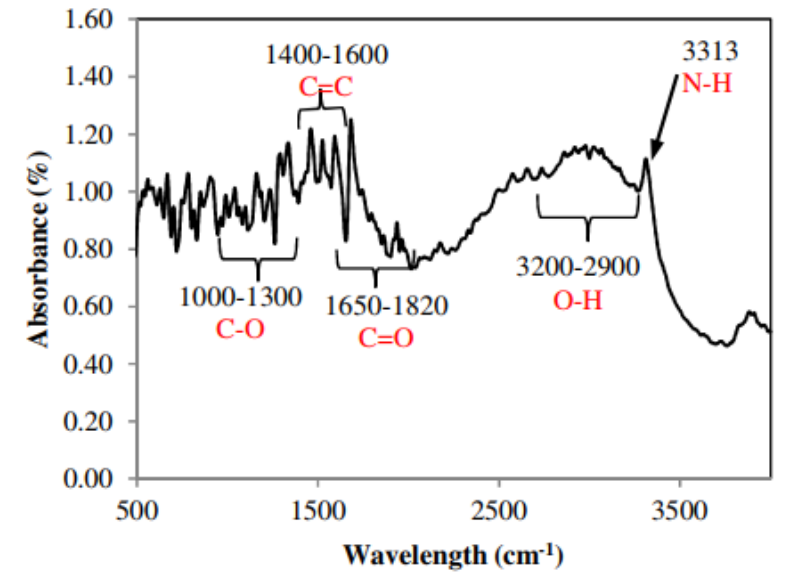
(b)



$g(r)$ plots of pure ethanol (a) Molecular interaction between $O1E \cdots H6E$ and (b) $O1E \cdots O1E$ in comparison with literature



The comparison of $g(r)$ plot of mefenamic acid/ ethanol solution
 (a) solvent-solvent; (b) solvent-solute and solute-solvent; (c) solute-solute



FTIR spectrum of mefenamic acid solid crystals obtained from ethanol solution.

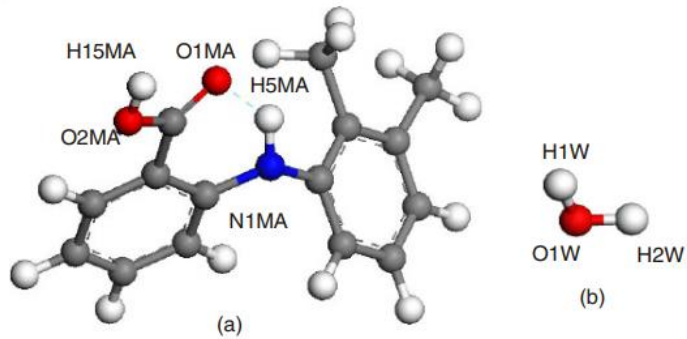
Molecular Recognition and Solubility of Mefenamic Acid in Water

Scopus, 0.6

Author: S.K. Abdul Mudalip, M.R. Abu Bakar, P. Jamal, F. Adam, And Z.M. Alam, *Asian Journal of Chemistry*, 2016

Method: Material Studio, COMPASS Forcefield.

Objective: To investigate the solubility and intermolecular interactions (i.e., hydrogen bonding) of water with mefenamic acid.



(a) Chemical structure of a mefenamic acid molecule with partial labelling; (b) Water;

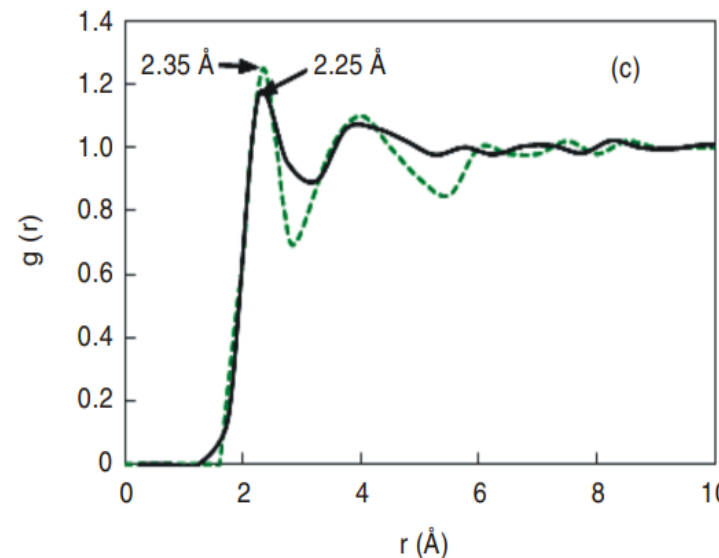
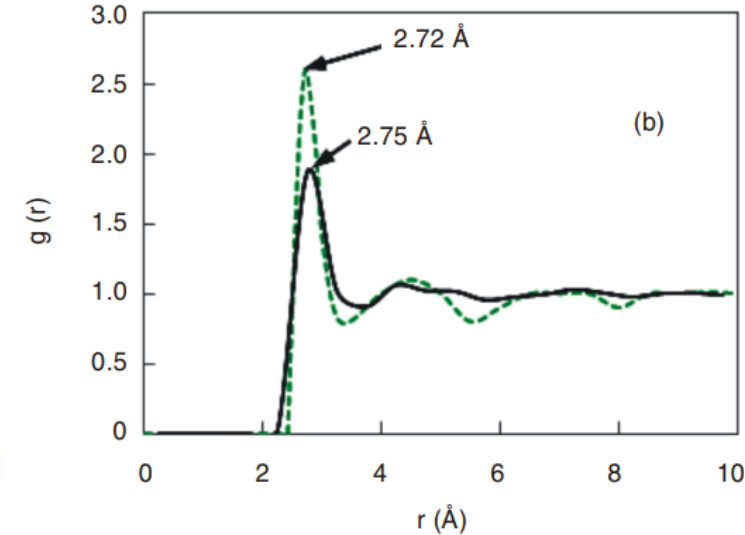
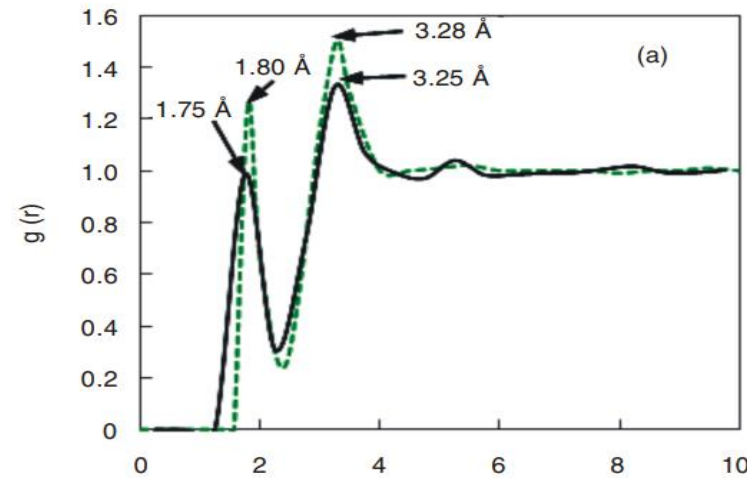
$$g_{xy}(r) = \frac{\langle N_y(r, r+dr) \rangle}{\rho_y 4\pi r^2 dr}$$

r = spherical radius distance from the reference atom,

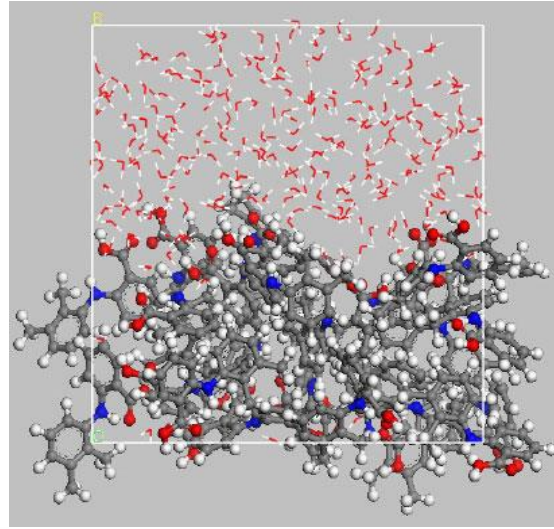
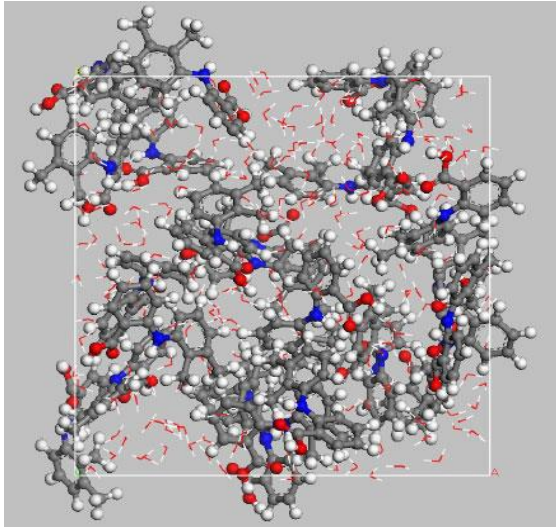
ρ_y = density of a y atom,

$\langle N_y(r, r+dr) \rangle$ = number of y atoms in a shell of width Δr at distance r

x = reference atom



$g(r)$ plots for pure water : (a) O1W...H1W; (b) O1W...O1W and (c) H1W...H1W. The solid line from this work, **green dashed from literature**

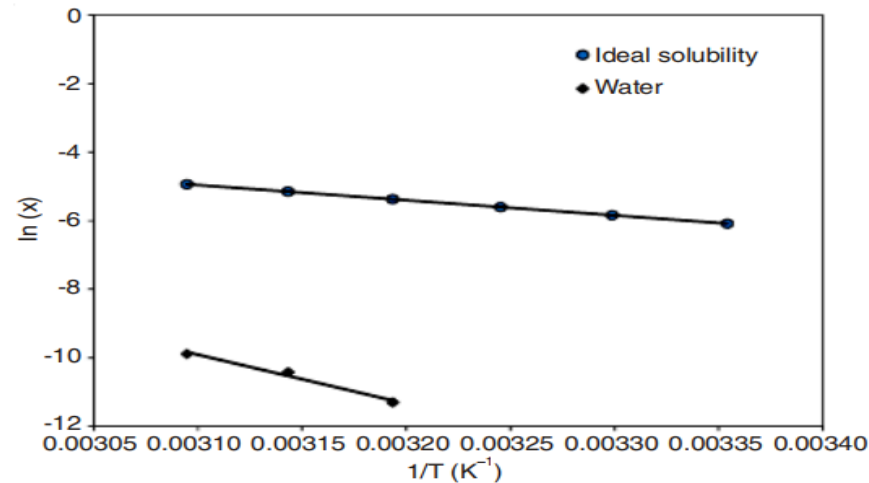


(a) **the initial distribution**; (b) the **final distribution** of mefenamic acid molecules in water.

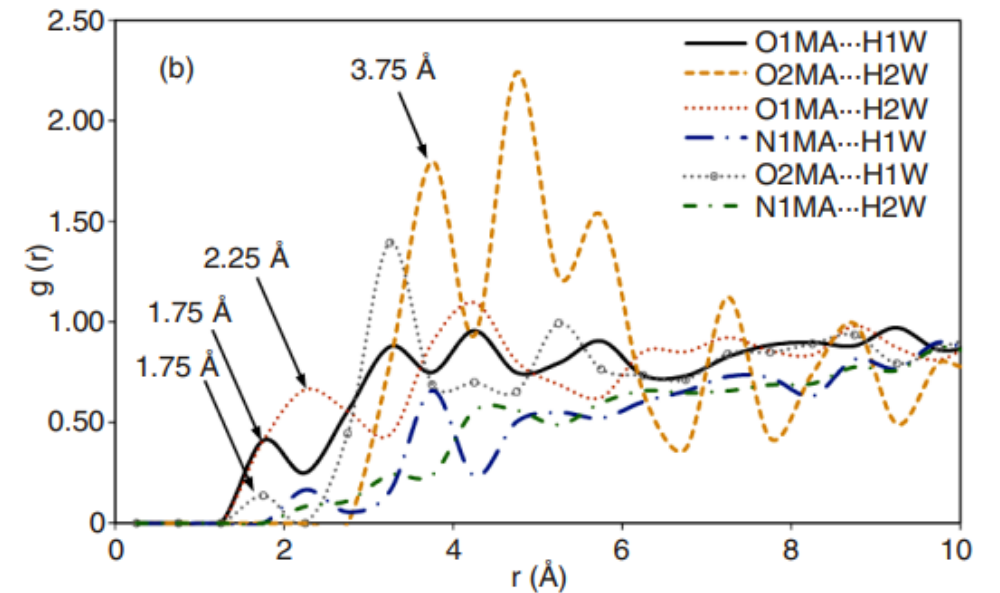
Van't Hoff Equation

$$\ln x = \frac{\Delta H_f}{R} \left(\frac{1}{T_f} - \frac{1}{T} \right)$$

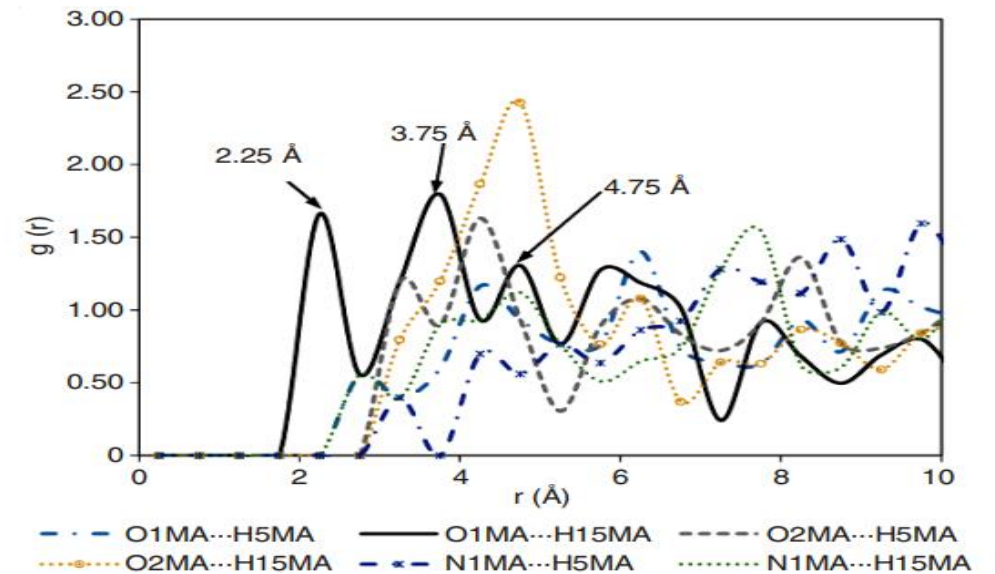
x = mole fraction of the solute in the solution,
 ΔH_f = the molar enthalpy of fusion of the solute (J/mol),
 R = gas constant,
 T_f = the fusion temperature of the solute (K)
 T = solution temperature (K).



van't Hoff plot of mefenamic acid solubility and ideal solubility values



Mefenamic acid molecules in water molecules (**solute-solvent interactions**)



Mefenamic acid/water system (**solute-solute interactions**)

Investigating The Role Of Molecular Interactions In Polymorphism Of Mefenamic Acid In Ethyl Acetate Solution

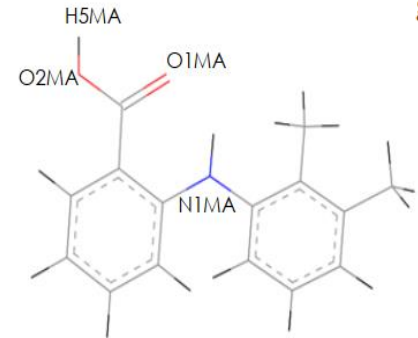
Scopus, 1.3

Siti Kholijah Abdul Mudalip, Mohd. Rushdi Abu Bakar, Fatmawati Adam, Parveen Jamal, Zahangir Md. Alam, Jurnal Teknologi, 2016

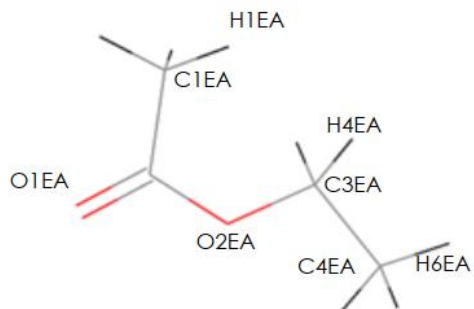
Method: Material Studio, COMPASS Forcefield.

Objective: To study crystallization of mefenamic acid in ethyl acetate using experimental and molecular dynamics simulation

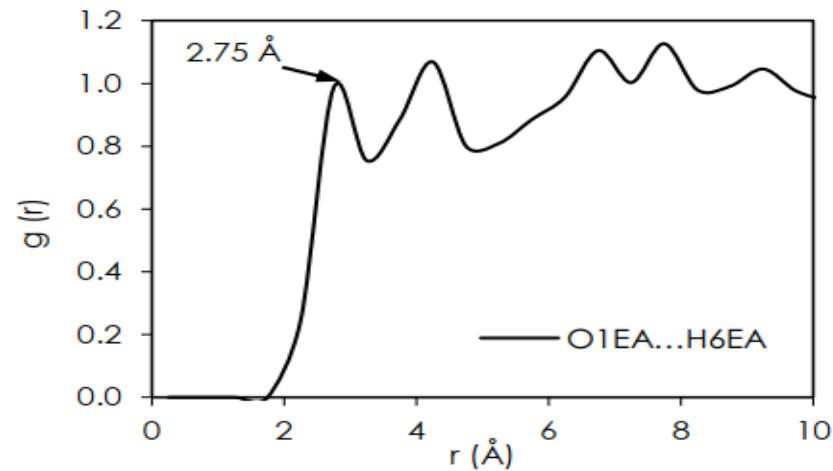
$$g_{xy}(r) = \frac{\langle N_y(r, r+dr) \rangle}{\rho_y 4\pi r^2 dr}$$



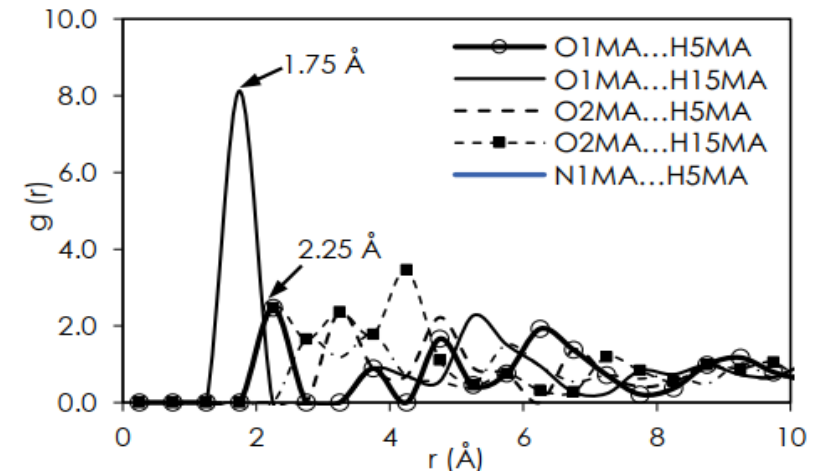
Mefenamic Acid



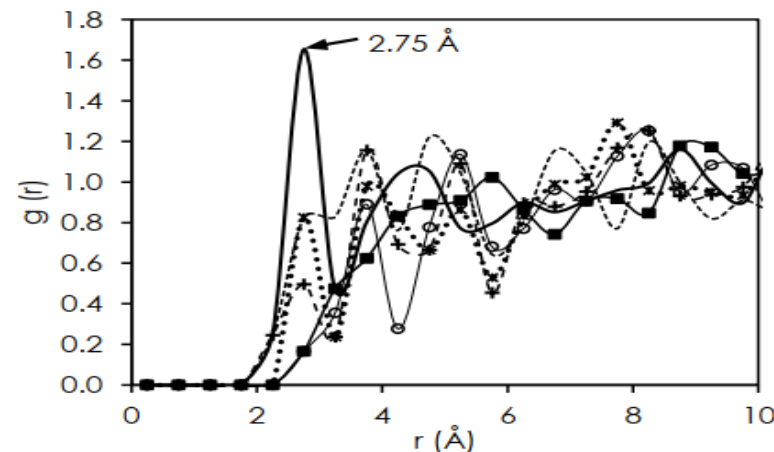
Ethyl Acetate



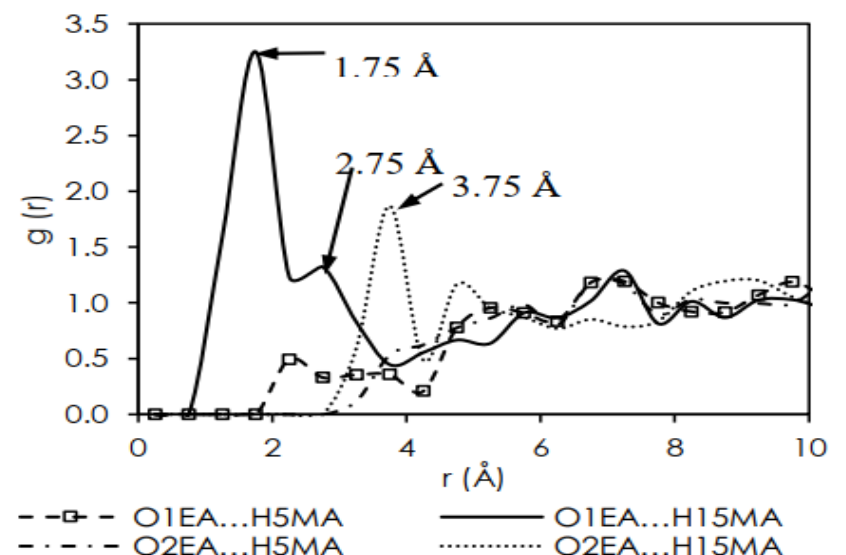
Solvent-solvent



Solute-solute



Solute-solvent



Solvent-solute

Prediction of Mefenamic Acid Solubility and Molecular Interaction Energies in Different Classes of Organic Solvents and Water

ISI: 3.573,
Scopus, 5.3

Siti Kholijah Abdul Mudalip, Mohd Rushdi Abu Bakar, Parveen Jamal, and Fatmawati Adam, Industrial and Engineering Chemistry Research, 2018.

Objective: To predicts the mefenamic acid solubility and molecular interaction energy, namely electrostatic (HMF), hydrogen bonding (H-HB) and van der Waals (H-VdW) in different solvents at temperatures from 298 to 323 K using Conductor-like Screening Model for Real Solvents (COSMO-RS)

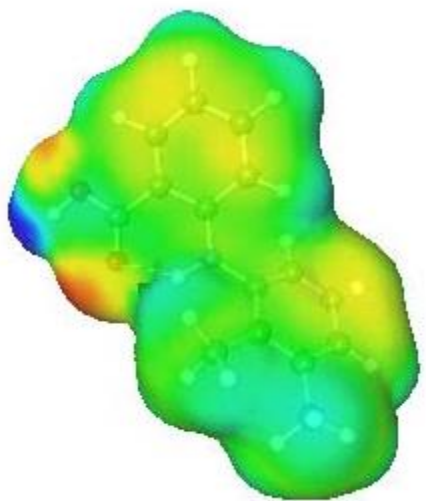
Method: COSMO-RS, Becke-Perdew triple valence plus polarization function (BP-TZVP)

COSMOthermX solubility iterative tool: $\log_{10}(x_j^{sol(n+1)}) = [\mu_j^{Pure} - \mu_j^S(x_j^{sol(n)}) - \max(0, \Delta G_{fus})] / (RT \ln(10))$

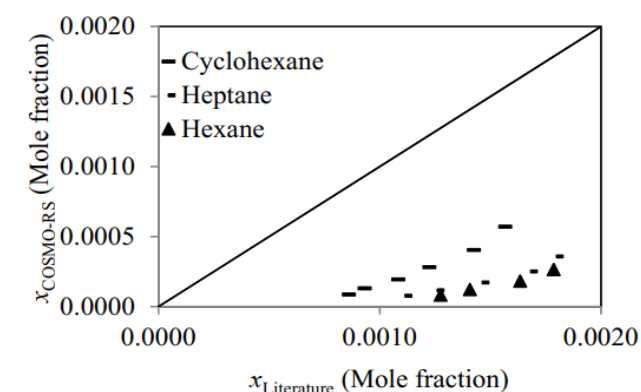
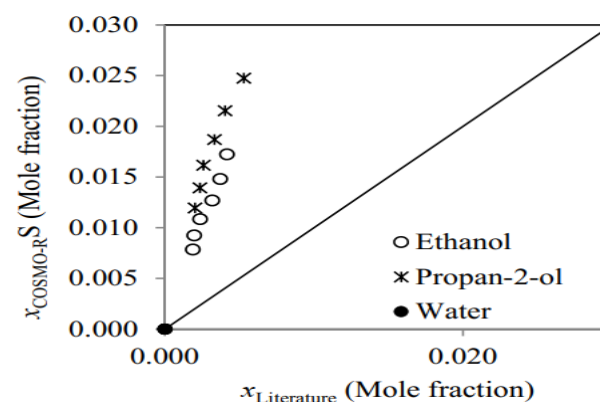
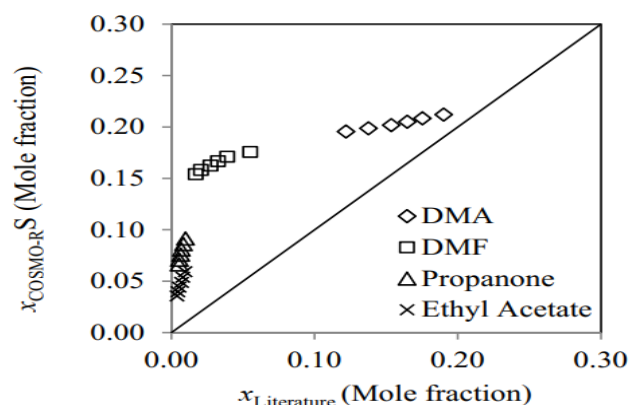
Modified van't Hoff:

$$\ln x = \frac{\Delta H_f}{R} \left[\frac{1}{T_f} - \frac{1}{T} \right] - \ln \gamma$$

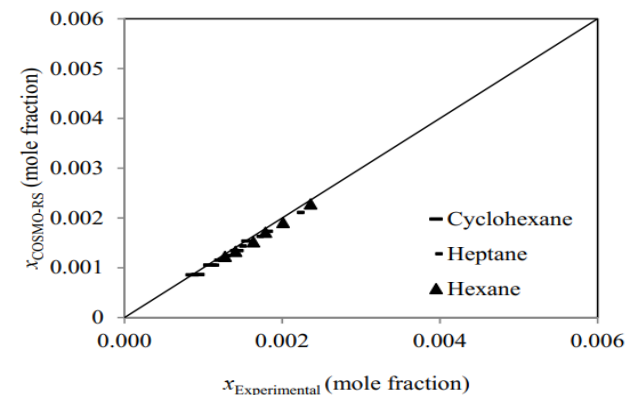
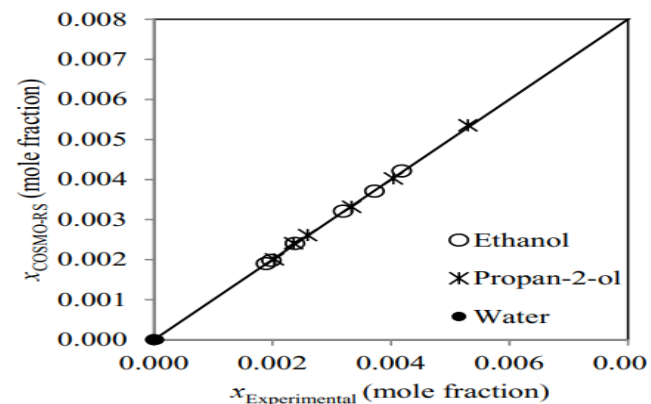
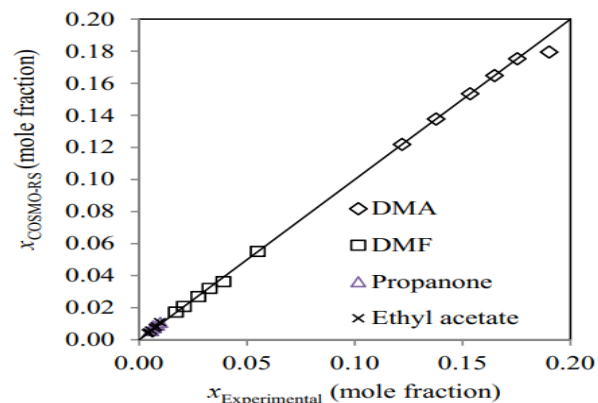
x_j^{sol} = the mole fraction of mefenamic acid dissolved in the targeted solvent,
 μ_j^{pure} = the chemical potential of pure compound j ,
 μ_j^S the chemical potential of pure compound j at infinite dilution in the solvent
 ΔG_{fus} = the Gibbs free energy of fusion



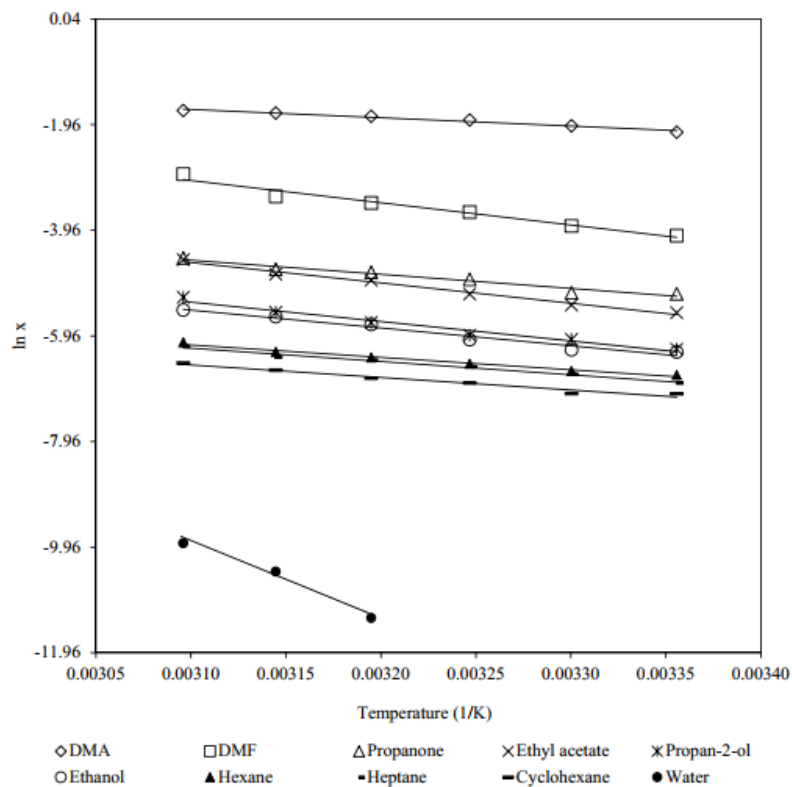
3D COSMO-surface screening charge densities of mefenamic acid



Predicted solubility COSMO-RS vs literature: (a) DMA, DMF, propanone and ethyl acetate (dipolar aprotic); (b) Ethanol and propan-2-ol (polar protic); and (c) Cyclohexane, heptane and hexane (Apolar aprotic)



Mefenamic acid solubility predicted by COSMO-RS vs experimental: (a) DMA, DMF, propanone and ethyl acetate (dipolar aprotic); (b) Ethanol and propan-2-ol (polar protic); and (c) Cyclohexane, heptane and hexane (Apolar aprotic)



Van't Hoff plot of mefenamic acid solubility in different organic solvents and water

Solvents	Average mean squared quadratic errors, MSE	
	Differential scanning calorimetry	Literature ⁵
DMA	0.13	0.0010
DMF	27.42	0.0002
Propanone	107.64	0.0200
Ethyl Acetate	44.85	0.0040
Ethanol	10.54	0.0001
Propan-2-ol	21.47	0.0010
Cyclohexane	0.80	0.0020
Heptane	0.74	0.0010
Hexane	0.93	0.0020

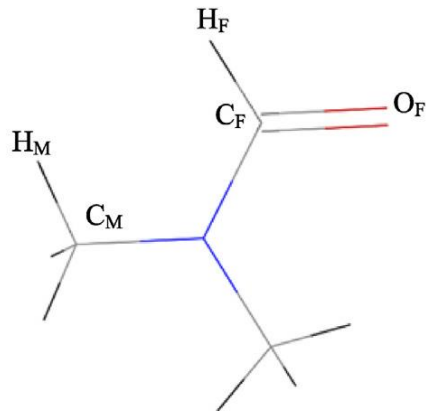
Mean squared quadratic errors (MSE) of COSMO-RS solubility prediction with enthalpy of fusion obtained from differential scanning calorimetry analysis and literature

Evaluation of the intermolecular interactions and polymorphism of mefenamic acid crystals in N,N-dimethyl formamide solution: A molecular dynamics simulation and experimental study

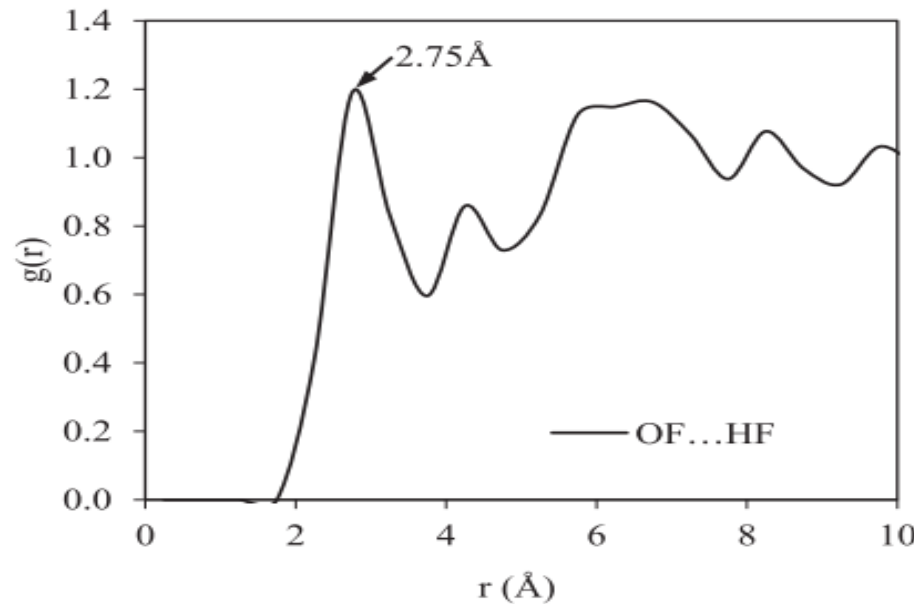
Siti Kholijah Abdul Mudalip a, b, *, Fatmawati Adam a, b, Mohd Rushdi Abu Bakar, Comptes Rendus Chimie, 2019

Objective: To investigate the polymorphism of mefenamic acid in N,N-dimethyl formamide (DMF) through the combination of molecular dynamic simulations and experimental study.

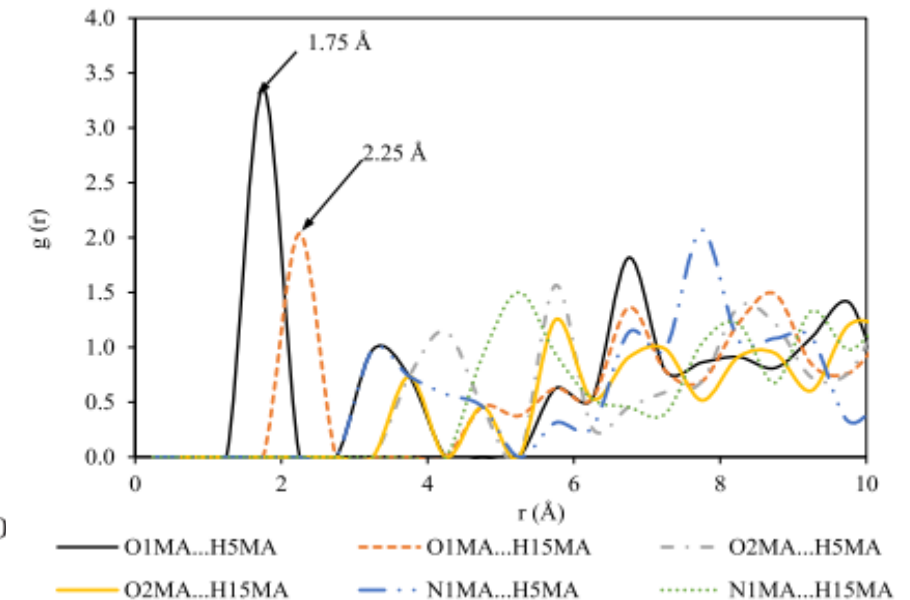
Method: Material Studio, COMPASS Forcefield.



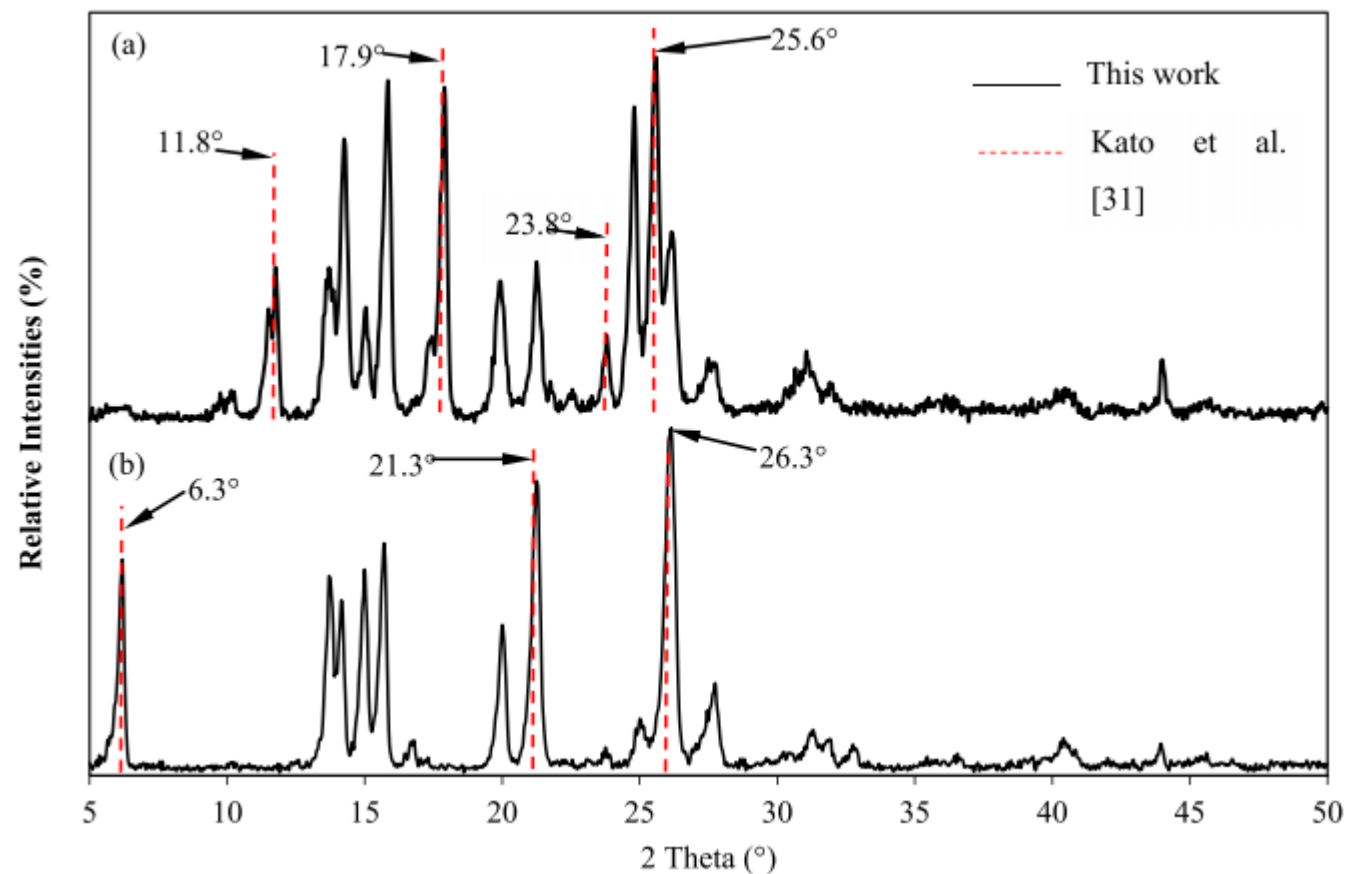
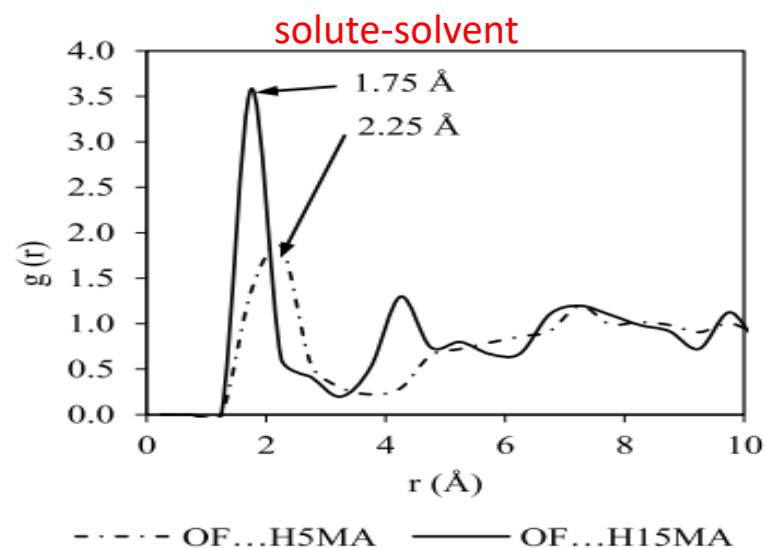
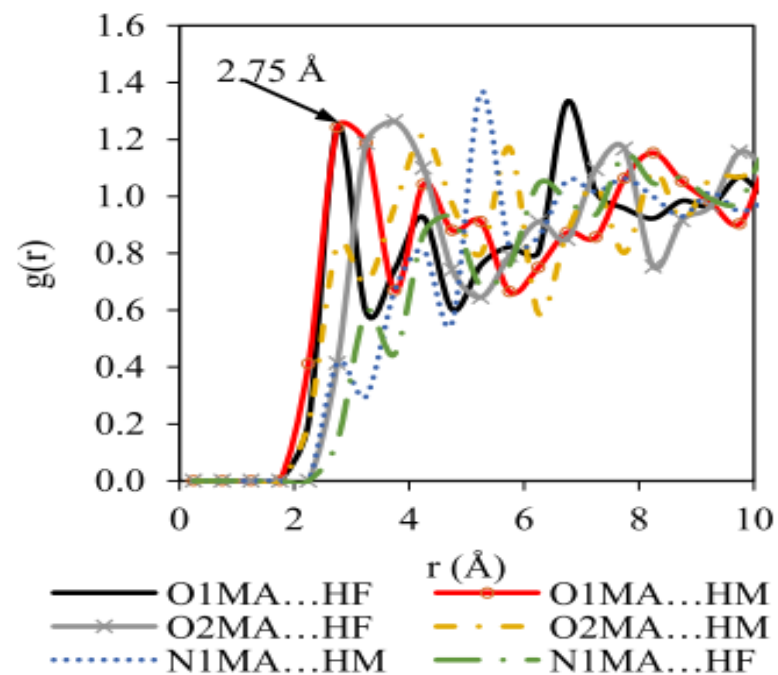
N,N-dimethyl formamide (DMF)




Solvent-solvent interaction binary system (mefenamic acid/DMF mixture)



solute molecules in DMF.



Comparison of the X-ray powder diffraction patterns of the mafenamic acid crystals (a) crystallized using DMF and (b) raw material in this work with the major peaks of the mafenamic acid form I crystals obtained by Kato et al

A rustic-themed photograph featuring a small, rectangular, light-brown cardboard tag with a torn left edge. The tag is placed on a weathered wooden surface. It has the words "Thank you!" written in a black, cursive script. To the right of the tag is a single white daisy with a bright yellow center. In the background, two more similar daisies are visible but out of focus. A dark, thin vine or string is draped across the scene, passing behind the tag and one of the background flowers.

Thank
you!

CMMS Application as a thickener and binder in Pharmaceutical Application

Associate Professor Dr Fatmawati binti Adam

Faculty of Chemical and Process Engineering Technology



Objective

- To evaluate the applications of **CMSS** in the pharmaceutical field with **tablet binder** and **solution thickener** as first focus as it is stable.
- As the plant origin material, the replacement of gelatine in solution thickener will ensure the **halal** pharmaceutical product which may attract **Muslim and vegetarian consumer**.
- Replacement of imported starch such as corn starch as tablet binder **using local sources**.

OBJECTIVES



1

To incorporate carboxymethyl sago starch as a **binder** before tablet pressing



2

To incorporate carboxymethyl sago starch as a solution thickener in producing **hard capsules** for drug delivery

Incorporate CMSS as a binder before tablet pressing



Granulator



Granules



Tablet press

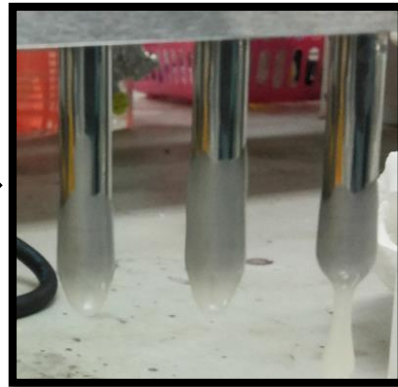


Tablets formed

To incorporate CMSS as a solution thickener in producing hard capsules



**Solution
formation**



**Capsule
moulding**

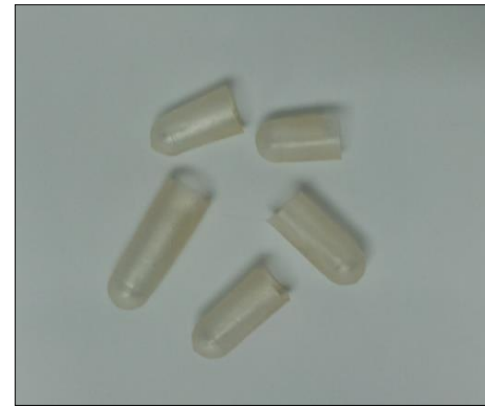


**Capsule
drying**



**Capsule
formation**

Some capsules that has been produced



DISINTEGRATION TEST ANALYSIS

Before the addition of additives

Mixture Composition (CMSS + water)	Disintegration in pH 1.00 (pH stomach pH 1 - 3)	Disintegration in pH 7.00
CMSS 10w/v%	10 minutes	11 minutes
CMSS 15w/v%	30 minutes	32 minutes
CMSS 20w/v%	Do not disintegrate after 1 hour	Do not disintegrate after 1 hour
CMSS 25w/v%	Do not disintegrate after 1 hour	Do not disintegrate after 1 hour
CMSS 30w/v%	Do not disintegrate after 1 hour	Do not disintegrate after 1 hour

After the addition of additives

Formulation	Disintegration in pH 1.00 (pH stomach pH 1 - 3)	Disintegration in pH 7.00
1	6 minutes	6 minutes
6	7 minutes	8 minutes
16	10 minutes	10 minutes
19	10 minutes	10 minutes

FILM MORPHOLOGY ANALYSIS

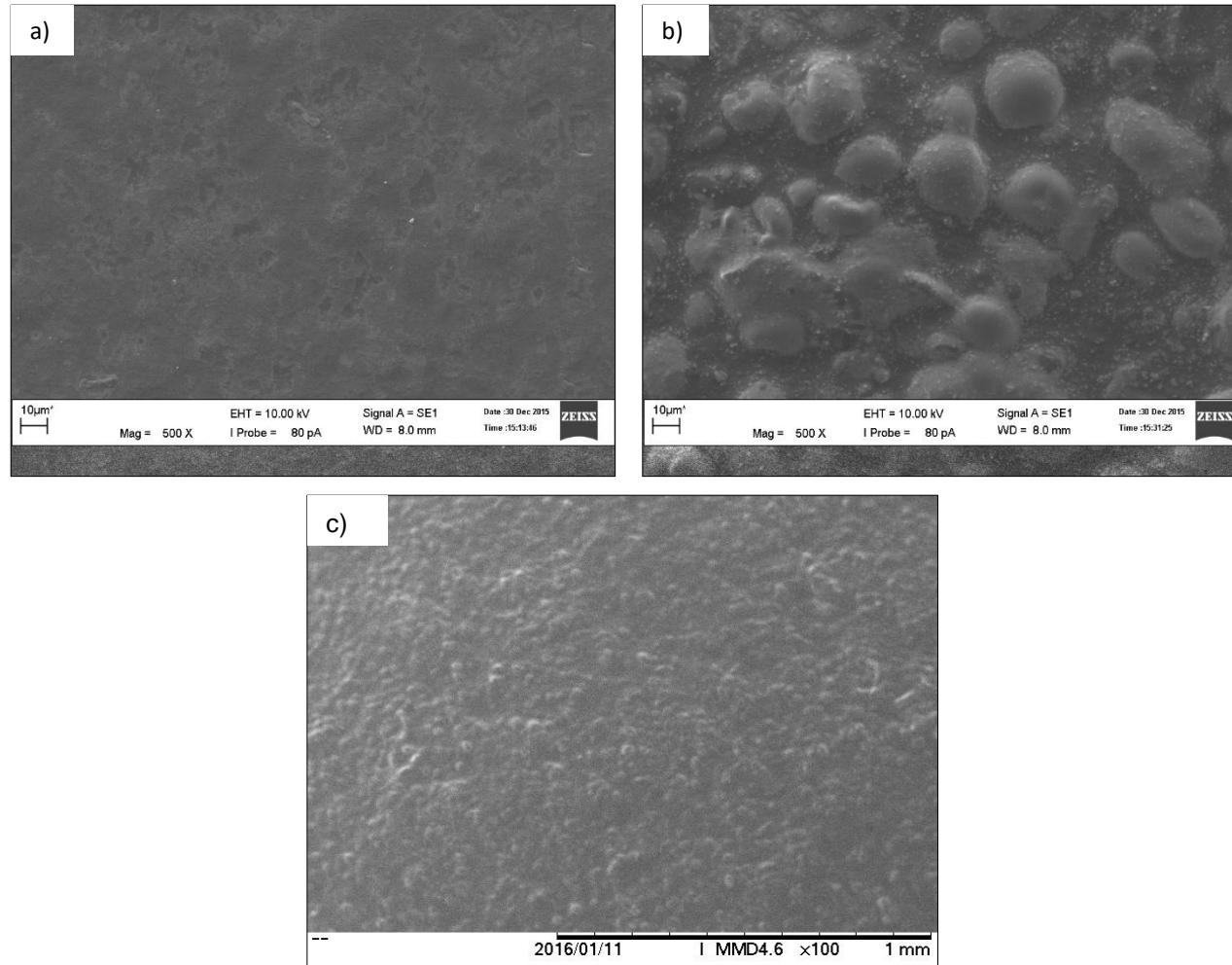
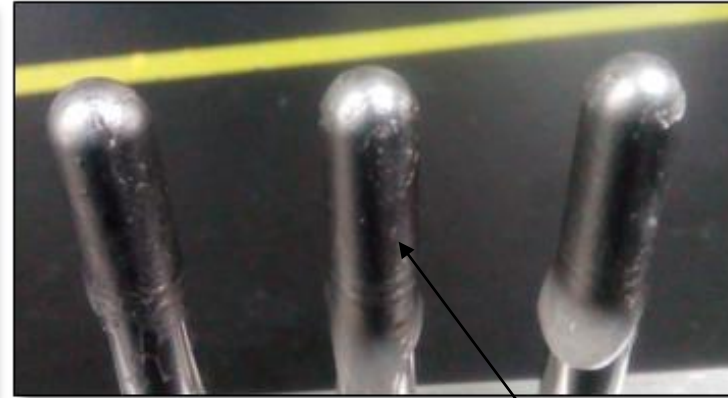
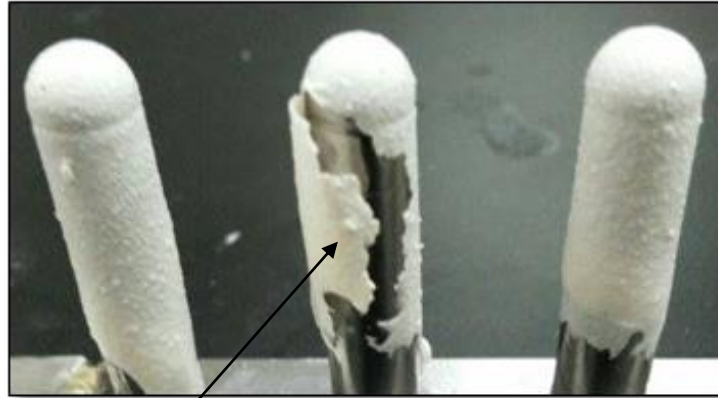
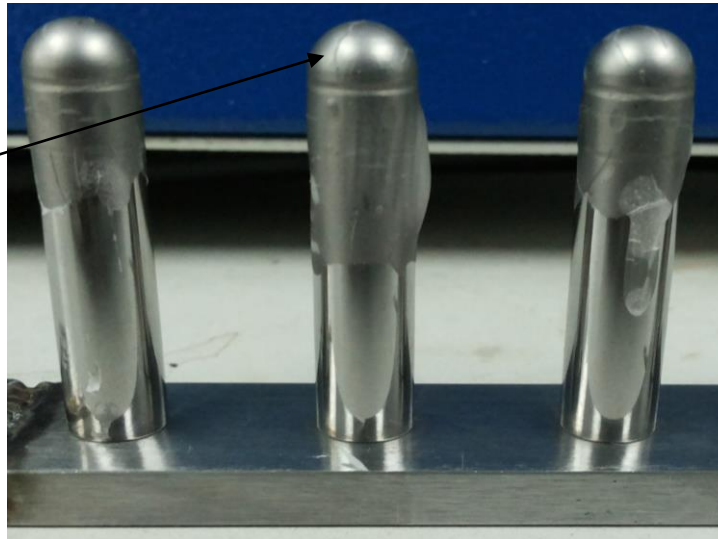


Figure 4: SEM analysis for capsule film: a) F1 (W+CMSS+G) b) F6 (W+CMSS+G+SC) c) F16(W+CMSS+G+SHC+SC+T)

Some of the capsules that cannot be stripped or removed



Capsule become brittle/crack



Capsule film formed is too thin

Capsules that are brittle after removed from the pin bar



Capsules after 2-3 weeks of storage start to demonstrate the instability properties



Capsules tend to absorb water from surrounding

Capsules produced that have formed some bubbles



- **CMSS** shows a potential as a solution thickener in producing hard capsule.
- The addition of **additive** such as carboxymethyl cellulose salt and titanium dioxide seems to increase the **tensile strength** of the film capsule.
- The addition of the **plasticiser** such as glycerol and PEG made the capsule film **less brittle**.
- **Further extensive formulation study** need to be conducted to **meet actual industrial specification and application** and to avoid the capsule film from becoming brittle, bubble formation and has similar tensile strength based on industrial specification.

DEVELOPMENT & CHARACTERISATION
OF GUM ARABIC-KAPPA CARRAGEENAN
FILM FOR HARD CAPSULE APPLICATION

OBJECTIVES

To formulate and produce the films by using gum arabic(GA) and the gum arabic-semi refined kappa carrageenan composite formulation with addition of toughening agent and plasticiser.

To investigate and characterize the mechanical, thermal, surface morphology properties and **disintegration** time of composite films.



LITERATURE REVIEW

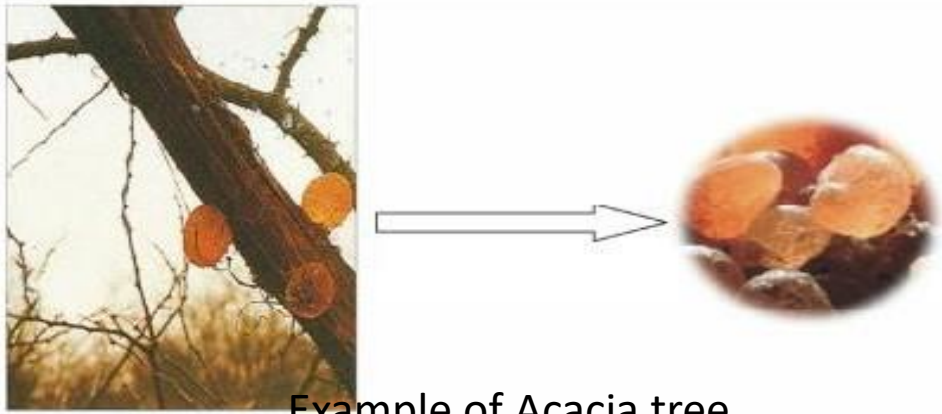
POLYSACCHARIDE

- ✓ Definition: (Demchenko, 2008)
 - **Complex** carbohydrate polymer
 - **long chain**
 - repeating monosaccharide
 - bond at glycosidic linkage
- ✓ Properties:
 - Water solubility, viscosity, gelling behaviour :structure molecule arrangement (Gidley and Reid, 2006)
 - **Film forming** easily modified (De Moura et al., 2009)
 - Well known as **viscosity builder**, gelling agent and stabiliser (Prajapati et al.2014)
- ✓ This study:
 - Gum arabic and semi refined kappa carrageenan

Structures and properties of gum arabic and kappa carrageenan

Structures and Properties	Gum arabic	Kappa carrageenan
Structures	<ul style="list-style-type: none"> ➤ From Acacia tree ➤ Consist of Carbon, Oxygen and Hydrogen (Stephen and Churms, 2006) 	<ul style="list-style-type: none"> ➤ Red seaweed ➤ <i>Eucheuma cottoni</i> and <i>Kappaphycus alvarezii</i> (Jiao et al., 2011) ➤ Consist of Carbon, Oxygen, Hydrogen and Sulphate esters. (Zia et al., 2016)
	<ul style="list-style-type: none"> ➤ Galactose, Arabinose, Rhamnose and Glucuronic acid (Espinosa-Andrew et al., 2007) 	<ul style="list-style-type: none"> ➤ D-galactose residue linked alternately to 3-linked-β-D-galactopyranose and 4-linked-β-D-galactopyranose units.
Properties	<ul style="list-style-type: none"> ➤ High water solubility ➤ Low viscosity (William et al., 2000) 	<ul style="list-style-type: none"> ➤ Fully soluble in hot and cold water (Zia et al., 2016) ➤ Excellent gelling ability (Li et al., 2014)

Gum Arabic & Seaweed



Example of Acacia tree
(Dauqan and Abdullah, 2013)



Example of Red seaweed

LITERATURE REVIEW

Functional	Gum arabic	Kappa carrageenan
Binder agent in tablet coating	√ Lu et al.,2003	x
Ingredient in edible film	√ Apandi et al.,2013	√ Paula et al.,2014; Ili balqis et al.,2017
Biocompatible Scaffold	√ Sarika et al., 2014	x
Food protection packaging	√ Li et al., 2014	√ Kanmani and Rhim, 2014; Farhan, 2017
Gelling agent for hard capsule	x	√ L.Zhang, 2013, Li et al., 2014
Ingredient of hard capsule	x	√ Fakharian et al., 2015
Reduced viscosity of binder solution	√ Singh et al., 2016	x

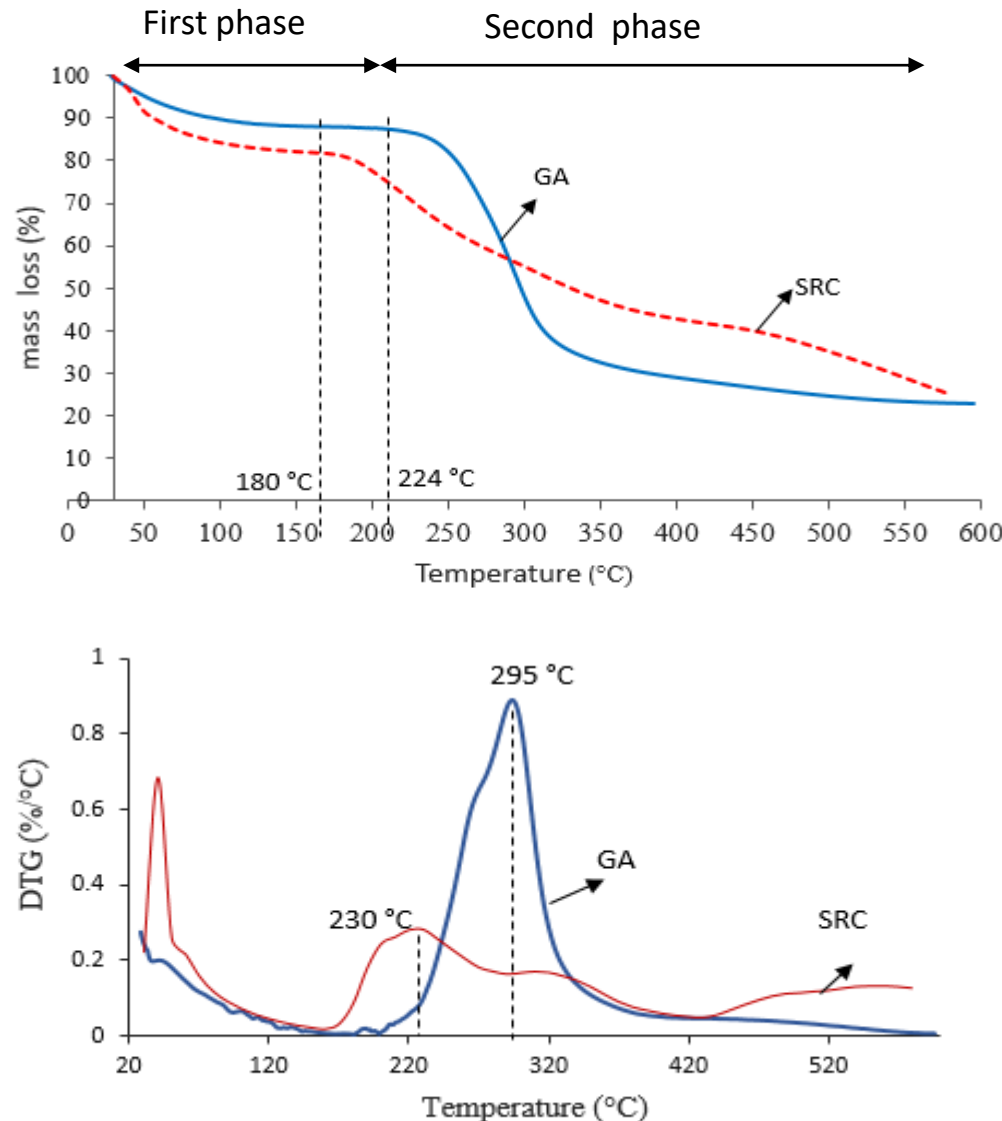
Potential of gum Arabic and kappa carrageenan in pharmaceutical and food industries

CHARACTERISATIONS of SAMPLES

Analysis	Purpose of analysis
X-diffraction (XRD)	To identify solid state of film
Scanning electron microscope (SEM)	To observe the film surface morphology changes after the addition of semi refined kappa carrageenan
Tensile strength (TS)	To study the mechanical property of mixture film after addition of semi refined kappa carrageenan
Viscosity measurement	To identify the viscosity value which the dipping process can be conducted
Disintegration test (DT)	To ensure the capsule disintegrate within 15 minutes
Differential scanning calorimetry (DCS)	To study the endothermic and exothermic heat flow transition To identify the glass transition temperature of film
Thermogravimetry analysis (TGA)	To study weight loss pattern during the film degradation To plot DTG curve to determine temperature with the maximum weight loss To calculation the activation energy from major weight loss and broido model .

Raw material characterisations

Thermal properties: TGA and DTG curves



Two phases of the mass loss: water loss and film degradation

- **Similar pattern** of GA

(Ali et al., 2018; Daoub et al., 2016; Ganie et al., 2015; Cozic et al., 2009).

- The mass loss of first phase and second phase about 11.8 % and 63.92 % respectively.

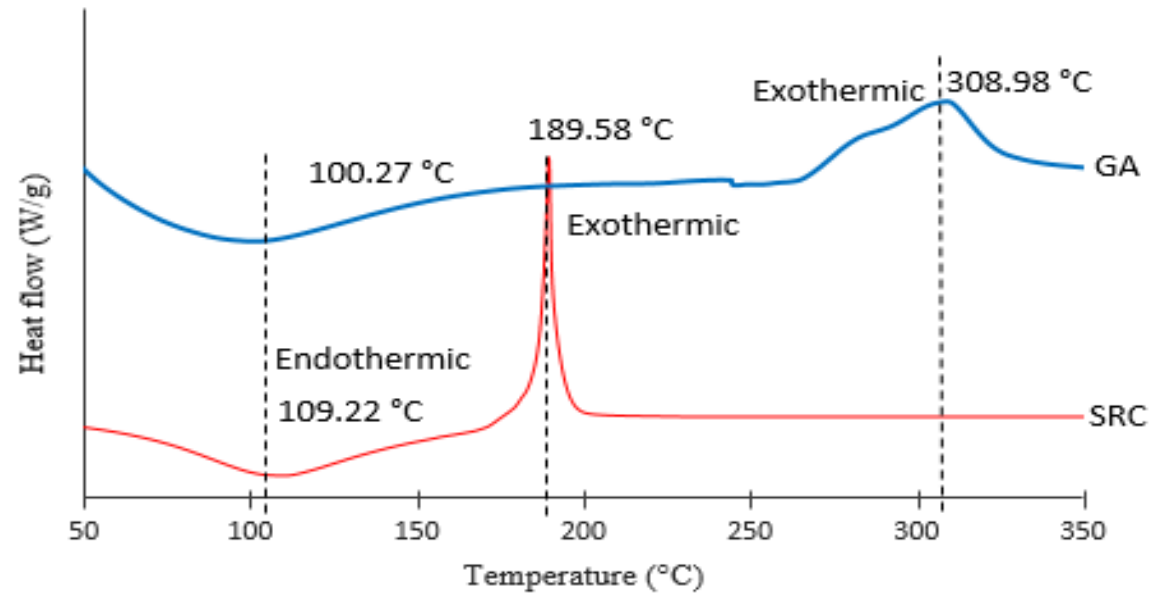
- SRC- two mass loss phases.
- The second phase mass loss is 56 % (Hezaveh & Muhamad, 2013).
- This different trend of the thermal degradation implies the **difference of their structure molecules and molecular weight** (Bothara & Singh, 2012)

- DTG

- GA : A strongly **sharp peak**. Ali et al., 2018; Zohuriaan & Shokrolahi, 2004)
- SRC: some **broad peaks**

Raw material characterisations

Heat flow transition



DSC curve of GA and SRC

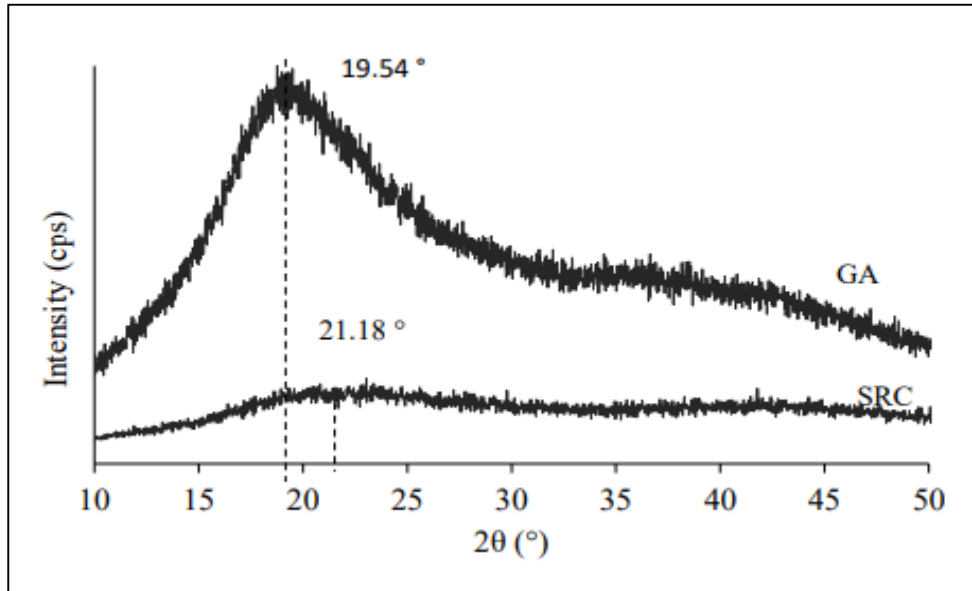
GA:

- Similar trend of GA (Zohuriaan & Shokrolahi, 2004)

SRC

- Similar trend of DSC curve was observed (Hezaveh & Muhamad, 2013).
- Endothermic and exothermic peaks at 100 °C and 180 °C respectively.
- Exothermic temperature of GA high because its complex structure which consisting several sugar units (Daoub et al., 2016).

Solid state and chemical elements of GA and SRC

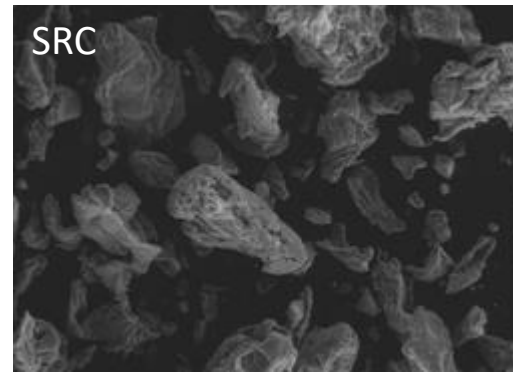
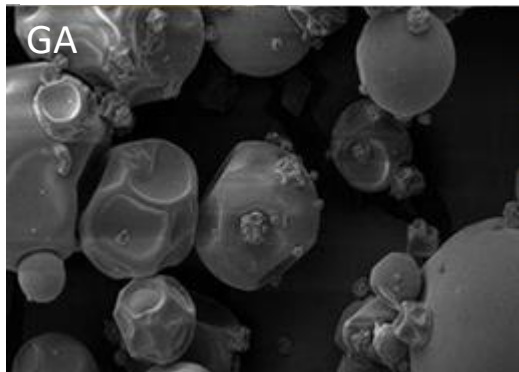
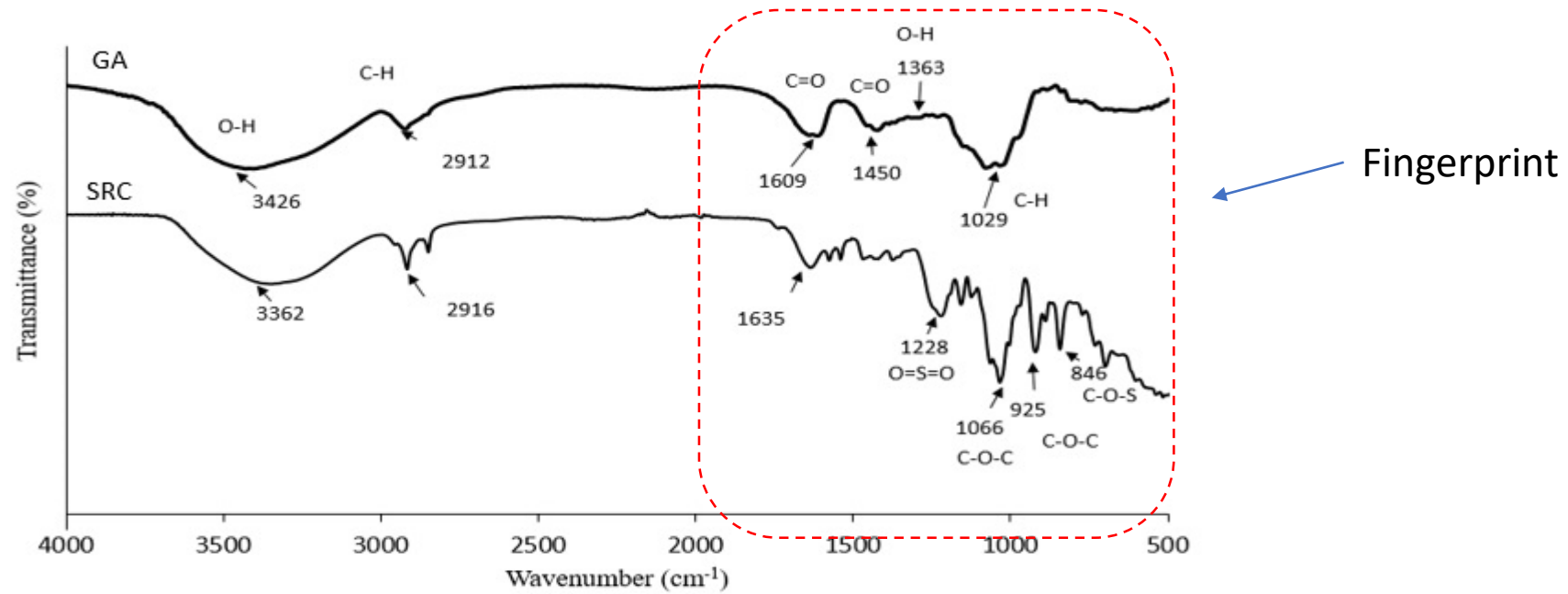


- GA and SRC are **amorphous**.
- XRD trends of GA: 2θ range of 19.50° to 19.88° (Ali et al., 2018; da S. Gulão et al., 2014; Cozic et al., 2009).
- SRC with $2\theta = 20.0^\circ$ (Ili Balqis et al., 2017).
- Less energy** is required to break down the amorphous structure (Weber et al., 2017).
- The **solubility and dissolution rate increased** (Riekens et al., 2010).

Elements	SRC (ppm)	GA (ppm)
Sodium(Na)	4504.70	455569.28
Magnesium(Mg)	673.74	2.06
Aluminium(Al)	150.10	406.45
Potassium(K)	65909.09	149.57
Calcium(Ca)	563.89	110.05

Elements	SRC (ppm)	GA (ppm)	JECFA (ppm)
Lead (Pb)	1.003	1.410	5
Arsenic(As)	0.921	Less than 0.5	3
Cadmium(Cd)	0.5395	0.0289	2

- The **impurities** in the GA and SRC.
- Potassium in SRC: contribute the **double helix formation** to form viscous solution (Campo et al., 2009).
- below the standard specification by **Joint FAO/WHO Expert Committee on Food Additives (JECFA)**



- GA: **Spherical** in shape with **many dents** (Ali et al., 2018; Uekane et al., 2016).
- SRC: uneven and **roughs surface** (Rudhziah et al., 2015)

FILM AND HARD CAPSULE PREPARATION

Preparation film is divided into 2 sections with different formulation:

Gum Arabic films (GF)

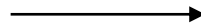
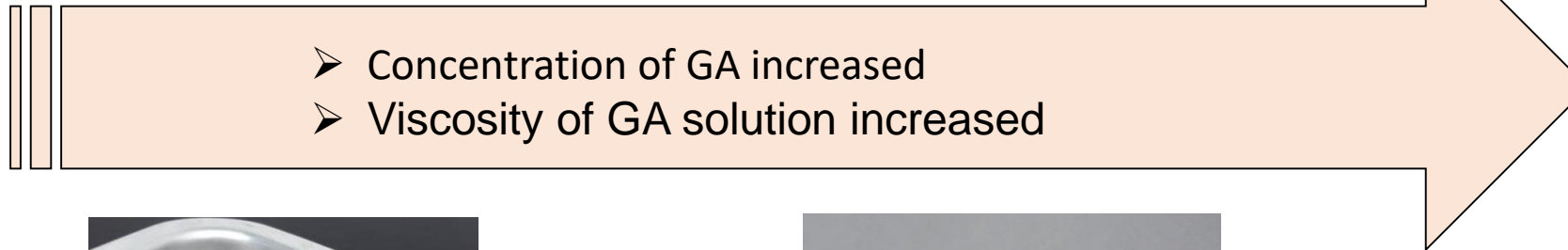
- At variation concentration
- 40% w/v to 90% w/v

GA and SRC composite film and hard capsule

- 33% w/w SRC
- 50% w/w SRC
- 67% w/w SRC
- PEG 400
- Alginate

GUM ARABIC FILMS

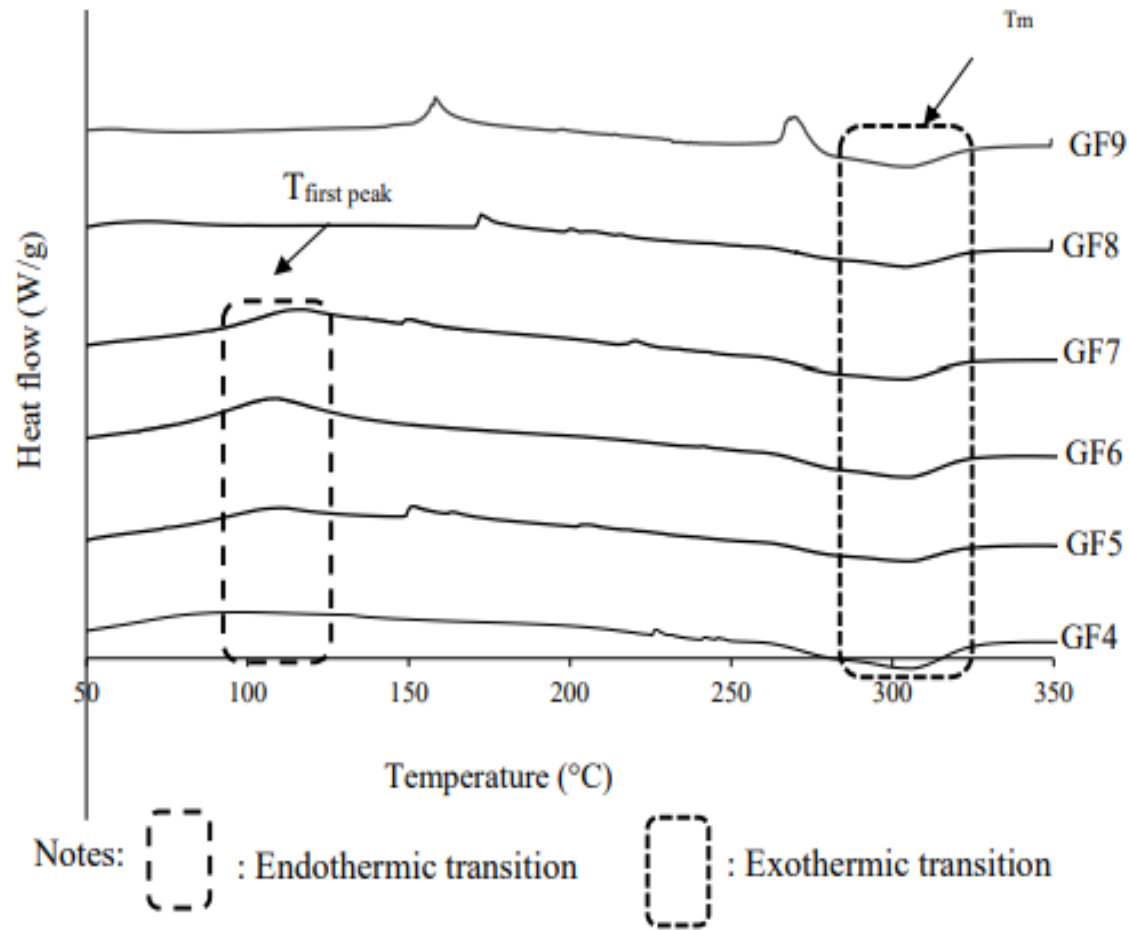
Visual observation on samples



Hard capsule
samples ruptured
during the capsule
removing.

Thermal properties of GA films

DSC cu



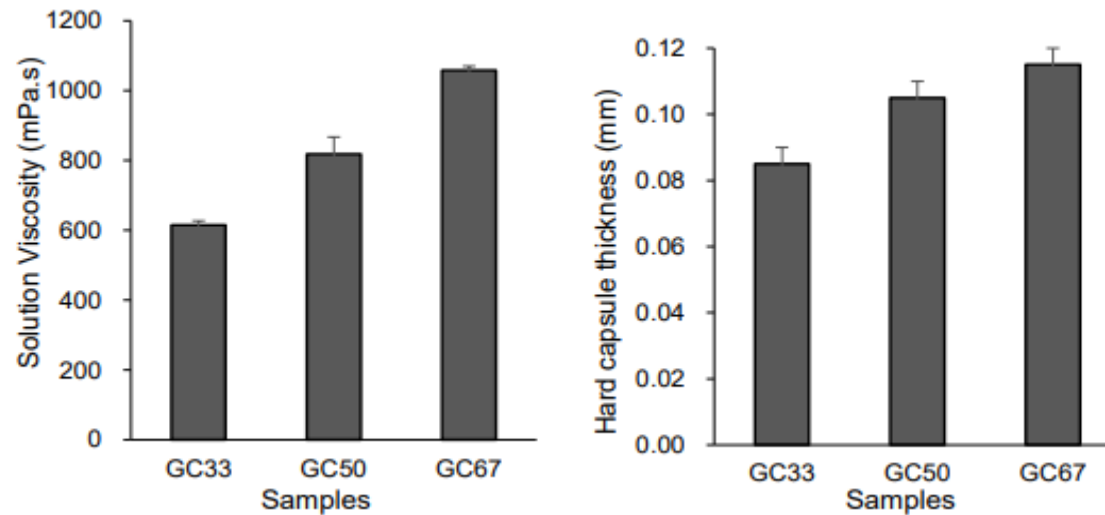
- Endothermic transition at 100 °C.
- Heat absorption for **dehydration of free and bonded water** (Mothe and Rao, 2000)
- Exothermic transition at around 300°C.
- **Film decomposition at high temperature** (Zohurian and Shokrolahi, 2004)

Conclusion of the GA films

- ✓ The ↑ GA concentration, The viscosity of GA solution ↑
- ✓ Viscosity value **above 600 mpa.s** managed to form hard capsule shell.
- ✓ The GA **capsule shell ruptured** during **the capsule removing** from the dipping bar.
- ✓ The GA films were **brittle and cracked** during placing it on the tensile strength machine. **Tensile strength test was not able to conduct.**
- ✓ GA formulation was modified by adding SRC

GA-SRC COMPOSITE HARD CAPSULE

- In this GA-SRC composite formulation, the addition of SRC is increased. (33 %w/w, 50 % w/w and 67 % w/w)



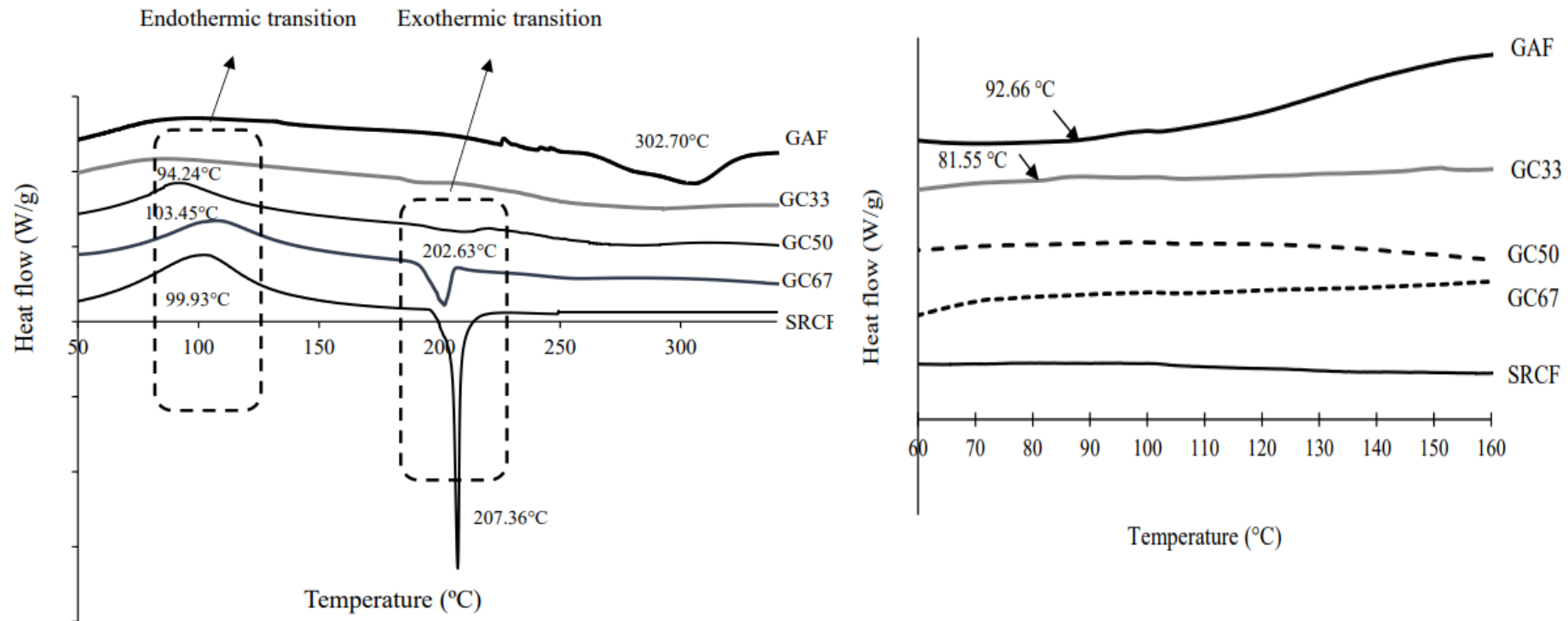
- The viscosity is increased with the increased of SRC
- The thickness of hard capsule is 0.08- 0.12mm
- All composite hard capsule were removed easily from dipping bar without ruptured.

Dented



Thermal properties of GA-SRC composites

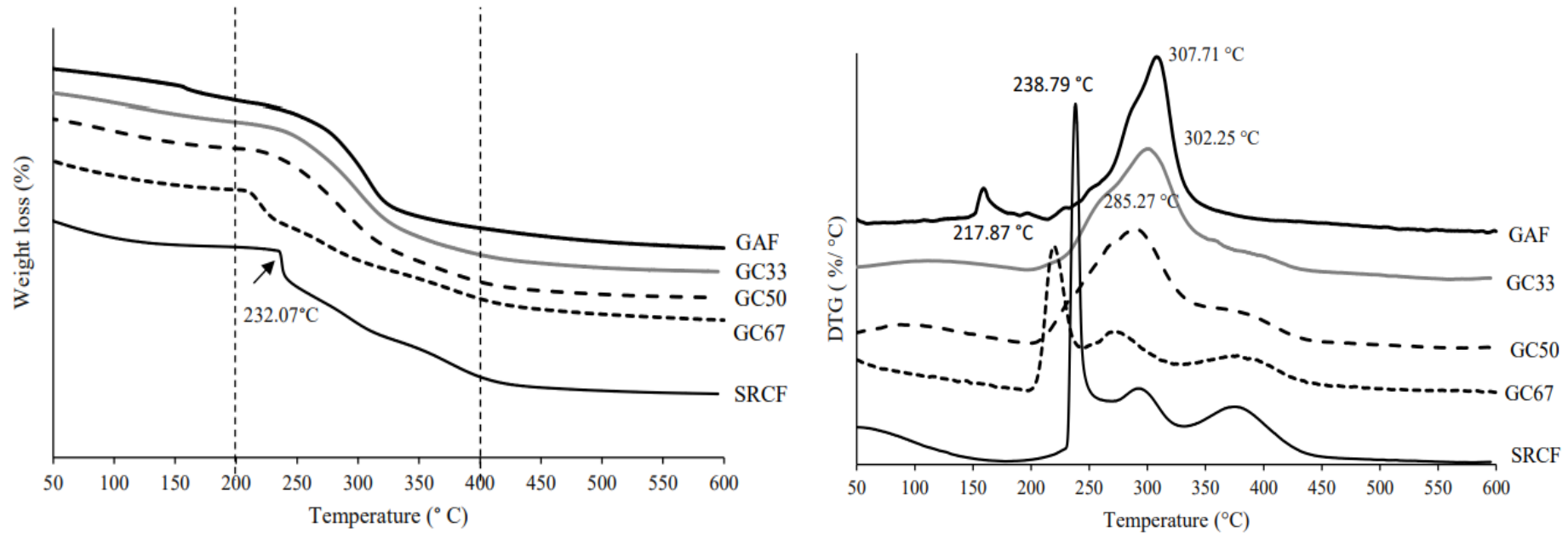
DSC curves of GA-SRC composites



- The changes on the DSC thermogram: probably the **changes on the molecule structures of the composites**.
- First exothermic peak is associated with the **SRC degradation**. (Ili balqis et al., 2017)
- Second exothermic peak is contributed by **GA degradation** (Zohuriaan and Shokrolahi, 2004).
- The addition of SRC is reduced the T_g as shown for GC33.
- GC50 and GC67 and SRCF do not exhibit the T_g . The set up of double heating with the minimum temperature at around 40°C.

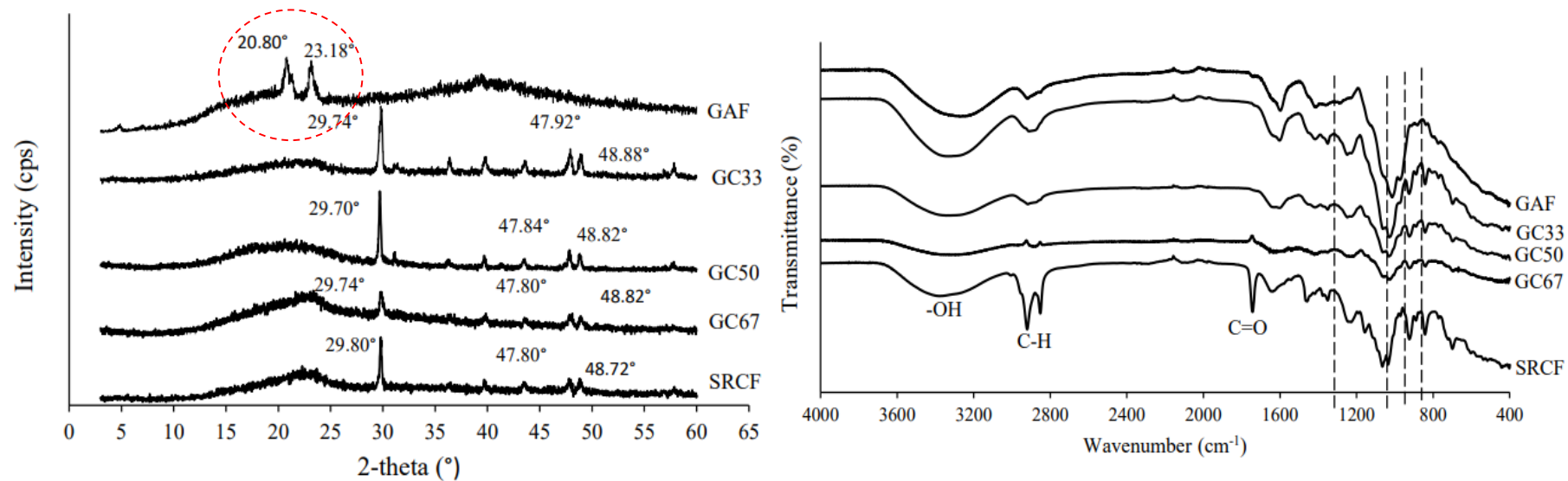
Thermal properties of GA-SRC composites

TGA and DTG curves of GA-SRC composites



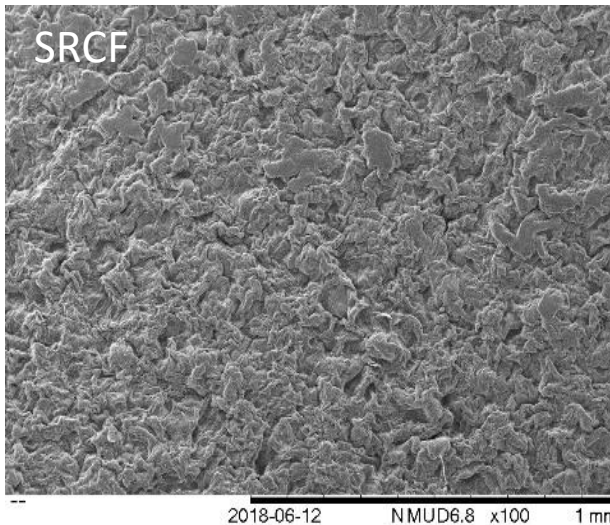
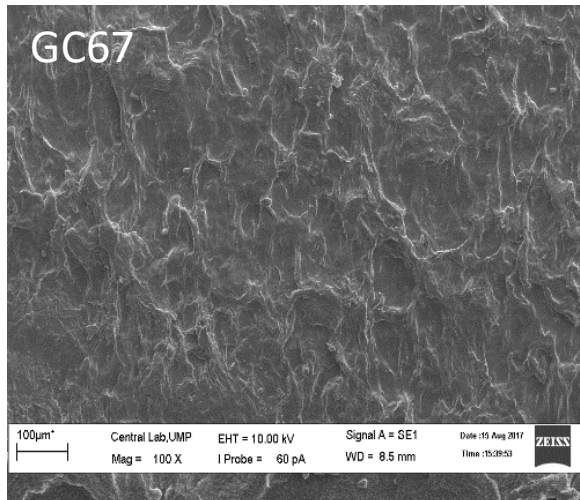
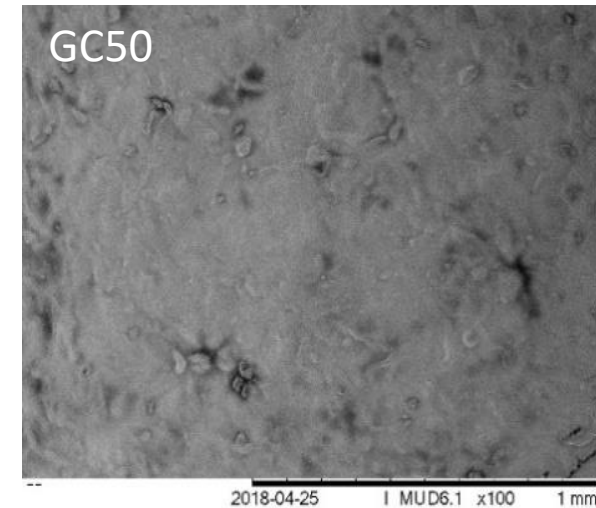
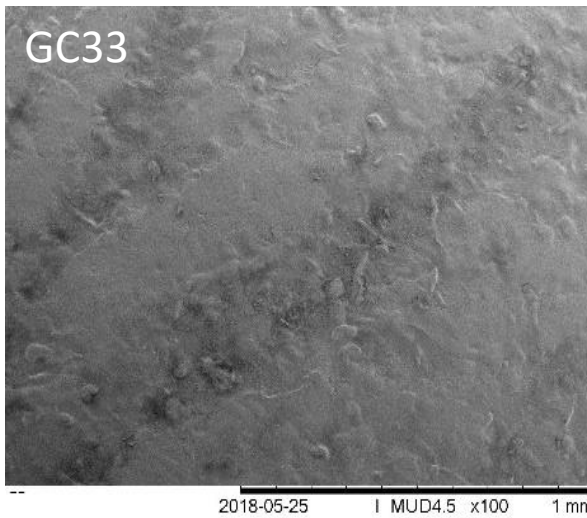
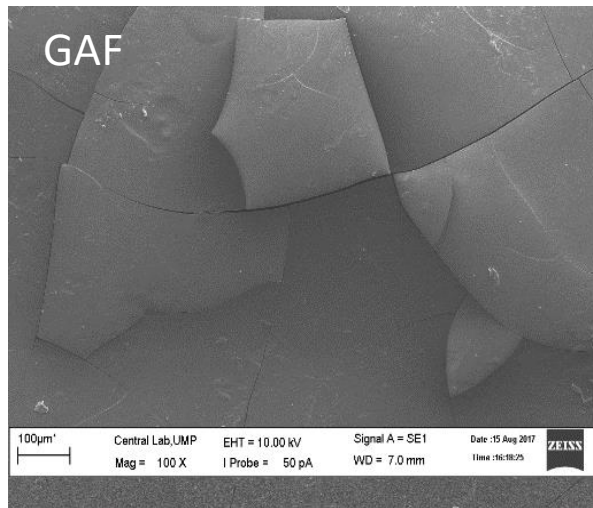
- The changes on TGA and DTG thermogram
- TGA patterns: **GC67** has the **lowest weight loss (53.69%)** with the highest of final residue (30.79%) at 600°C.
- Weight loss and final residue in range of 60.98-60.99% and 25.29-25.97% respectively.
- DTG of GC67 showed **the lowest value of T_{max} ; 217.87 °C.**
- The addition of SRC above 60% w/w into the hard capsule formulation, thermal properties were altered.
- **Thermal stability is reduced.**

XRD and FTIR Trends of GA-SRC composites



- GAF and SRCF : Amorphous with crystalline region.
- The addition of alginate and PEG 400 into the GA-SRC composites, two peaks disappeared.
- Addition of plasticiser dissolved the crystalline region (Ili Balqis,2017).
- The amorphous hard capsule probably can **increase sample solubility and dissolution rate**. (Riekes et al.,2010).
- GA-SRC composite, some new bands were observed between 400 cm⁻¹ to 1034 cm⁻¹ and 1240 cm⁻¹.
- The changing of peak intensity and broadness of regions.

Surface morphologies of samples

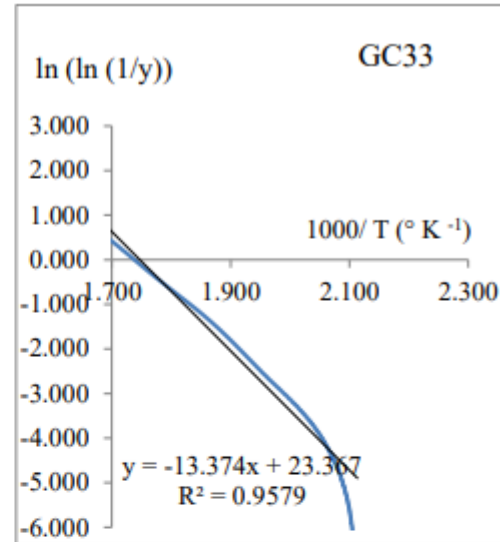
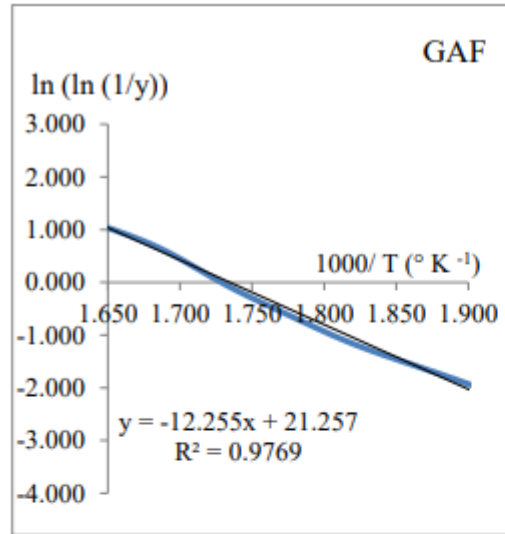


- ❑ GAF film : smooth surface with some cracks and brittle.
- ❑ SRCF film : Rough surface due to the entanglement behaviour (Roldán et al., 2017)
- ❑ GA-SRC composites; no cracks were observed. SRC weight ratio increased, the surfaces roughness increased.

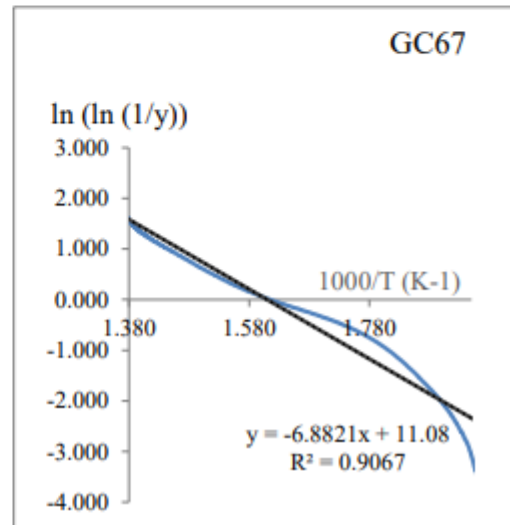
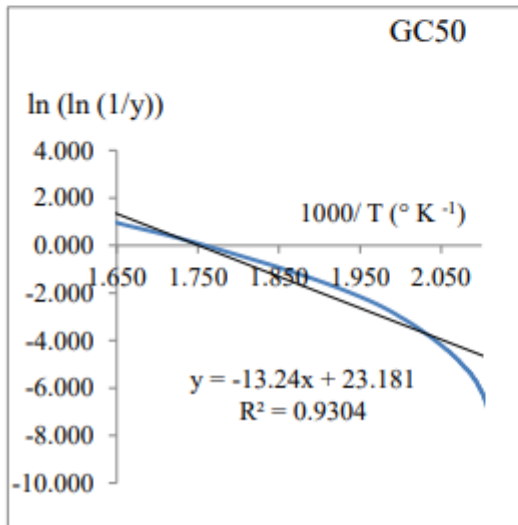
Activation Energy

- Activation energy calculated : Broido model and TGA data.
- A **minimum energy** to **break the molecule bond** of material structure during **thermal degradation** (Maleque, 2013).
- An indicator of material **thermal stability study** (Barreto et al., 2003) and useful to **predict product life time** (Iqbal et al, 2013).
- Activation energy is **changed with the changes of the natural molecule structure** film (Iqbal et al., 2011; Maciel et al., 2005).
- Activation energy of films was **reduced due to sulfate group** from kappa carrageenan (Roman & Winter, 2004).
- Based on the E_a values, thermal stability is in the order of:

GAF > GC33 > GC50 > GC67



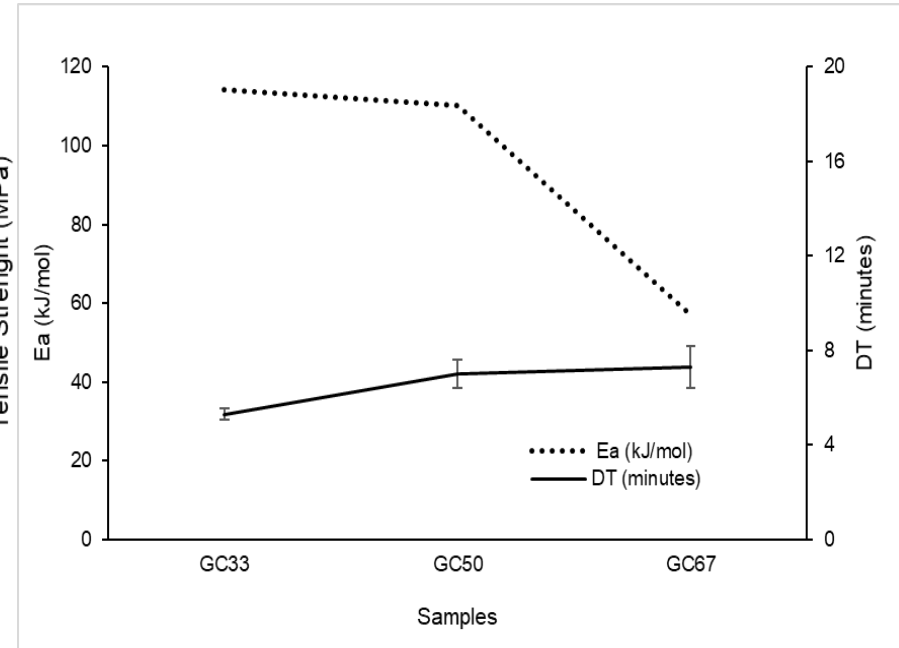
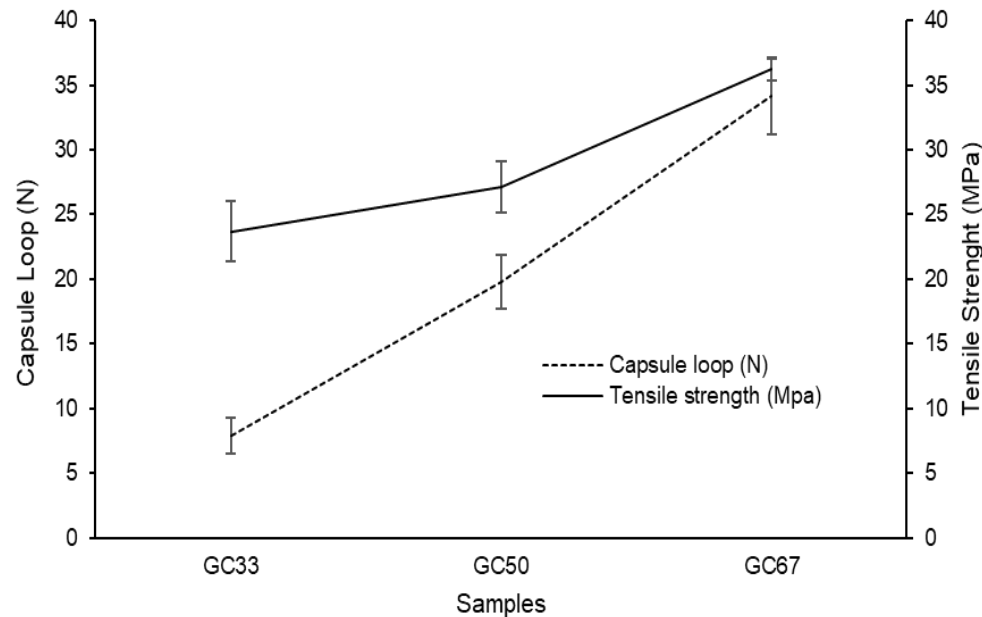
E_a (kJ/mol)	
Samples	
GAF	168.10
GC33	114.18
GC50	110.08
GC67	57.08



$$\ln [\ln 1(1-\alpha)] = - \left(\frac{E_a}{RT} \right) + \text{constant}$$

$$\ln [\ln 1(1-\alpha)] = \ln \ln (1/y)$$

$$\left(\frac{E_a}{R} \right) \left(\frac{1}{T} \right) = x \left(\frac{1000}{T} \right)$$



- Indicators for the hard capsule resistance.
- Potential applications as hard capsule materials
- Tensile strength and capsule loop increased with increases SRC.

- The DT of composite **does not change a lot with the increased of SRC.**
- The **thickness of capsule shell also influenced the DT results.**
- GC33 with **0.08mm** showed the **faster of DT time.**
- No significant effect between of activation energy and DT time.

CONCLUSION

1. Gum arabic film (GAF) alone is **not suitable** for hard capsule application:

- ❑ **Brittleness** problem
- ❑ The **low viscosity** property of gum arabic solution lead to the **failure of dipping process**
- ❑ GA hard capsule was **not able to produced**.

2. GA-SRC composite hard capsule:

- ❑ **Showed the good improvement** of almost film and hard capsule characterisation.
- ❑ The **hard capsules** were **successfully developed** and the **tensile strength result** was obtained.

The summarised of important parameters of the mixture hard capsule:

- ❑ The **viscosity of solution** must be **above 1100mpa.s** to ensure the dipping process conducted.
- ❑ The obtained thickness of hard capsule **around 0.1mm**
- ❑ All composite hard capsule **disintegrated below 15 minutes**.

The characterisation of GA-SRC composites:

The increased of SRC in composite formulation caused:

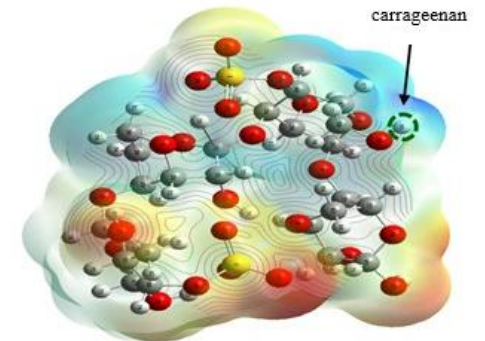
- ❑ The **melting temperature** of mixture film was reduced.
- ❑ The **thermal stability and activation energy** were decreased
- ❑ The mixture solution **viscosity and tensile strength** of film were increased
- ❑ In term of tensile strength, GC67 has **the highest value** about 58.26 kN/m² and become the best formulation.

Thank You

From Molecule to Product: Development of Stable Kappa Carrageenan Capsule Through Molecular Properties Manipulation

Associate Professor Dr Fatmawati binti Adam

Faculty of Chemical and Process Engineering Technology



Project Background

- Hard capsule – **easy and versatile drug delivery carrier** –
- Muslim population increasing – expected in 2030, 1 of 3 person will be muslim (Population Reference Bureau), **1.6 billions**
- **100 millions vegetarian**
- At present, the application of hard capsule has been increased which **not limited to the solid powder**, but can be used to **deliver the liquid or granule form** of filling such as illustrated in Figure 1.



Figure 1: Several types of potential hard capsule applications (Doshi et al., 2011).

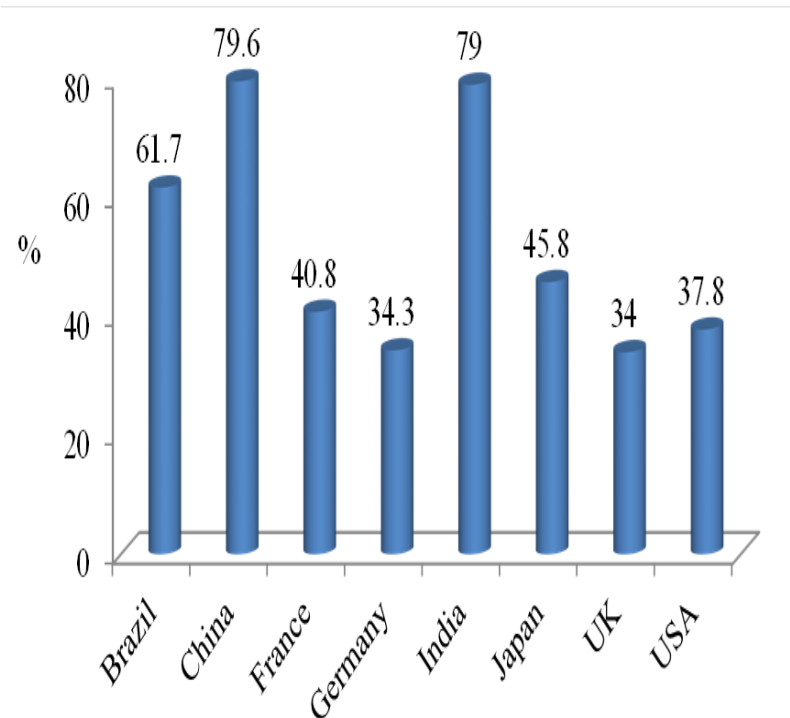


Figure 1=2: Consumer survey on **their willingness to pay extra** for **vegetarian hard capsule** by Capsugel (2015).

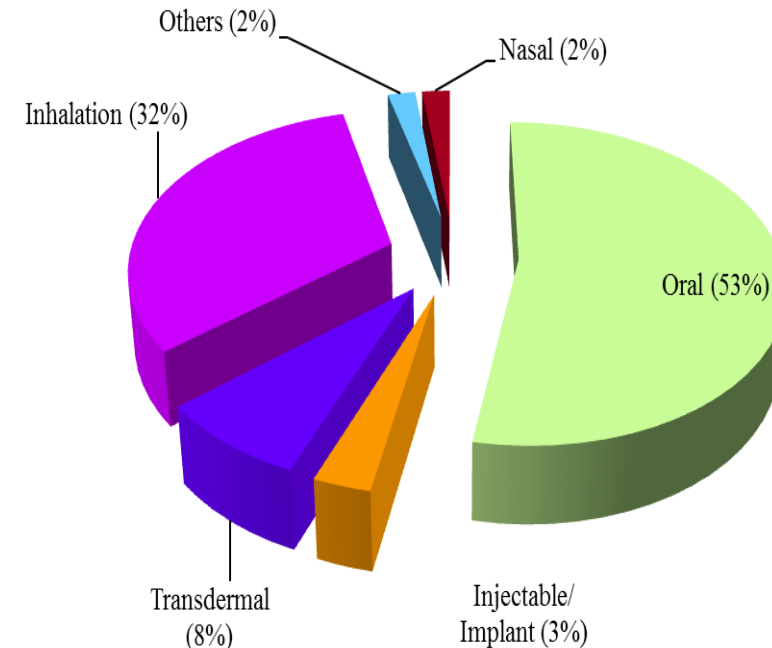


Figure 3: Global **drug delivery market** by administration mode (Senthilk, 2015).

- Carrageenan (**local** Rhodophyceae **seaweed**)
 - Polysaccharides – Vege base- inexpensive, **easy cultivation** and renewable
 - **3,6-anhydro group** promotes α helix formation which is important for gelling (Lamond, 2004) -
 - increased its flexibility
 - **ester sulfated groups** - **hydrogen bond** with crosslinker agent - leads to a physical crosslink – easy to disintegrate (DT)
- Manipulation of crosslink method was used to produce film which can be **disintegrate** rather than **swelled**
 - Crosslinker which has a good **H-bond network** – with natural compound extracted from plant base as targeted compound
- The **quantum mechanics** is one of the physical concepts used to explain the nano and microscale phenomena. The matrix mechanic and wave mechanic are the two subjects within this concept

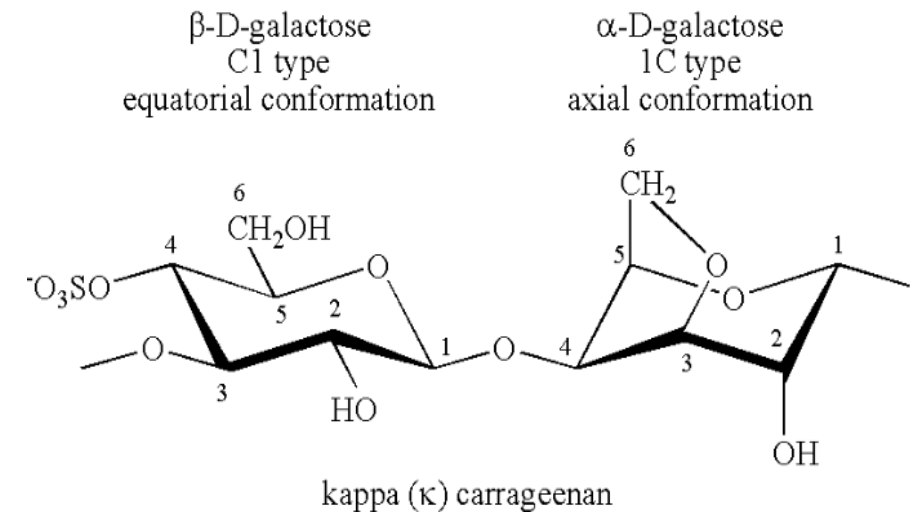


Figure 4: Monomer of κ Carrageenan.

Objective

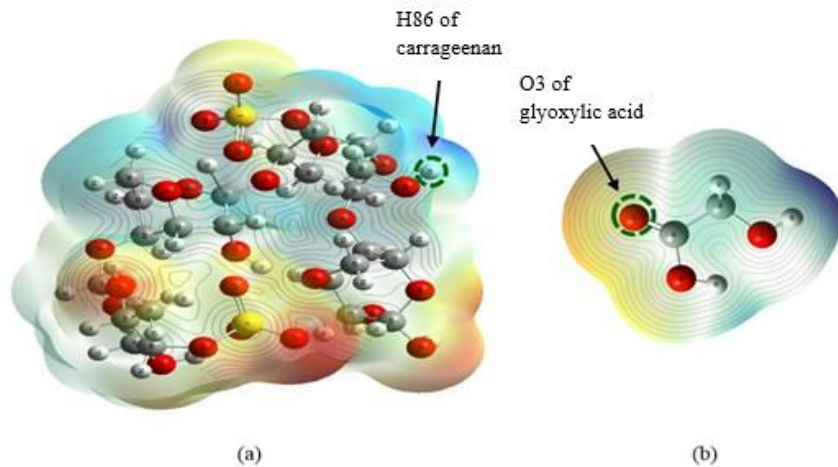
- To **simulate the structure of solid kappa-carrageenan capsule** as a **function of cross-link agent type at molecular scale**. The molecular interaction strength presence in the system will be calculated through the hydrogen bonding interaction and radial distribution function.
- To **formulate and produce the hard carrageenan capsule** which can improve its properties through **molecular recognition approach** by using **crosslink technique** on kappa-carrageenan. Possibility of forming different degree of hydrogen bonding (synthons) between k-carrageenan molecule and cross-link agent molecule will influence **the final product property of kappa-carrageenan capsule**.
- To **analyse and characterise the macroscopic and microscopic properties** of produced kappa-carrageenan capsule viz morphology, strength, hydrogen bonding, structure and swelling.

.

Determination Of Physical Crosslink Between Carrageenan And Glyoxylic Acid Using Density Functional Theory Calculations

Objective: To predict the possible location of the physical crosslink in the conjugate complex between carrageenan and glyoxylic acid (film of carrageenan and glyoxylic acid)

Method: Gaussian 09W software at B3LYP (Becke's three-parameter functional and nonlocal correlation of LYP expression).



The order of increasing electron is arranged as per following sequence:

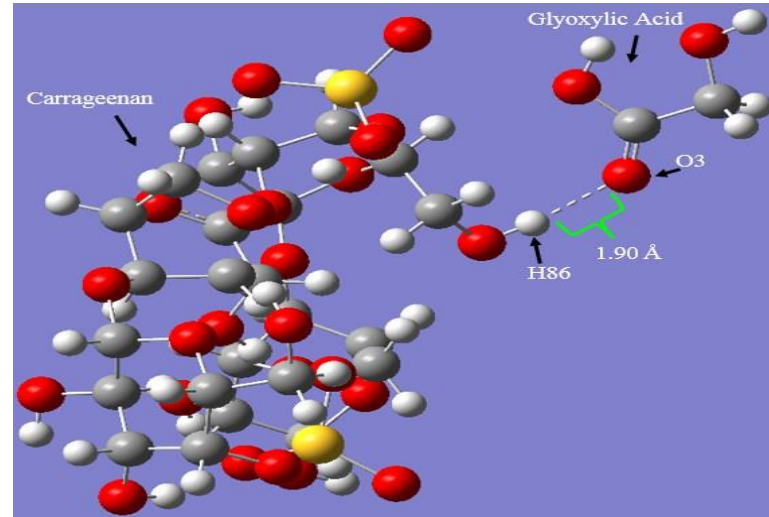
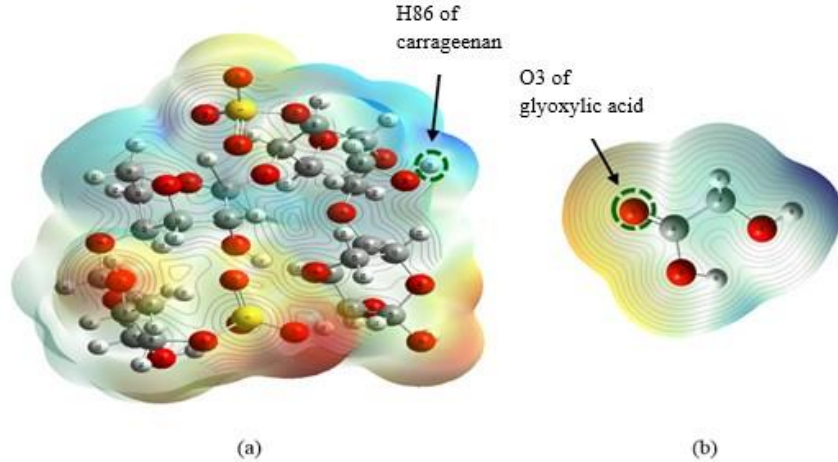
red < orange < yellow < green < blue.

Potential increases (electron rich)

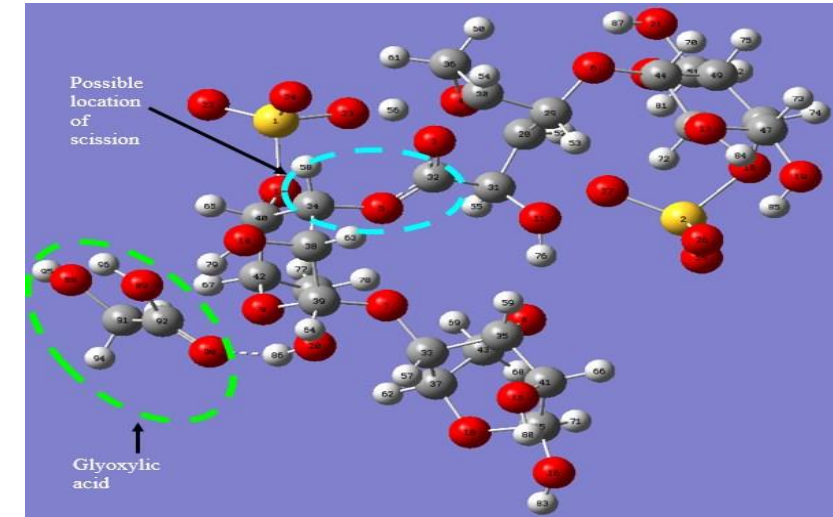
The **molecular electrostatic surface potential (MESP)** analysis for optimized molecule structure of (a) k-carrageenan and (b) glyoxylic acid

most electron rich surface is in red colour while poor of electron surface is in blue colour.

Determination Of Physical Crosslink Between Carrageenan And Glyoxylic Acid Using Density Functional Theory Calculations



Hydrogen bond point between H86 --- O3 generated from the optimization calculation



Probability of scission effect in conjugate complex k-carrageenan-glyoxylic chains

Determination Of Physical Crosslink Between Carrageenan And Glyoxylic Acid Using Density Functional Theory Calculations

Objective: To predict the possible location of the physical crosslink in the conjugate complex between carrageenan and glyoxylic acid (film of carrageenan and glyoxylic acid)

Method:Gaussian 09W software at B3LYP (Becke’s three-parameter functional and nonlocal correlation of LYP expression .

Component	SCF energy for optimized molecule (kJ mol ⁻¹)
k-Carrageenan	-938 9839.095
Glyoxylic acid	-798 961.796
k-Carrageenan – glyoxylic acid	-1 018 876.626
Interaction energy (ΔSCF energy)	-75.735

Component	C32	O5	C34	ΔMC	C32 – O5	ΔMC	O5 – C34
k-Carrageenan	-1.850	0.180	0.617		2.030		0.437
k-Carrageenan - glyoxylic acid	0.054	-0.442	0.691		0.492		1.133

Synthetic crosslinker	Funtional group available
Glyoxylic acid	Double bond O, Hydroxyl

SCF energy value for optimized k-carrageenan, glyoxylic acid and conjugate complex k-carrageenan-glyoxylic acid

Mulliken atomic charges, and absolute Mulliken atomic charges (ΔMC) obtained for optimized k-carrageenan and conjugate complex of k-carrageenan-glyoxylic acid.

$$\text{Interaction energy} = E_{\text{SCF complex}} - \{E_{\text{SCF polysaccharide}} + E_{\text{SCF crosslinker agent}}\}$$

$$\Delta H_{\text{formation complex}} = H_{\text{complex}} - \{H_{\text{polysaccharide}} + H_{\text{crosslinker agent}}\}$$

H = Sum of electronic and thermal Enthalpies

In the geometry optimization calculation, the lowest self-consistent field (SCF) energy was produced. The SCF energy is the electronic energy of the system at 0 Kelvin

Molecular recognition of isovanillin crosslinked carrageenan biocomposite for drug delivery application

Method: Gaussian 09w

Objective: to evaluate carrageenan as a potential biocomposite for hard capsule in the drug delivery application

H – bond interaction energy

= ESCF_{complex} – (ESCF_{polysaccharide} + ESCF_{isovanillin})

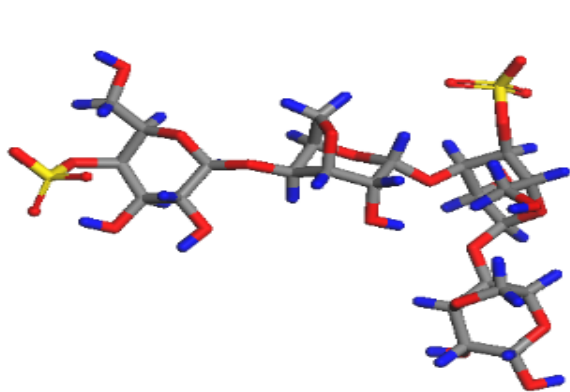
(1)

ΔH formation complex

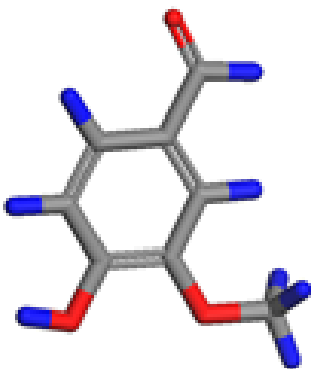
= H_{complex} – (H_{polysaccharide} + H_{isovanillin})

(2)

H is the sum of electronic and thermal enthalpies from frequency calculation.



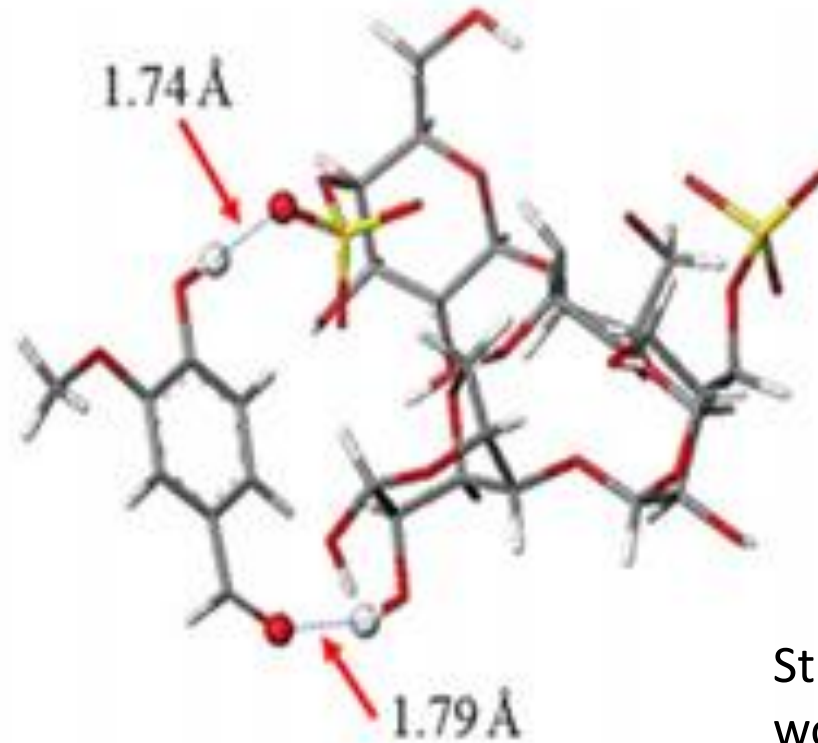
carrageenan–isovanillin.



Natural crosslinker	Funtional group available
Iso vanillin	Double bond O, Hydroxyl

κ-carrageenan	Double bond O, hydroxyl, ester sulfate
Monomer = C ₂₄ H ₃₆ O ₂₅ S ₂	

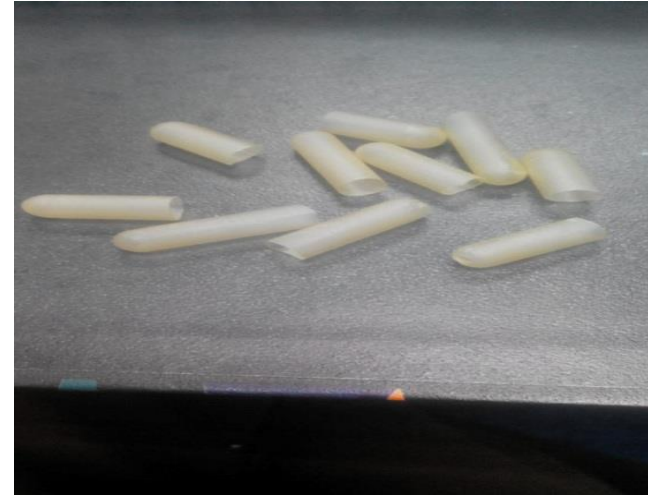
Molecular recognition of isovanillin crosslinked carrageenan biocomposite for drug delivery application



The H-bond interaction energy between isov. and carrageenan is - 235.997 kJ mol⁻¹ with a H-bond length of 1.74–1.79 Å

Strong intermolecular interaction would lead to a strong tensile strength of the biocomposite film

Early Work of Hard Capsule Product Prototype



Photos of hard capsule samples through manual dipping process.



Tuning mechanical properties of seaweeds for hard capsules: A step forward for a sustainable drug delivery medium

Most of the renewable polymers do not meet sufficient mechanical strength for developing hard capsules.

However, after drying process, carrageenan tends to become brittle due to formation of double helices upon heating (Farahnaky, Azizi, Majzoobi, Mesbahi, & Maftoonazad, 2013; Zarina & Ahmad, 2015).

It caused the carrageenan film to have low mechanical stability, thereby offering significant challenges in removing carrageenan films from the capsule mold without breaking.

One of the solutions to solve the brittleness issue is by incorporating plasticizer and crosslinker in the product formulation.

Plasticizers such as glycerol and polyethylene glycol (PEG) have been incorporated in the carrageenan biocomposite formulation and successfully reduced the brittleness and improve the flexibility of the films (Phan The et al., 2009). Meanwhile the incorporation of crosslinker improved the mechanical property.

Hydrogen bonding formation in the Biocomposite Film

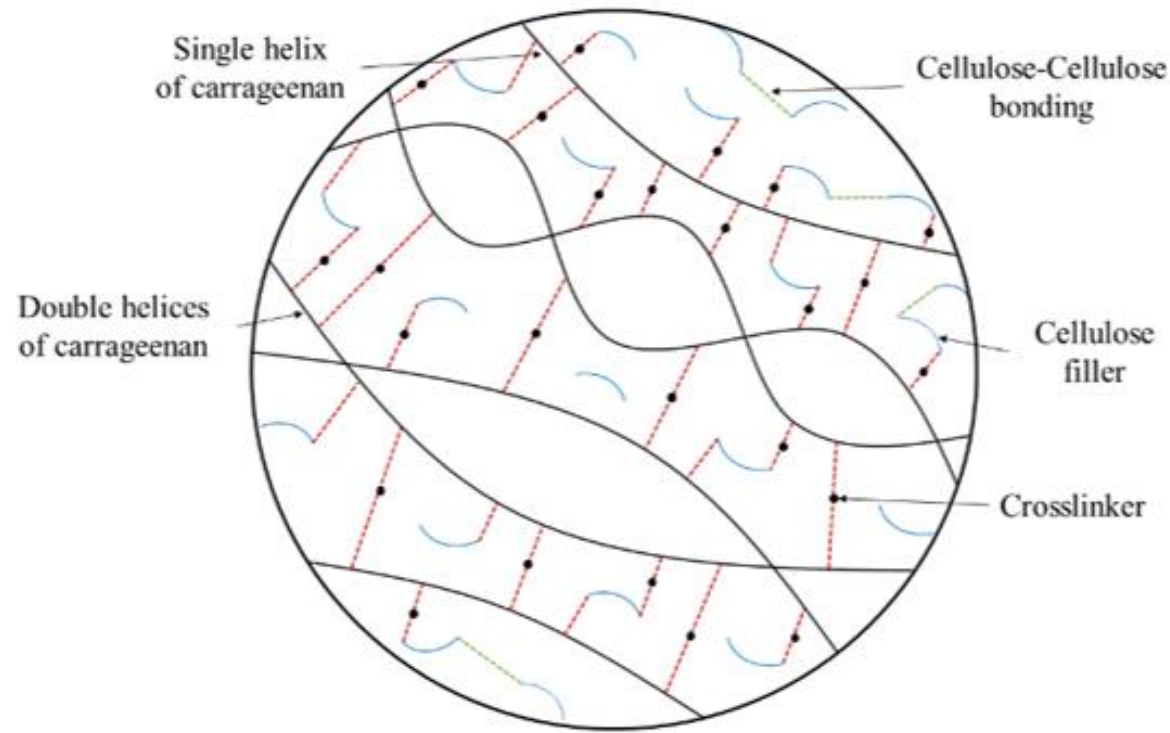
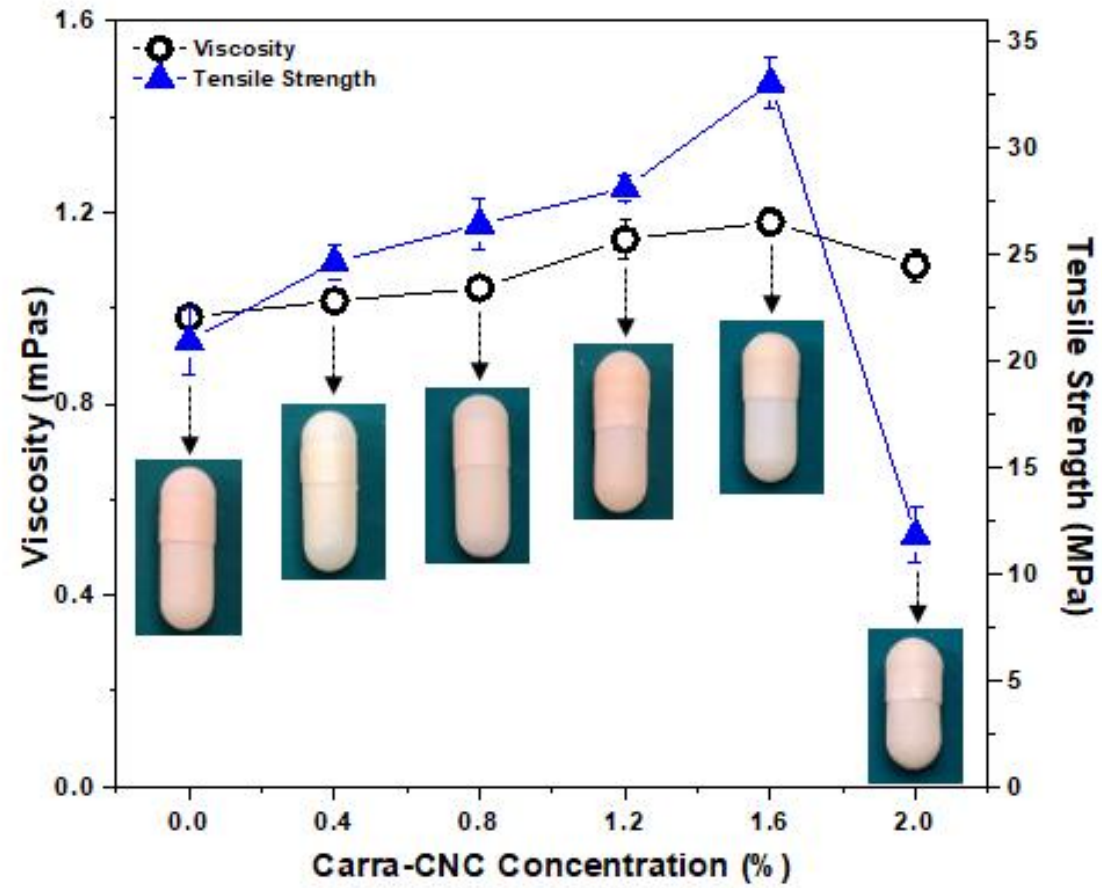


Illustration showing the mechanism of CNC as a filler in the carrageenan matrix

Mechanical and Rheological Properties







Viscosity of carrageenan solution, tensile strength of sample film, and physical appearance of carrageenan hard capsule.

Hard Capsule Disintegration Test

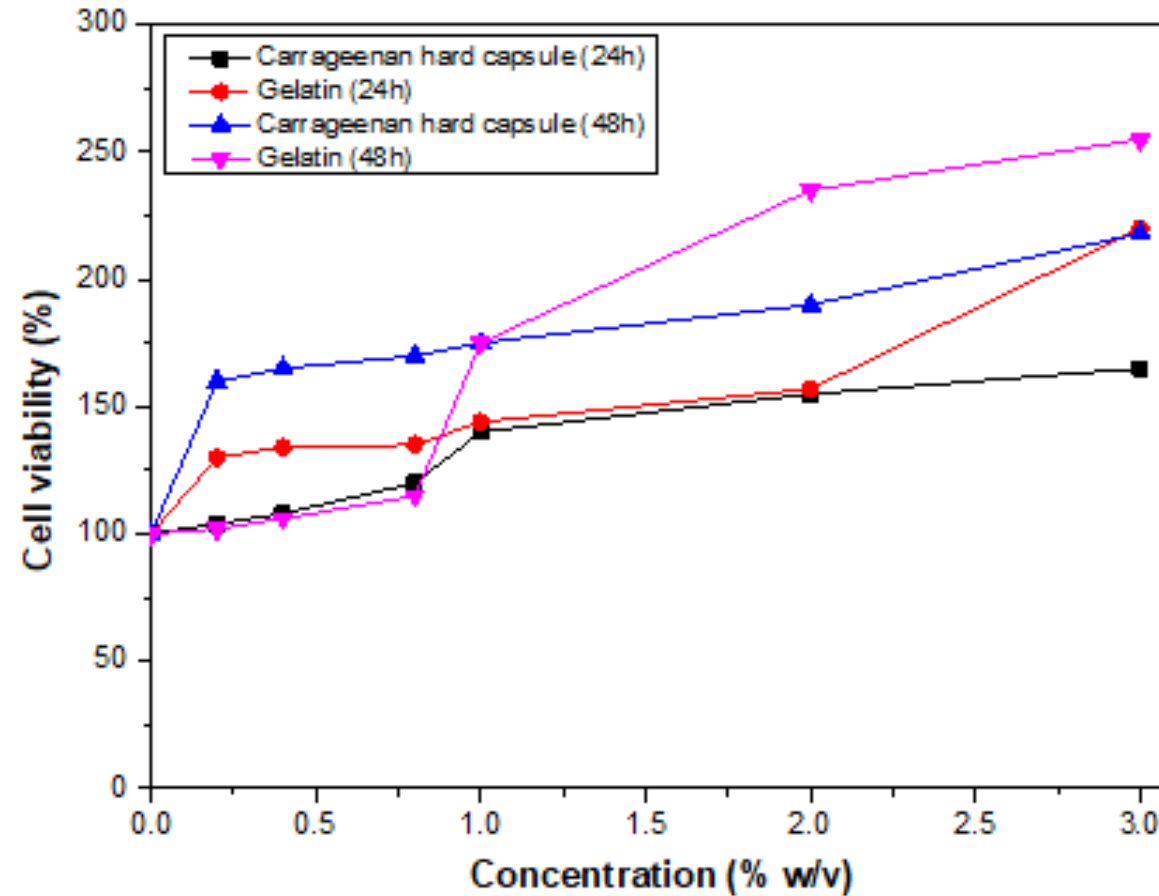
Hard capsule disintegration time of carrageenan film and its nanocomposites

Sample	Disintegration Time (min)
Control	11.96 ± 0.50
Carra-CNC0.4	12.38 ± 0.55
Carra-CNC0.8	11.85 ± 0.58
Carra-CNC1.2	8.39 ± 0.53
Carra-CNC1.6	11.27 ± 0.15
Carra-CNC2.0	13.12 ± 0.16

Antibiotic stability test of carrageenan hard capsule

Antibiotic name	pKa of antibiotics	Physical properties observation after 14 days	Hard capsule sample image
Blank	-	No changes observed in hard capsule and powder colour and odour	
<u>Amoxycillin</u> 500 mg	2.4	No changes observed in hard capsule and powder colour and odour	
Ampicillin 500 mg	2.5	No changes observed in hard capsule and powder colour and odour	
Doxycycline 100 mg	3.5	No changes observed in hard capsule and powder colour and odour	

Cytotoxicity Study of Carrageenan Hard Capsule



Cell viability was measured using MTT assay at 24 and 48 hours of cell treatment for control and anisyl crosslinked sample.

Study Summary

Cellulose nanocrystals (CNC) filler can increase the mechanical strength of carrageenan film for their application as a hard capsule.

The CNC is a rod shaped with length in the ~52-265 nm and diameter in the ~19-71 nm ranges and had an average aspect ratio of ~2.7.

The CNC toughened carrageenan had a tensile strength up to 58% compared to the films without the filler which carrageenan films containing 1.6 wt./v% of CNC is optimum for producing stable films. This composition also had the favourable rheological properties for formation of stable hard capsules.

A disintegration test conducted on the stability of the hard capsule at physiological conditions showed complete disintegration in less than 15 mins.

The hard capsule passed the stability test with three types of antibiotics, which suggested that it is suitable for application as a drug delivery system. This study also indicated that this solvent free CNC is suitable for food and pharmaceutical application especially incorporation with carrageenan.

Reinforced Bioplastic Film at Different Microcrystalline Cellulose Concentration



Plastic pollution has led to the development of bioplastic to replace conventional petroleum-based plastic.

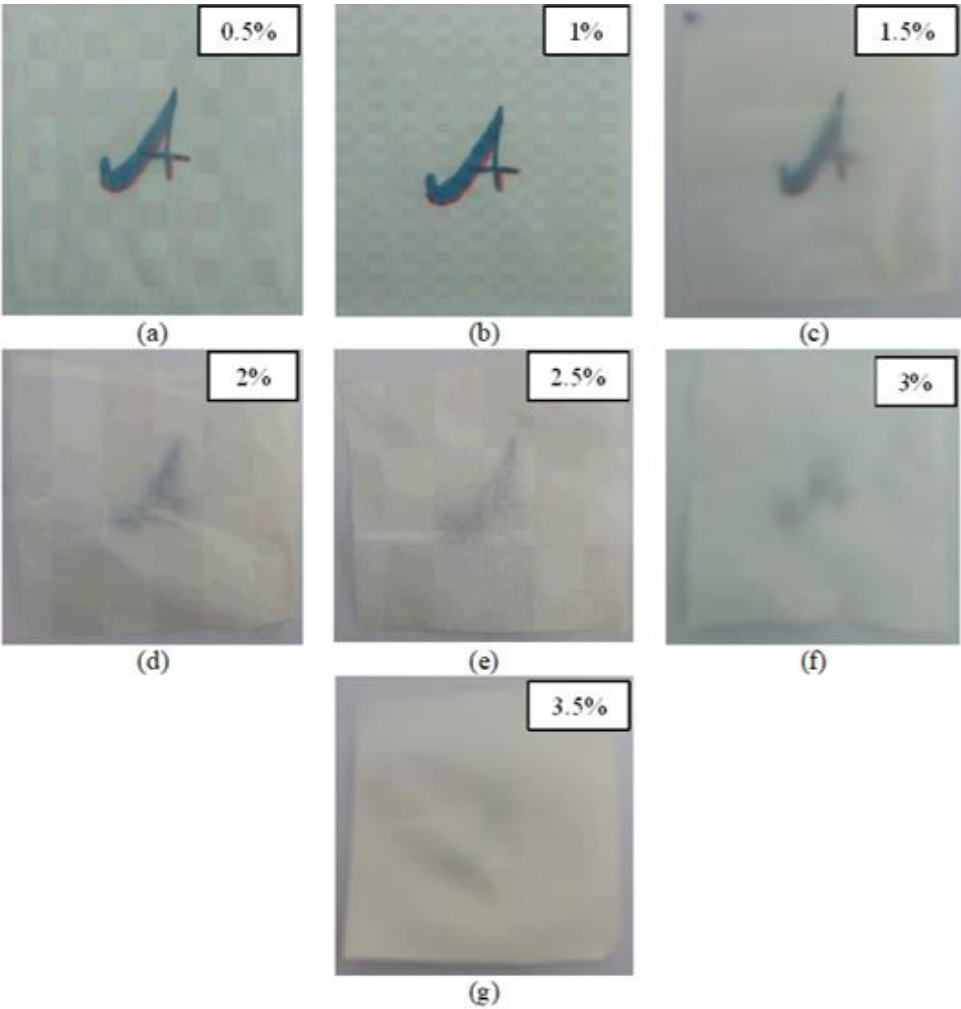
- ✓ China, Indonesia, Philippines, Sri Lanka and Vietnam generate **50% of global plastic pollution**
- ✓ Malaysia contribute 5% of plastic pollution

This study is to formulate and produce bioplastic films reinforced from a renewable resource using carrageenan, microcrystalline cellulose (MCC), polyethylene glycol (PEG), glyoxylic acid and hydroxypropyl methylcellulose (HPMC) to produce.

Moisture content of bioplastic

Moisture content of the carrageenan-cellulose films.

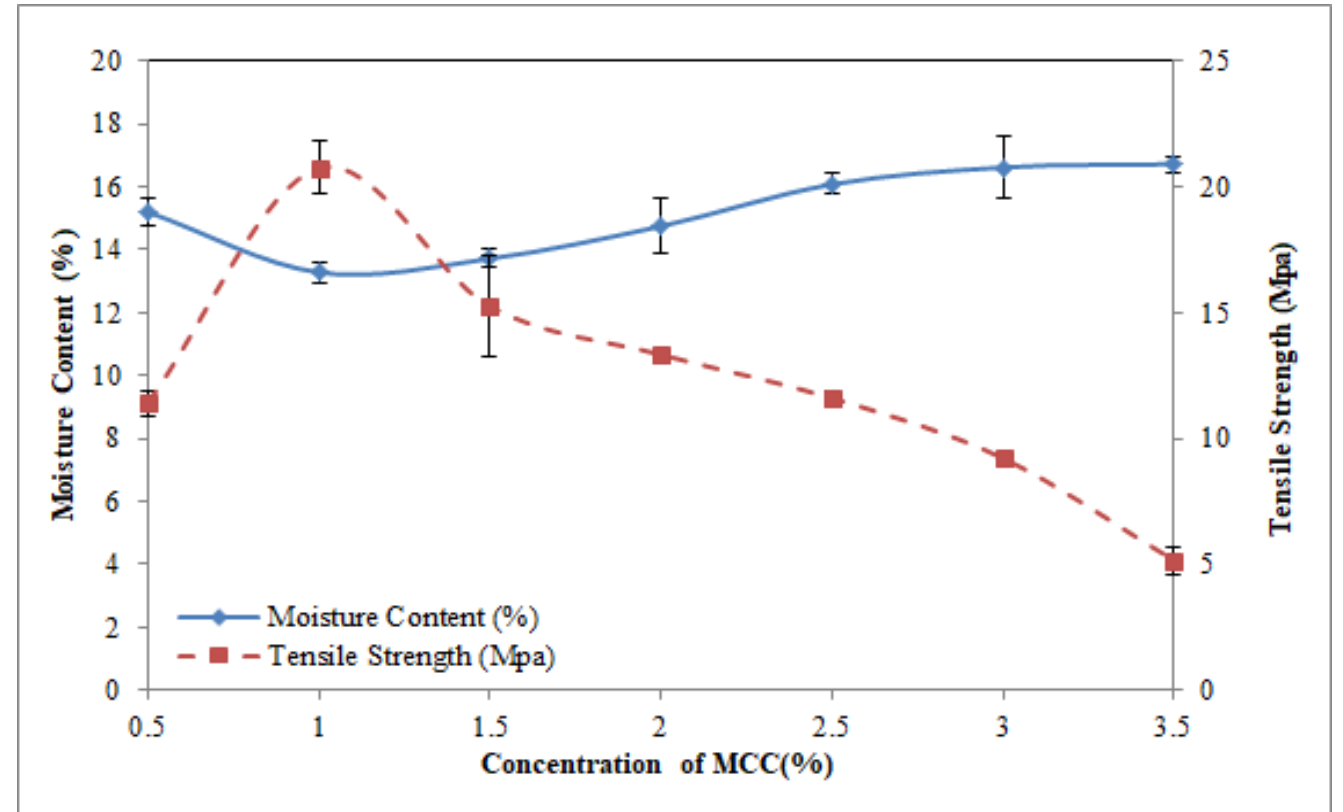
Concentration of MCC (%)	Moisture Content (%)
0.5	15.20 ±0.43
1	13.28 ±0.31
1.5	13.72 ±0.31
2	14.75 ±0.86
2.5	16.08 ±0.33
3	16.62 ±1.02
3.5	16.72 ±0.25



Moisture Content and Appearance of the Biofilm



Production Date:
Feb 2020

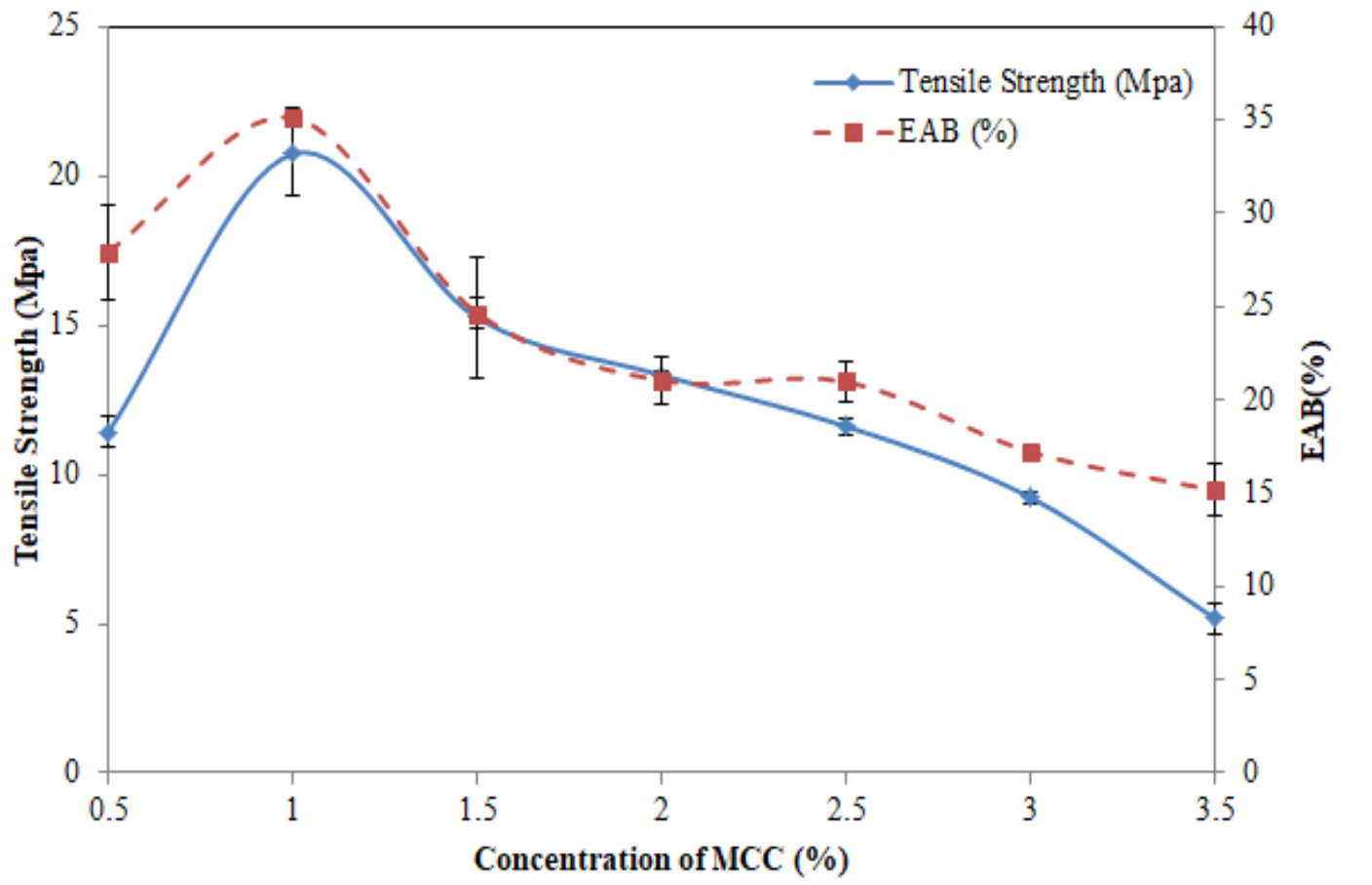


Moisture content and tensile strength of carrageenan-cellulose films.



Production Date:
Feb 2020





Relationship of (a) tensile strength and viscosity and (b) tensile strength and EAB of carrageenan-cellulose films.

tensile strength (MPa) = (load at break) / (original width)(original thickness)

elongation at break (%) = (elongation at rupture/initial gage length) × 100

Study Summary

In conclusion, the addition of the MCC into the matrix of carrageenan biocomposite improved the tensile strength EAB, water content & the appearances of the films.

However, as the percentage of the MCC increased from 0.5% until 3.5% the mechanical and physical of the films changed where the results shows that biofilm with 1% of MCC give the most favorable properties for bioplastic. The film has the highest value of viscosity, tensile strength and EAB which were 352.55 mPa/s, 20.74 MPa and 35.12%, respectively. Thus, 1% of MCC bioplastic holds the priority to be further explored as a potential packaging material.

Active Packaging Semi-refined carrageenan film incorporated with α -tocopherol: Application in food model

Objective:

To formulate Semi-refined carrageenan (SRC) film plasticized with glycerol and incorporated with α -tocopherol was prepared for food packaging application.

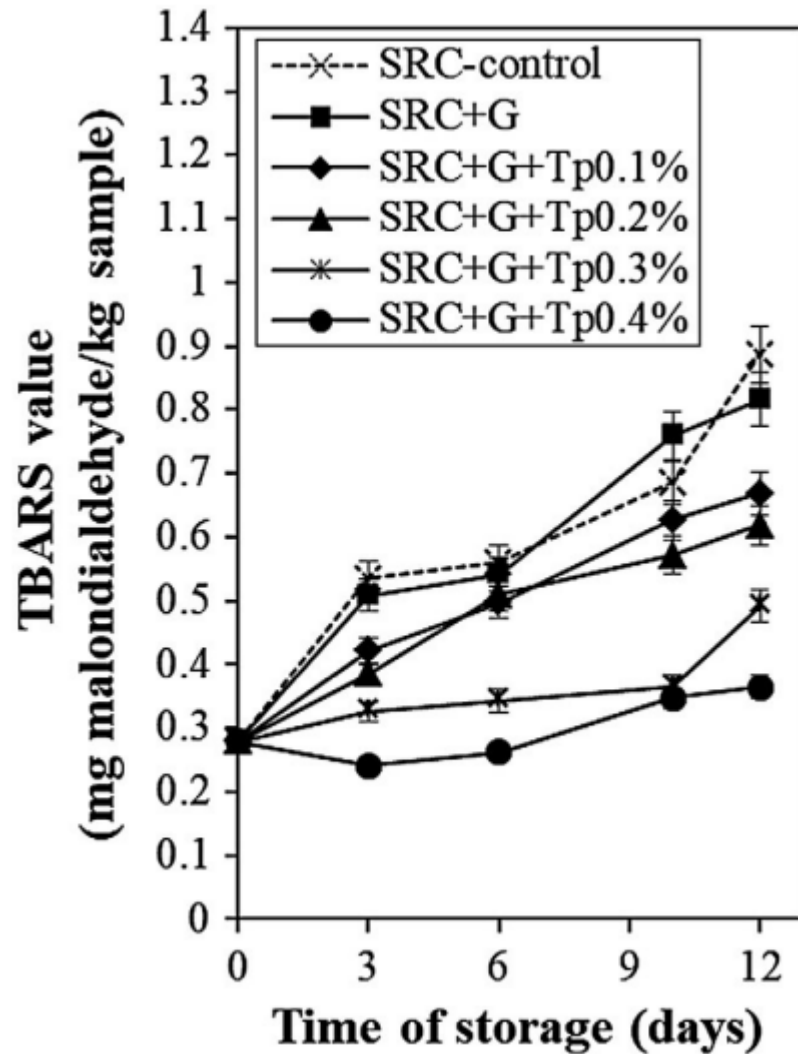
To study the effects of antioxidant α -tocopherol from SRC-based film were studied based on thio- barbituric acid-reactive substance assay, metmyoglobin assay, and pH value in food model (meat patties) for 12 days of storage.

Evaluation on maintaining and extending meat patty product shelf life using this active packaging bioplastic from carrageenan based.

Method

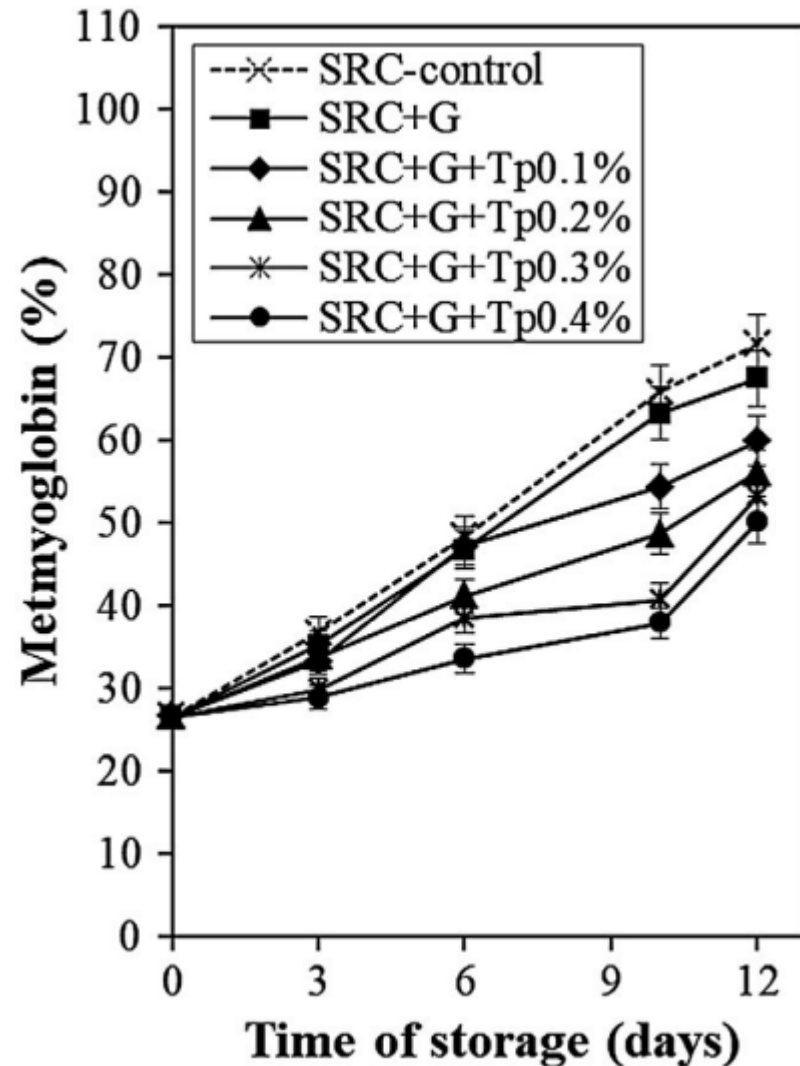
The meat patties were purchased 7 days after slaughtering process to allow it to mature and kept at $-4 \pm 1^{\circ}\text{C}$ for further treatment. Approximately 20 g of meat was wrapped with different types of the SRC-based films: SRC-control, SRC + G, SRC + G + Tp0.1%, SRC + G + Tp0.2%, SRC + G + Tp0.3%, and SRC + G + Tp0.4%. The films sample were placed on the top and bottom to cover the whole meat with approximate size of 7 cm diameter. Each meat patty wrapped with treated films were prepared in triplicate. All the samples were placed in sterilized trays and stored in a chiller at $4 \pm 2^{\circ}\text{C}$ for 12 days of storage for analysis.

TBARS

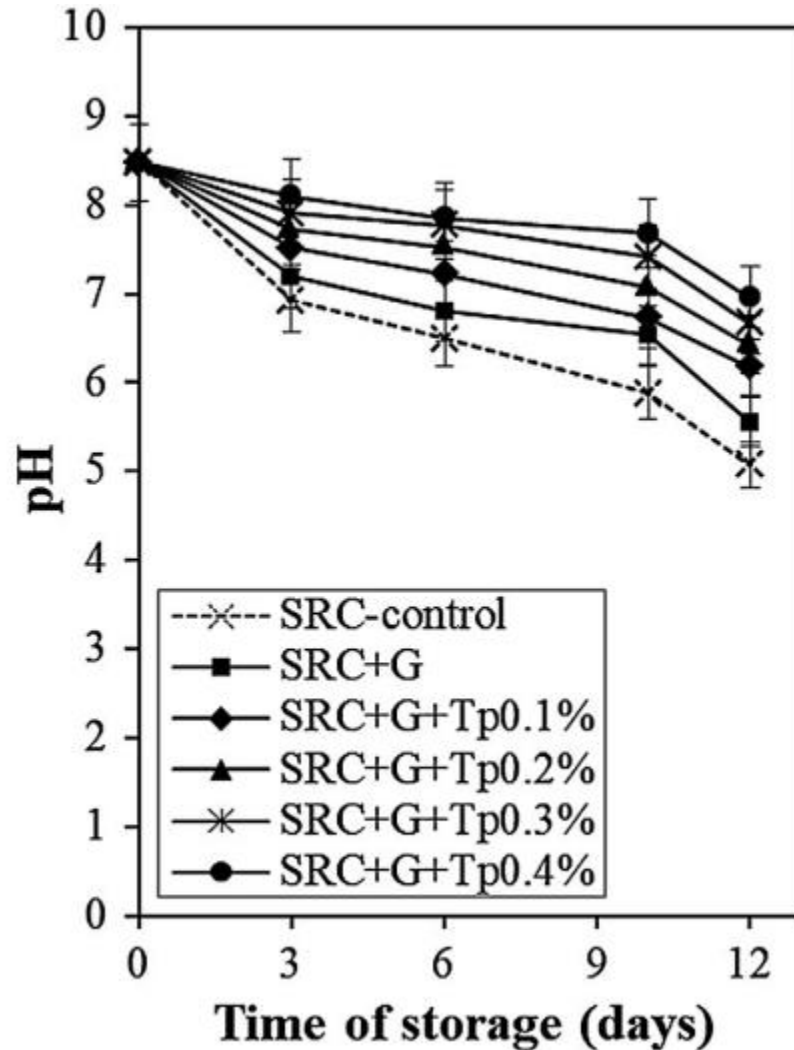


TBARS analysis of meat patties wrapped with SRC-control, SRC + G, SRC + G + Tp0.1%, SRC + G + Tp0.2%, SRC + G + Tp0.3%, and SRC + G + Tp0.4% films for 12-day storage at 4°C

Metmyoglobin assay



Metmyoglobin percentage in meat patties wrapped with SRC-control, SRC + G, SRC + G + Tp0.1%, SRC + G + Tp0.2%, SRC + G + Tp0.3%, and SRC + G + Tp0.4% films for 12-day storage at 4°C



pH values of meat patties wrapped with SRC-control, SRC + G, SRC + G + Tp0.1%, SRC + G + Tp0.2%, SRC + G + Tp0.3%, and SRC + G + Tp0.4% films for 12-day storage at 4°C

Study Summary

The antioxidant effect of Tp in the SRC-based films was tested using meat patties and the highest antioxidant effect was shown by the incorporation of the highest concentration of Tp in the SRC-based film.

The antioxidant film delayed the development of lipid oxidation and brown color formation in the meat patties during storage.

The pH value of the meat patties treated with the antioxidant film showed a positive effect where the value decreased steadily throughout the storage.

In conclusion, the formulation of SRC incorporated with Tp may be an alternative not only to prolong the shelf life but also to avoid the direct contact of synthetic preservative with foods.

THANK YOU